6-21-2019 12:45 PM

Absence of Activating Transcription Factor 3 Reduces Severity of Recurrent Pancreatitis and K-RAS Mediated PDAC in Mice

Nawab Azizi, *The University of Western Ontario*

Supervisor: Pin, Christopher L., *The University of Western Ontario*

A thesis submitted in partial fulfillment of the requirements for the Master of Science degree in Physiology and Pharmacology

Abstract

Pancreatic ductal adenocarcinoma (PDAC) is a terminal cancer projected to become the leading cause of cancer-related deaths in North American by the year 2030. Constitutive activation of KRAS is seen in >90% of PDAC cases. In addition to oncogenic KRAS activity, pancreatic injury is key contributor to PDAC initiation and progression. Activating transcription factor 3 (ATF3) is required for the formation of preneoplastic lesions in acute pancreatitis. However, unlike recurrent or chronic forms of pancreatitis, acute pancreatitis is not predictive of PDAC. Therefore, the goal of this thesis is to determine the role of ATF3 in recurrent pancreatitis and PDAC. *I hypothesize that* ATF3 *is required for persistent acinar-to-ductal cell metaplasia (ADM) and* pancreatic intraepithelial neoplasia *(PanIN) in recurrent pancreatitis and PDAC*. To address this hypothesis, I used mice carrying a targeted deletion of the *Atf3* translation start site (*Atf3*$^{-/-}$) and exposed them to an experimental model of recurrent pancreatic injury or bred them with mice allowing inducible activation of oncogenic KRAS (*KRAS*$^{LSL\text{-}G12D/+}$) specifically in pancreatic acinar cells. The absence of ATF3 reduced ADM and improved pancreatic tissue regeneration in response to recurrent pancreatitis. In addition, *KRAS-G12D* mice lacking *Atf3* showed reduced high grade PanIN lesions compared to mice expressing *KRAS-G12D* and ATF3. These results suggest an important role for ATF3 in PDAC initiation and progression from recurrent forms of pancreatitis.

Keywords

Pancreatic ductal adenocarcinoma, pancreatitis, acinar-to-ductal cell metaplasia, activating transcription factor 3, unfolded protein response pathway

Summary for Lay Audience

This thesis examines the role of a protein called Activating Transcription Factor 3 (ATF3) in experimental models of pancreatitis and pancreatic cancer in mice. Pancreatitis is the inflammation of the pancreas as a result of injury, which increases the susceptibility of developing pancreatic cancer. Previous work done in our laboratory looked at acute forms of pancreatitis and showed that the germline loss of *Atf3* expression was beneficial for pancreatic tissue regeneration. Next, I wanted to know if the loss of ATF3 was also beneficial in the context of recurrent forms of pancreatitis (greater susceptibility for pancreatic cancer in comparison to acute forms) and pancreatic cancer. My work showed that mice lacking ATF3 expression in recurrent forms of pancreatitis had better tissue regeneration and lower number of lesions, which have the potential of developing into cancer. In my pancreatic cancer model, the loss of ATF3 reduced the number of highly developed lesions. My results indicate that there may be a potential in therapeutically targeting ATF3 in pancreatic cancer for better outcome.

Co-authorship Statement

Nawab Azizi completed all the experiments along with the data analysis in this study, with the exception of (**Figure 3.4 C-E**), which was completed by Mickenzie Martin.

Acknowledgements

Firstly, I would like to thank Dr. Christopher Pin for providing me the opportunity that allowed me to grow and become more confident as a researcher. The technical and critical thinking skills I have gained over the past two years are invaluable to me. This is thanks to you. Your constant availability, feedback, and knowledge was truly appreciated. Thank you for your guidance over the years!

Secondly, I would like to thank my parents Wali and Farida Azizi for their constant support over the past 2 years. Thank you for being understanding when I could not make time for family matters due to time related constraints from my research. I strive to be humble hearted like the two of you. Thank you for bringing homemade food with each visit to London. It did not go unnoticed! Truly appreciated it. Thank you.

I would like to next thank my committee members, Drs. Gabriel Dimattia, Samuel Asfaha, and Thomas Drysdale. Thank you for the input and guidance that has shaped my project for the better! I would like to specially thank Dr. Drysdale for reviewing my thesis and providing critical feedback.

Finally, to all the past and current Pin lab members that have helped me learn certain techniques in the lab and have helped me with mouse dissections, thank you. In particular, I would like to thank Kurt Berger for his knowledge and assistance by the bench side.

Table of Contents

List of Tables

List of Figures

List of Appendices

List of Abbreviations

ADM	Acinar-to-Ductal cell Metaplasia
ATF/CREB	ATF/cAMP responsive element binding
ATF	Activating Transcription Factor
ARE	Antioxidant Response Elements
bHLH	Basic Helix-Loop-Helix
BMI	Body Mass Index
BRCA2	Breast Cancer Type 2 Susceptibility Protein
bZIP	Basic Leucine Zipper
CAF	Cancer Associated Fibroblast
CARE	C/EBP-ATF Response Element
CCK	Cholecystokinin
CCL2	C-C Motif Chemokine Ligand 2
CK19	Cytokeratin 19
CI	Confidence Interval
CIP	Cerulein Induced Pancreatitis
ChIP	Chromatin Immunoprecipitation
CP	Chronic pancreatitis
CTRC	Chymotrypsin C
DAPI	4',6-Diamidino-2-Phenylindole
DRG1	Developmentally Regulated GTP Binding Protein 1
ECM	Extracellular Matrix
ERK	Extracellular Signal-Regulated Kinases
EGF	Epidermal Growth Factor
EGFR	Epidermal Growth Factor Receptor
eIF2α	Translation Initiation Factor 2 Alpha
EMT	Epithelial-to-Mesenchymal Transition
ERAD	ER-Associated Degradation
FITC	Fluorescein Isothiocyanate
GADD34	Growth Arrest and DNA Damage Inducible 34

GAP	GTPase-Activator Protein
GDP	Guanosine Diphosphate
GEF	Guanine-Nucleotide Exchange Factors
GRP94	Glucose-Regulated Protein 94
GTP	Guanosine Triphosphate
HAT	Histone Acetyltransferase
HDAC6	Histone Deacetylase 6
H&E	Hematoxylin & Eosin
HNF6	Hepatocyte Nuclear Factor 6
ICAM1	Intracellular Adhesion Molecule 1
IF	Immunofluorescence
IHC	Immunohistochemistry
IKKα	IκB Kinase α
IL-6	Interleukin 6
IRE1	Inositol Requiring Enzyme 1
JNK	c-Jun N-terminal Kinase
JUN	Transcription Factor AP-1
KRAS	Kirsten Rat Sarcoma Viral Oncogene Homolog
MAPK	Mitogen Activated Protein Kinase
MCP-1	Monocyte Chemoattractant Protein-1
MMP2	Matrix Metallopeptidase 2
MUC	Mucin
NFATc1	Nuclear Factor of Activated T cells c1
NFDM	Non-Fat Diary Milk
NRF2	Nuclear factor erythroid 2–Related Factor 2
NSCLC	Non-Small-Cell Lung Carcinoma
PanIN	Pancreatic Intraepithelial Neoplasms
PDAC	Pancreatic Ductal Adenocarcinoma
PDX1	Pancreatic and Duodenal Homeobox 1
PERK	PKR-like Endoplasmic Reticulum Kinase
PI3K	Phosphatidylinositol 3-Kinase

PKB	Protein Kinase B
PMAIP1	Phorbol-12-Myristate-13-Acetate-Induced Protein 1
PRSS1	Serine Protease 1
PSC	Pancreatic Stellate Cell
PTF1a	Pancreas Associated Transcription Factor 1a
PVDF	Polyvinylidene Difluoride
RAF	Rapidly Accelerated Fibrosarcoma
RBPJ	Recombining Protein Suppressor of Hairless
RER	Rough Endoplasmic Reticulum
ROS	Reactive Oxygen Species
RP	Recurrent Pancreatitis
RR	Relative Risk
RT	Room Temperature
RTK	Receptor Tyrosine Kinases
SAL	Saline
SMA	Smooth Muscle Actin
SMAD4	SMAD family member 4
SOX9	Sry-Related High-Mobility Group Box 9
SPINK1	Serine Protease Inhibitor Kazal Type-1
TAM	Tumour Associated Macrophage
TGF-α	Transforming Growth Factor Alpha
TRITC	Tetramethylrhodamine
UPR	Unfolded Protein Response
WT	Wild-Type
YFP	Yellow Fluorescent Protein

CHAPTER 1

1 INTRODUCTION

1.1 Overview

This thesis provides important insights for the transition from recurrent pancreatitis (RP) to pancreatic ductal adenocarcinoma (PDAC). Activating Transcription Factor 3 (AFT3), mediator of the unfolded protein response pathway (UPR), has been associated with multiple cancer types and previous work from our laboratory suggests it is required for the de-differentiation of acinar cells in the context of acute pancreatic injury (Thompson et al., 2009; Yin et al., 2010; Wu et al., 2010; Fazio et al., 2017). However, ATF3 to our knowledge has not been studied in murine models of chronic or recurrent pancreatitis, nor in PDAC to date. While a wide range of intrinsic and extrinsic signalling pathways have been studied in PDAC, there is still a gap in understanding the molecular events that promote KRAS-mediated initiation and progression of PDAC (Bryant et al., 2014; O'Hagan & Heyer, 2011; Liu & Kaufman, 2003; Ron & Walter, 2007). Therefore, examining additional signalling factors, such as ATF3 will help us understand how the cellular response to recurrent forms of injury promote progression to PDAC. Previous work in our laboratory showed ATF3 is a mediator of preneoplastic lesions in acute pancreatitis (Fazio et al., 2017). This thesis investigates ATF3's role in recurrent pancreatic injury and in the context of oncogenic *KRAS*-(*G12D*). Molecular markers of preneoplastic lesions were examined during injury, recovery and in advanced PanIN lesions in the absence of ATF3.

1.2 PDAC

PDAC constitutes 95% of pancreatic cancers and has a very poor overall 5-year survival rate of only 8%. PDAC is projected to be the leading cause of cancer-related deaths in North America by the year 2030 (Conroy et al., 2011; Koikawa et al., 2018). A large majority of PDAC patients are diagnosed at the late stages of the disease, when metastasis has already taken place (Zhang et al., 2019). The lack of early clinical symptoms before PDAC develops and metastasizes makes early detection difficult (Zhang et al., 2019). Surgical resection is considered the most effective treatment, although 80% of these patients are noted to relapse soon after surgery (Low et al., 2011). Cancerous tissue that is surgically resected is commonly noted as a solid mass upon gross morphologically examination. This is reflective of the tumour microenvironment being highly fibrotic in addition to showing high levels of immune cell infiltration (Kleeff and Jorg, 2016; Sener et al., 1999). Due to the highly heterogenous and stromal nature of the disease, effective drug delivery remains a problem when treating PDAC (Jacobetz et al., 2013). Patients with late stage PDAC without the option of resection are treated with either gemcitabine (median survival 6.8 months) or FOLFIRINOX (median survival 11.1 months) chemotherapeutics (Ahn et al., 2017; Von Hoff et al., 2013; Conroy et al., 2011). Combining both gemcitabine and FORFIRINOX shows no beneficial outcome compared to either drug alone (Conroy et al., 2011). Based on these findings, there is a dire need for better biomarkers that are able to detect and diagnose the disease at earlier stages.

The origin of PDAC as demonstrated by animal and human studies show emergence from late stage neoplastic lesions called pancreatic intraepithelial neoplasms (PanINs) (Hruban et al., 2000). Histologically, PanIN development and progression occurs in stages. Early PanINs (PanIN1A/B and PanIN2) are classified by the replacement of cuboidal duct structures with columnar mucinous epithelium with low levels of dysplasia. Focal PanIN1A/B lesions are known to be observed in non-diseased pancreatic tissue (Di Magliano & Logsdon, 2013). Intermediate (PanIN2) and high-grade PanINs (PanIN3) are characterized by varying degrees of nuclear irregularity (nuclear atypia), loss of cell

polarity, luminal necrosis and increased levels of dysplasia (Makohon-Moore et al., 2016; Hruban et al., 2008; Basturk et al., 2015).

The cell of origin of precursor lesions is debated (Ferreira et al., 2017; Bailey et al., 2014; Rooman & Real, 2012). It has been demonstrated that PDAC can arise from ductal cells which form the conduit system that carries secreted enzymes from pancreatic acinar cells to the duodenum (Ferreira et al., 2017; Lee et al., 2018) or from pancreatic acinar cells (Chen et al., 2018; Bailey et al., 2014; Rooman & Real, 2012). Pancreatic acinar cells are highly polarized, enzyme secreting cells within the exocrine pancreas, which makes up the majority of the pancreas (>90%) (Tsunoda et al., 1996). Upon neuronal or hormonal stimulation (Tsunoda et al., 1996; Ogami & Otsuki, 1998) acinar cells release synthesized and stored pro-enzymes by regulated exocytosis into the ductal network (Reichert and Rustgi, 2011). In addition to lesion formation from acinar cells, the cells of the stromal microenvironment during injury also play a role in further progressing PanIN lesions by cell-to-cell crosstalk.

1.2.1 PDAC microenvironment

The microenvironment in PDAC plays a major role in progression and metastasis of PDAC (Macherla et al., 2018; Ogier et al., 2018). Standard therapies including immune-based therapies are difficult to develop due to the encapsulation of PDAC cells in the tumour-associated fibroinflammatory network (Zhang et al., 2019). The highly stromal nature of PDAC prevents drug delivery and the mobilization of anti-tumour cells from destroying cancer cells (Olive et al., 2009; Neesse et al., 2011; Hingorani & Tuveson, 2003). Fibroblast cells normally reside between pancreatic cells and help model the extracellular matrix (ECM; Bailey et al., 2008). Early PanIN lesions secrete the sonic hedgehog signalling (shh) molecule and activate fibroblast cells into cancer-associated fibroblast cells (CAFs; Yauch et al., 2008; Bailey et al., 2008). The deregulation of the ECM by CAFs results in significantly more deposits of collagen protein leading to fibrosis (Zhang et al., 2019). CAFs make up a large proportion of the dysplastic constituents of the stroma and are one of the known hallmarks of PDAC (Collins et al.,

2012). CAFs are known to have different potential roles in PDAC; studies have demonstrated both a pro-tumorigenic role (Yauch et al., 2008) or a tumour suppressor role (Kalluri & Zeisberg, 2006).

In addition to fibroblast activation and extensive fibrosis, immune cell signalling has a major role in PDAC (Gardian et al., 2012; Kurahara et al., 2011; Helm et al., 2014). Immune cells that are highly prevalent in PDAC and are derived from hematopoietic stem cells of the bone marrow (Nowarski et al., 2013). In particular, myeloid cells derived from hematopoietic stem cells can be subcategorized into granulocytes, mast cells, monocytes, dendritic cells, macrophages and play a vital role in fighting infection and help heal wounds (Nowarski et al., 2013). One of the best characterized subsets of these cells in PDAC are tumour associated macrophages (TAMs). TAMs can either be derived from circulating monocytes or activated locally by cytokine signalling on resident macrophages (Clark et al., 2007). In PDAC, cytokines secreted by neoplastic ductal lesions include monocyte chemoattractant protein-1 (MCP-1), more currently known as C-C Motif Chemokine Ligand 2 (CCL2) (Rambaldi et al., 1987; Murdoch et al., 2004). In addition to local activation of macrophages to TAMs, increased serum levels of CCL2 correlate with increased TAM attraction and infiltration of neoplastic lesions from the blood stream (Monti et al., 2003). TAMs have been implicated in the initiation and expansion of tumour cells (Mitchem et al., 2013) along with promoting epithelial to mesenchymal transition (EMT) (Helm et al., 2014) and PDAC metastasis (Gardian et al., 2012; Kurahara et al., 2011).

1.2.2 Genetic mutations linked to PDAC

A number of studies assessing genetic risk factors for PDAC show an estimated 10% of patients have an inherited susceptibility for PDAC (Lynch, et al., 2010; Hruban et al., 1998; Schenk et al., 2001). Case-control and cohort studies demonstrate individuals with a family history of PDAC have a 1.9- to 13-fold risk factor for PDAC when compared to individuals with no family history (Ghadirian et al., 1991; Jacobs et al., 2010; Klein, 2012). In addition, the odds of PDAC increase with increasing number of first-degree

relatives with the disease. The odds ratio for PDAC is 1.76-fold higher for an individual with one first-degree relative with PDAC and 4.26-fold higher with two first-degree relatives (Jacobs et al., 2010). Individuals that have greater odds of PDAC development are typically carriers of multiple genetic mutations that have been linked to the disease (Reznik et al., 2014; Pogue-Geile et al., 2006).

Specific inherited mutations for breast cancer type 2 susceptibility protein (BRCA2), p16 and PALLADIN increase the risk for PDAC development (Reznik et al., 2014). The *BRCA2* gene is involved in the Fanconi anemia pathway and is responsible for double stranded DNA break repair and synthesis phase DNA damage checkpoint control (van der Heijden et al., 2005; B. Xia et al., 2006). Inherited mutations in *BRCA2* result in impaired cytokinesis, proliferation arrest and genomic instability (Sharan et al., 1997; Patel et al., 1998; Couch et al., 2007). Individuals with this mutation have a 3.5- to 10-fold risk factor for PDAC development compared to non-carriers (Breast Cancer Linkage Consortium, 1999; van Asperen et al., 2005). In addition, *PALLD* overexpression has been linked to PDAC development (Pogue-Geile et al., 2006). PALLADIN is responsible for encoding components of the cytoskeleton that help with cellular motility. Cells with *PALLD* overexpression show increased cellular motility (Pogue-Geile et al., 2006). Furthermore, germline mutations in the tumour suppressor gene *CDKN2A,* encoding both $p16^{INK4A}$ and $p19^{ARF}$, increases the risk for PDAC. The $p16^{INK4A}$ protein is responsible for the regulation of cell cycle through the G1 to S phase transition (Schneider & Schmid, 2003). The mutated $p16^{INK4A}$ protein has been reported to act jointly with oncogenic kirsten rat sarcoma viral oncogene homolog (KRAS) and accelerate tumour progression (Hezel, et al., 2006).

1.2.3 Oncogenic KRAS and downstream effectors

The most common mutation in early neoplastic lesions (PanIN1) occur in the *KRAS* gene. More than 90% of PDAC patients carry an activating mutation in *KRAS*, with a G12D conversion observed 98% of the time (Bryant et al., 2014; O'Hagan & Heyer, 2011; James et al., 2018; Eser et al., 2014). The G12D mutation causes constitutive activation of KRAS by preventing GTP hydrolysis (Bos, 1989; O'Hagan & Heyer, 2011). Physiologically, the human *RAS* protein is a small (21 kDa) plasma membrane bound GTPase protein, responsible for proliferation, differentiation and cell migration by linking multiple downstream signalling pathways. KRAS activation promotes mitogen activated protein kinase (MAPK) and phosphatidylinositol 3-kinase (PI3K) signalling (Bryant et al., 2014). In the pancreas, KRAS cycles between a GTP-bound "ON switch" and GDP-bound "OFF switch" (Bryant et al., 2014; Di Magliano & Logsdon, 2013). The proteins responsible for affecting the molecular switch in KRAS include guanine nucleotide exchange factors (RasGEFs) and GTPase-activating proteins (RasGAPs) (Bryant et al., 2014) respectively. RasGEFs activate KRAS by replacing GDP with GTP, while RasGAPs hydrolyze GTP to GDP and inactivate KRAS activity (Bryant et al., 2014). Genetic mouse models that utilize the cre/loxP system, which allow for temporal oncogenic KRAS activation, demonstrate constitutively active KRAS is needed for progression, and maintenance of preneoplastic lesions as well as promote metastasis (Ying et al., 2012; Collins et al., 2012). The development of therapy targeting constitutively active KRAS has been unsuccessful to date due to the lack of direct, potent and selective inhibitors (Nussinov et al., 2018) along with random spontaneous KRAS mutations with age (Di Magliano & Logsdon). Further, Singh et al., (2009) showed a subset of PDAC cells associated with epithelial to mesenchymal transition (EMT) that did not respond to KRAS inactivation. Despite these findings, there have been increasing efforts made in developing potential inhibitors to target *KRAS*-(*G12D*) (Holderfield, 2018; Lu, et al., 2016; Zeng et al., 2017).

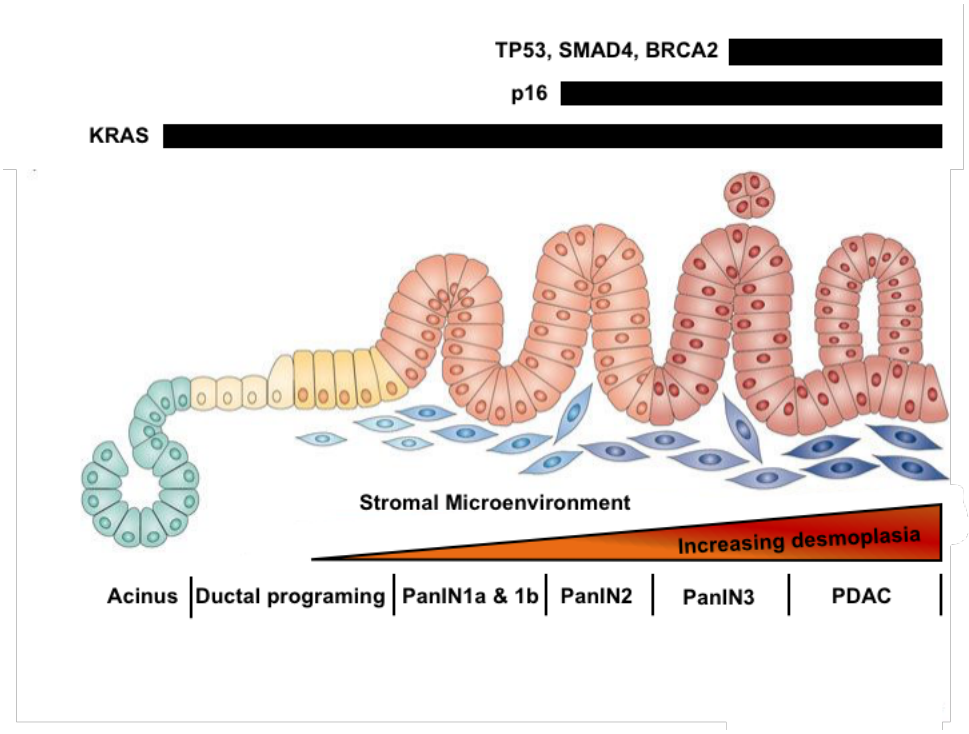

Figure 1.1. Progression from normal to diseased pancreas with the temporal association of known genetic mutations. The *Kras* gene is initially mutated resulting in constitutive activation of KRAS in acinar cells leading to ductal programing. Lower grade PanIN1A/B lesions form in the presence of oncogenic KRAS and are characterized by columnar mucinous epithelium. The second most common mutation is in the p16 protein which further progresses PanIN1 lesions to PanIN2 in the presence of oncogenic KRAS characterized by nuclear atypia and a lower degree of surrounding desmoplasia. Further mutations in *TP53*, *SMAD4* and *BRCA2* result in high grade PanIN3 lesions and PDAC, which is characterized by high levels of nuclear atypia, epithelial folding and higher levels of surrounding desmoplasia (Figure adapted from Morris et al., 2010).

Currently the inability to directly target oncogenic KRAS has led to targeting potential downstream effectors of KRAS. The two major downstream pathways include RAF-MEK-ERK (MAPK) and PI3K-AKT signalling (Lim et al., 2005; Feldmann et al., 2010; Collisson et al., 2012; Eser et al., 2013). The MAPK pathway involves a series of downstream phosphorylation events where RAF (MAPKKK) is activated by GTP bound KRAS. Subsequently, RAF phosphorylates MEK (MAPKK) and further MEK phosphorylates ERK (MAPK). Phosphorylated ERK translocates to the nucleus and phosphorylates transcription factors, which induce gene expression (Crespo & León, 2000; Schubbert et al., 2007). Oncogenic RAF alone is sufficient to induce PanIN lesion formation in the absence of constitutively active KRAS (Collins et al., 2012b). The presence of oncogenic KRAS along with constitutively active RAF shows more severe high-grade PanIN formation compared to oncogenic KRAS alone (Collisson et al., 2012). This highlights that downstream mediators are capable of inducing lesion formation even in the absence of oncogenic KRAS.

The second major intrinsic pathway involved in cell survival is PI3K-AKT signalling. Phosphatidyl inositol 3 kinase (PI3K) is phosphorylated by receptor tyrosine kinases (RTKs) and further phosphorylates downstream PIP2 producing phosphatidylinositol (3,4,5)-trisphosphate (PIP3) (Castellano & Downward, 2011). PIP3 subsequently binds and activates AKT/PKB leading to a cascade of phosphorylation events downstream (Castellano & Downward, 2011; Eser et al., 2013). Blocking both RAF-MEK-ERK and PI3K-AKT results in a delayed induction of lung tumours compared to non-inhibitor controls (Castellano & Downward, 2011). In contrast, mutations in the EGFR signalling pathway and focal low grade PanIN lesions do occur spontaneously and are present in normal pancreatic tissue. Therefore, it is believed that additional genetic or environmental factors are necessary to initiate full blown carcinogenesis in addition to constitutively active KRAS (Di Magliano & Logsdon, 2013).

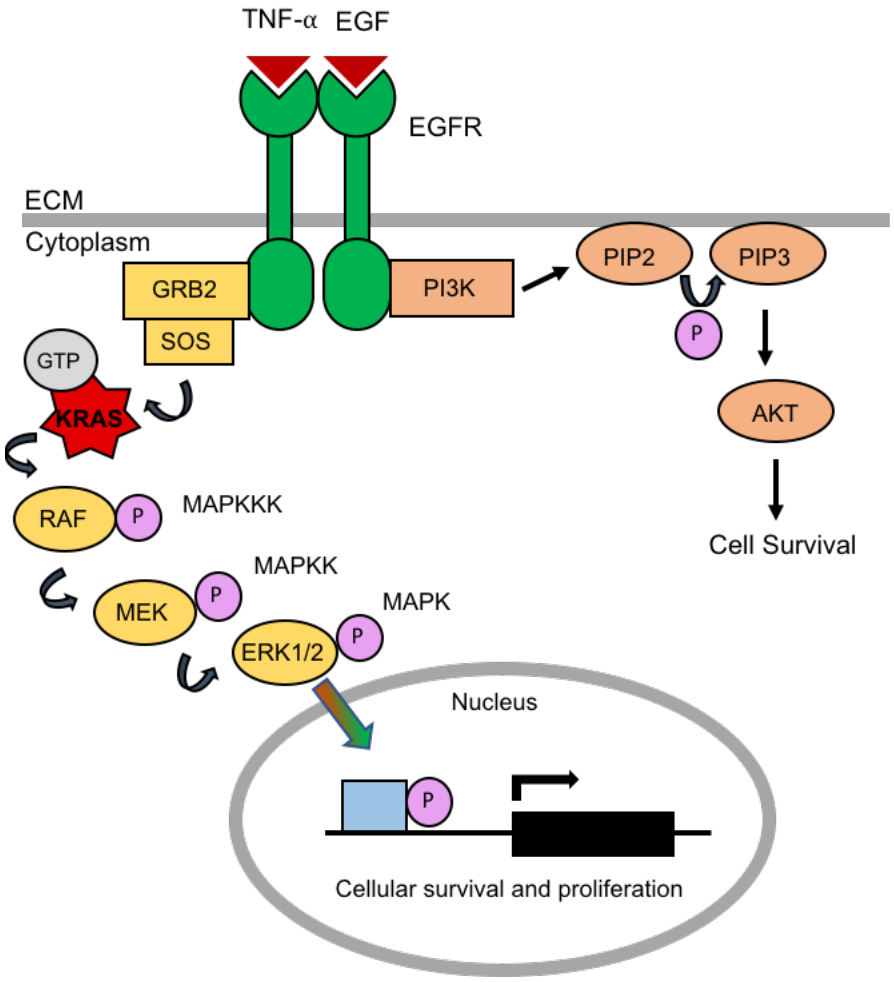

Figure 1.2. EGFR signalling pathway. The EGFR pathway is split into two main intracellular signalling streams (MAPK and PI3K) involved in cell survival and proliferation. The intracellular MAPK signalling stream is activated by a cascade of phosphorylation events that results in the translocation of phosphorylated ERK1/2 to the nucleus where it phosphorylates transcription factors. In the second signalling stream, PI3K is phosphorylated by RTKs where it subsequently phosphorylates PIP2 to PIP3 and as a result AKT is activated downstream.

1.2.4 Additional Genetic Mutations

Additional mutational burden helps progress low grade neoplastic ductal lesions with oncogenic KRAS into PDAC (Bryant et al., 2014; O'Hagan & Heyer, 2011; James et al., 2018). Progression through the PanIN stages to PDAC includes additional mutations in *TP53*, *SMAD4* and other key genes. In 50-75% of PDAC cases the *TP53* gene is mutated (Morton et al., 2010; The Cancer Genome Atlas Research Network, 2017). Mutations in *TP53* specifically drive KRAS-induced neoplastic lesions to PDAC (Morton et al., 2010) and is thought to further induce metastasis (Weissmueller et al., 2014). Further mutations in *SMAD4* (30-64% of PDAC show *SMAD4* mutations) have been implicated in progression of low grade PanIN lesions to PDAC as demonstrated by genomic sequencing and immunohistochemistry techniques (Waddell et al., 2015; Ormanns et al., 2017). Physiologically, SMAD4 is a transcription factor involved in the transforming growth factor beta (TGF-β) pathway, which induces genes expression based on microenvironmental factors (Waddell et al., 2015; Ormanns et al., 2017). Conversely, genetics is not a major factor (90% PDAC cases have no additional mutated gene) therefore, environmental factors most likely are involved for the progression of PDAC.

1.2.5 Environmental factors linked to PDAC

Environmental factors such as chronic alcohol consumption and smoking are linked to PDAC development (Tramacere et al., 2010; Yadav & Whitcomb, 2010). Chronic alcohol consumption remains to be a significant risk factor for PDAC (Schenker & Montalvo, 1998; Tramacere et al., 2010). In addition, it is estimated that 25% of PDAC cases are due to the high prevalence of smoking worldwide (Maisonneuve & Lowenfels, 2010; Vrieling et al., 2010). This is complicated by individuals who abuse both alcohol and smoke concurrently (Yadav & Whitcomb, 2010).

Other factors that are linked to the development of PDAC include obesity and type 2 diabetes mellitus (T2DM). Obese individuals (BMI > 40 kg/m^2) have a 3-fold higher risk factor for PDAC both in men and women compared non-obese controls (Calle et al., 2003). Secondly, individuals with high insulin resistance have an estimated 3-fold increase for the risk of developing PDAC (Stolzenberg-Solomon et al., 2005). These studies suggest a strong correlation between stressors of the pancreas and PDAC. However, the strongest risk factor for PDAC is pancreatitis, in particular, recurrent and chronic forms of pancreatitis (Yadav & Lowenfels, 2006; Fagenholz et al., 2007; Krishna et al., 2017; Lew et al., 2017).

1.3 Pancreatitis

Pancreatitis is a severe disease marked by parenchymal and systemic inflammation, fibrosis, and necrosis (Lew et al., 2017). Pancreatitis can be classified into three main categories: acute, recurrent, and chronic (Yadav & Lowenfels, 2013). Acute pancreatitis is defined by the rapid onset inflammation of the pancreas and is known to be reversible (Crockett et al. 2018). If acute pancreatic injury occurs more than twice it is defined as recurrent pancreatitis (RP) (Lankisch et al., 2009; Nøjgaard et al., 2011). The incidence of RP worldwide is 8-10/100,000 and can substantially increase the likelihood of developing irreversible chronic pancreatitis (CP) (Machicado & Yadav, 2017). CP occurs as a result of repeated insult from RP producing inflammation and fibrosis of the exocrine pancreas leading to lasting changes of pancreatic architecture (Machicado & Yadav, 2017). The literature strongly correlates RP to the development of CP (Yadav & Lowenfels, 2006; Fagenholz et al., 2007; Krishna et al., 2017; Lew et al., 2017). Chronic pancreatitis is a significant risk factor for PDAC development (Guda et al., 2018; Yadav & Lowenfels, 2013).

1.3.1 Genetic and environmental factors linked to pancreatitis

Genetic factors linked to the development of pancreatitis are well known (Schneider et al., 2004; Rosendahl et al., 2008; Mayerle et al., 2018). The first gene mutation identified as being correlated to pancreatitis was in the serine protease 1 (*PRSS1*) gene which encodes cationic trypsinogen (Whitcomb et al., 1996). In physiological conditions, trypsinogen is maintained within acinar cells in an inactive state and only becomes active when released into the duodenum and enzymatically cleaved (Whitcomb et al., 1996; Mayerle et al., 2018). Gain of function mutations in *PRSS1* lead to premature activation of trypsinogen within acinar cells that is resistant to inhibition and causes autodigestion of the cell leading to pancreatitis. Mutations in the *PRSS1* gene are inherited in an autosomal dominant manner but do not show complete penetrance (Whitcomb et al., 1996; Charnley, 2003). Additional mutations that can lead to pancreatitis occur within serine protease inhibitor Kazal-type 1 (*SPINK1*) and chymotrypsin C (*CTRC*) genes (Schneider et al., 2004; Rosendahl et al., 2008). Both *SPINK1* and *CTRC* regulate trypsin by encoding proteins that inhibit its premature activation. Loss of function mutations in either *SPINK1* and *CTRC* can lead to the premature activation of trypsinogen to trypsin (Schneider et al., 2004; Rosendahl et al., 2008). In addition, intracellular activation of proteases, like trypsin, can result in the activation of nuclear factor kappa-light-chain-enhancer of activated B cells (NF-κB): a master regulator of the inflammatory pathway, which can further propagate the disease (Jakkampudi et al., 2016). However, NF-κB can be activated independent of premature protease activation and work independently of proteases in acinar cells to initiate pancreatitis (Baumann et al., 2007).

Environmental factors also contribute to the formation of pancreatitis. Risk factors include smoking, a Western diet and chronic alcohol consumption, which are correlated with the development of pancreatitis (Maisonneuve & Lowenfels, 2010; Vrieling et al., 2010; Tramacere et al., 2010). Additional factors, such as blockage of the common bile duct, also pose a risk for the development of pancreatitis. Normally, digestive enzymes of the pancreas flow through the common pancreatic duct into the duodenum. Blockage of the common bile duct can restrict the flow of digestive enzymes into the duodenum

causing a back flow of enzymes into parenchymal tissue leading to inflammation and digestion of healthy cells (Malik, 2015). The blockage of the pancreatic common duct is the most common cause of AP in the human adult population (35-75% of acute pancreatitis cases; Trust et al., 2011). Further, anatomical abnormalities can lead to the development of pancreatitis. For example, pancreas divisum (abnormal anatomy of pancreatic ducts) can cause RP and subsequently result in CP (Lew et al., 2017). On the other hand, it is important to note that 10-30% of patients with pancreatitis have no attributable cause, which can later lead to idiopathic onset of CP in patients and increase the risk for PDAC development (Lew et al., 2017).

1.4 Models used to study pancreatitis and PDAC

1.4.1 Environmental models of pancreatitis

To delineate the mechanisms that affect progression and severity of pancreatitis a wide range of animal models have been utilized (Saluja et al., 1985; Zhan et al., 2016; Hegyi et al., 2004). The introduction of L-arginine is one method of inducing pancreatitis (Hyun & Lee, 2014; Cuthbertson & Christophi, 2006). A single injection (500 mg/100 g body weight) induces severe acute necrotizing pancreatitis in rats (Hegyi et al., 2004; Tani et al., 1990). This model emulates clinical features of sudden onset acute pancreatitis such as multi-organ failure (Steinberg & Tenner, 1994; Renner et al., 1985; Karimgani et al., 1992). However, L-arginine's pathogenic mechanism of pancreatitis is unclear, although proposed mechanisms do exist in the literature (Czakó et al., 1998; Takács et al., 2002; Rakonczay et al., 2003). Secondly, to mimick pancreatitis caused by gallstone restriction of the main pancreatic duct, experimentally blocking the main duct by means of ligation can be used (Zhan et al., 2016; Kirkbride, 1912; Sendler et al., 2015; Xiao et al., 2017). This model is highly technical, invasive and is rarely used for CP studies (Lerch & Gorelick, 2013). Mainly, the pancreatic ductal ligation model is used in rodents to induce and study acute pancreatitis which mimicks human biliary acute pancreatitis and at later time points: chronic pancreatitis (Zhan et al., 2016). Despite the two models mentioned,

cerulein-induced-pancreatitis (CIP) remains the most common method of studying pancreatitis.

Cerulein is a cholecystokinin (CCK) hormone analog (Niederau et al., 1985) that can be administered at supraphysiologic levels preventing zymogen granule exocytosis within acinar cells. This results in pancreatitis as a result of acinar cell autolysis (Saluja et al., 1985). Intracellular changes in calcium signalling and the activation of the inflammatory pathway NF-kB are responsible for inducing pancreatitis as a result of CIP (Krüger et al., 2000; Mooren et al., 2003). The activation of the inflammatory pathway and autolysis of acinar cells produce chemokines and cytokines such as interleukin 6 (IL-6) and chemoattractant proteins that signal inflammatory cells such as neutrophils and macrophages to the surrounding tissue (Abdulla et al., 2011; Brady et al., 2002). The inflammatory response in CIP is representative of what is seen in human pancreatitis (Lew et al., 2017). In addition, the CIP model results in high levels of fibrosis representative of what is seen in human patients (Lew et al., 2017). Further, CIP activates resident fibroblast cells to active pancreatic stellate cells (PSC) (Yauch et al., 2008; Bailey et al., 2008). Once activated, PSCs secrete ECM proteins (mainly collagen 1) that results in extensive fibrosis. This is further exacerbated by macrophages that release TNF-α and signal the activation of stellate cells (Sendler et al., 2013). To recapitulate RP, multiple injections of cerulein can be given over the course of several weeks. This results in persistent exocrine tissue damage, immune cell infiltration and fibrosis, consistent with human patients that have CP (Neuschwander-Tetri et al., 2000). One caveat to this model is that pancreatitis completely resolves after the cessation of cerulein administration in mouse models (Lugea et al., 2006). This is unlike the self-sustained, irreversible CP seen in human patients (Etemad & Whitcomb, 2001).

1.4.2 Genetic models of pancreatitis and PDAC

A number of transgenic mouse models have been generated to study pancreatitis. Since pre-mature activation of trypsinogen is a key initiator of pancreatitis, transgenic mice carrying the mutant variant of the *PRSS1* gene have been generated (Archer et al., 2006;

Selig et al., 2006; Athwal et al., 2014). Mice carrying the mutant human *PRSS1* transgene fail to develop pancreatitis spontaneously (Archer et al., 2006). This is likely due to low penetrance of the transgene (Archer et al., 2006; Archer et al, 2014). However, a more severe pancreatitis phenotype occurs upon cerulein injection in mice carrying the mutant *PRSS1* gene compared to wild-type mice treated with ceruelin (Archer et al., 2006; Athwal et al., 2014). Secondly, the IKKα complex, which is a regulator of NF-κB, can also be specifically targeted to induce pancreatitis (Li et al., 2013). Loss of IKKα causes spontaneous pancreatic injury, along with acinar cell atrophy, fibrosis and the presence of tubular structures in the pancreas of mice (Li et al., 2013).

The number of different transgenic mouse models developed for studying PDAC is significant (Hingorani et al. 2003; Guerra et al., 2007; Guerra et al., 2011; Westphalen & Olive, 2012). The vast majority of the genetic mouse models express the mutant $KRAS^{G12D}$ by pancreas-specific cre-recombination (Guerra et al., 2007; Guerra et al., 2011; Krah et al., 2015). In non-inducible models, $KRAS^{G12D}$ is expressed early in embryonic development (E8.5) using promoters specific to the pancreas such as pancreatic and duodenal homeobox 1 (*Pdx1*) and pancreas associated transcription factor 1a (PTF1a) (Hingorani et al., 2003). These mice develop PanIN lesions that progress to metastatic PDAC within 1-year of $KRAS^{G12D}$ activation (Hingorani et al., 2003). Often, the transgenic models also incorporate mutations in tumour suppressor genes such as *TP53*, *SMAD4* and *CDKN2A* (Guerra et al., 2007; Guerra et al., 2011; Pérez–Mancera et al 2012; Westphalen & Olive, 2012). Mice carrying *TP53* mutations along with mutant $KRAS^{G12D}$ (*lox-stop-lox [LSL]* $KRAS^{G12D/+}$*; LSL-* $Trp53^{R172H/+}$; $Pdx\text{-}1^{Cre}$; *KPC*) do not show any signs of pancreatitis or neoplastic lesions at birth (Guerra et al., 2011). However, *KPC* mice develop PanIN lesions and show fibrosis by 8-10 weeks of age (Guerra et al., 2007; Guerra et al., 2011). Interestingly, the *KPC* model has an immuno-microenvironment that mirrors the one seen in human patients (Bayne et al., 2012; Beatty et al., 2011). In addition, PDAC clinical features are present in *KPC* mouse models: ascites, biliary obstruction and cachexia (Feig et al., 2013; Jacobetz et al., 2013). One caveat to this mouse model is that *KRAS* and *TP53* mutations occur as soon as the driver gene is activated embryonically, which does not resemble the developmental timeline of

PDAC seen in older human adults (Guerra et al., 2007; Guerra et al., 2011; Pérez–Mancera et al 2012; Westphalen & Olive, 2012). Therefore, I have chosen to use a mouse model that utilizes the loxP/creERT system to induce $KRAS^{G12D}$ expression temporally in adult acinar cells (Krah et al., 2015). The activation of $KRAS^{G12D}$ in adult acinar cells alone is generally not sufficient to induce PDAC on its own. Additional environmental stress like cerulein based pancreatitis is needed for PDAC development (Krah et al., 2015). In this thesis the loxP/creERT system was utilized to induce $KRAS^{G12D}$ expression in the adult pancreas and cerulein was further administered to induce PDAC development.

1.5 Acinar-ductal-cell metaplasia

To define the origin of precursor PanIN lesions, reporter genes can be included in the transgenic mouse models. Multiple reporter systems exist (Vacaru et al., 2014; Chen et al., 2018; de Latouliere et al., 2016) including *Gfp*, *Yfp*, *mCherry,* that are targeted to the *Rosa26R* allele (Krah et al., 2015). Lineage tracing experiments show acinar cells undergo trans-differentiation or de-differentiation to ductal-like complexes by a process called acinar-to-duct cell metaplasia (ADM) (Stanger & Hebrok, 2013; Pinho et al., 2011; Rooman & Real, 2012). This process is believed to be essential for the regeneration of parenchymal tissue from progenitor-like cells to cope for the loss of tissue mass associated with injury (Liou et al., 2013; Houbracken et al. 2011). However, when pancreatic injury is persistent or when genetic mutations are acquired, ADM is prevented from re-differentiation back to acinar cells and can further progress to form PanIN lesions increasing the risk of PDAC development (Kopp et al., 2012). There is evidence that ADM occurs in both mouse models (Sandgren et al., 1990) and in humans (Liu et al., 2016). In both mice and humans, transcription factors and signaling pathways are known to regulate the formation of ADM (Ardito et al., 2012; Guerra et al., 2007; Wagner et al., 1998; Campos et al., 2013). Therefore, it is critical to study and understand molecular factors involved in ADM development and progression.

1.5.1 Transcription factors involved in ADM

Transcription factors involved in maintaining acinar cell identity are down-regulated in cells undergoing ADM (Rodolosse et al., 2004). In addition, transcription factors involved in the maintenance of ductal cell identity are up-regulated (Park et al., 2011; Miyatsuka, 2006; Shi et al., 2013; Liou et al., 2013). Two key basic helix-loop-helix transcription factors, pancreas transcription factor 1 complex (*Ptf1)* and *Mist1* are vital in maintaining acinar cell identity (Krapp et al., 1998; Rodolosse et al., 2004; Pin et al., 2001). Along with maintaining acinar cell identity, PTF1 regulates the production of digestive enzymes such as amylase and carboxypeptidase 1 in acinar cells (Krapp et al., 1998; Rodolosse et al., 2004). The PTF1 protein exists in a complex with recombining protein suppressor of hairless (RBPJ) and PTF1A (Masui et al., 2010). Mechanistically, the PTF1 complex signals p300/CREB to acetylate the PTF1A subunit which induces its transcriptional activity (Campos et al., 2013). The complete loss of *Ptf1a* in the adult pancreas promotes metastatic PDAC development as a result of ADM progression (Krah et al., 2015). A second key regulator of acinar cell identity is *Mist1*, which is required for complete acinar cell maturation, establishment of cellular polarity, gap junction communication and appropriate regulation of exocytosis (Pin et al., 2001). Inflammation as a result of pancreatitis results in the downregulation of *Mist1* (Kowalik et al., 2007; Karki et al., 2015). Forced expression of *Mist1* rescues the pancreatitis phenotype and prevents ADM development. In contrast, complete ablation of *Mist1* results in incomplete acinar cell maturation increasing susceptibility to pancreatic injury (Rukstalis et al., 2003; Karki et al., 2015).

Conversely, the main transcription factors that are upregulated in the ADM program are the Sry-related high-mobility group box 9 (*Sox9*) and pancreatic and duodenal homeobox 1 (*Pdx1*) (Park et al., 2011; Miyatsuka, 2006; Shi et al., 2013; Liou et al., 2013). Physiologically, SOX9 protein expression is minimal in acinar cells but is expressed in some duct cells and centroacinar cells (Kopp et al., 2011; Furuyama et al., 2011). Expression of SOX9 is up-regulated in acinar cells as a response to inflammation or other forms of pancreatic injury. High levels of SOX9 expression up-regulate expression of

genes such as *cytokeratin 19 (Ck19)*, which is a marker of duct cells (Prévot et al., 2012; Carrière et al., 2011). In patient PDAC samples, SOX9 is expressed in PanIN lesions and tumour cells (Shroff et al., 2014). In addition, resected human PDAC samples show a correlation between SOX9 expression and increased EGFR signalling (Grimont et al., 2015). In mice, the absence of SOX9 results in lower EGFR signalling and reduces precursor lesion progression (Grimont et al., 2015). Secondly, PDX1 is vital for pancreatic development and is expressed in progenitor cells as well as β cells of the endocrine pancreas, but it is not normally expressed in adult acinar cells. (Wescott et al., 2009; Marty-Santos & Cleaver, 2016; Hale et al., 2005; Gu et al., 2002). Like *Sox9*, *Pdx1* is up-regulated in acinar cells during pancreatic injury and has an oncogenic role upon neoplastic transformation (Roy et al., 2016; Park et al., 2011; Miyatsuka, 2006). Constitutively active *Pdx1* expression in mice leads to spontaneous formation of duct-like structures (Miyatsuka, 2006).

1.5.2 Signalling pathways involved in ADM

Signalling pathways promoting ADM have been extensively studied in animal and cell culture models (Sandgren et al., 1990; Liou et al., 2015; Morris et al., 2010). Early work done on acinar cell culture models focused on the EGFR signaling pathway and demonstrated a correlation between EGFR signalling and ADM formation (Sandgren et al., 1990). Similarly, activating SMAD4 in human pancreatic cultures with transforming growth factor beta (TGF-β) have been correlated to the development of ADM (Liu et al., 2016). Secondly, in animal models, early cross-talk between inflammatory cells and KRAS activation has been linked to irreversible ADM development (Liou et al., 2016). Other known signalling pathways involved in ADM include NOTCH, Wnt and Hedgehog (Siveke et al., 2008; Fendrich et al., 2008; Morris et al., 2010). To better understand the interaction between intracellular and extracellular signalling pathways, additional pathways that promote ADM need to be studied. The unfolded protein response pathway (UPR) is one potential pathway that may help better understand ADM formation.

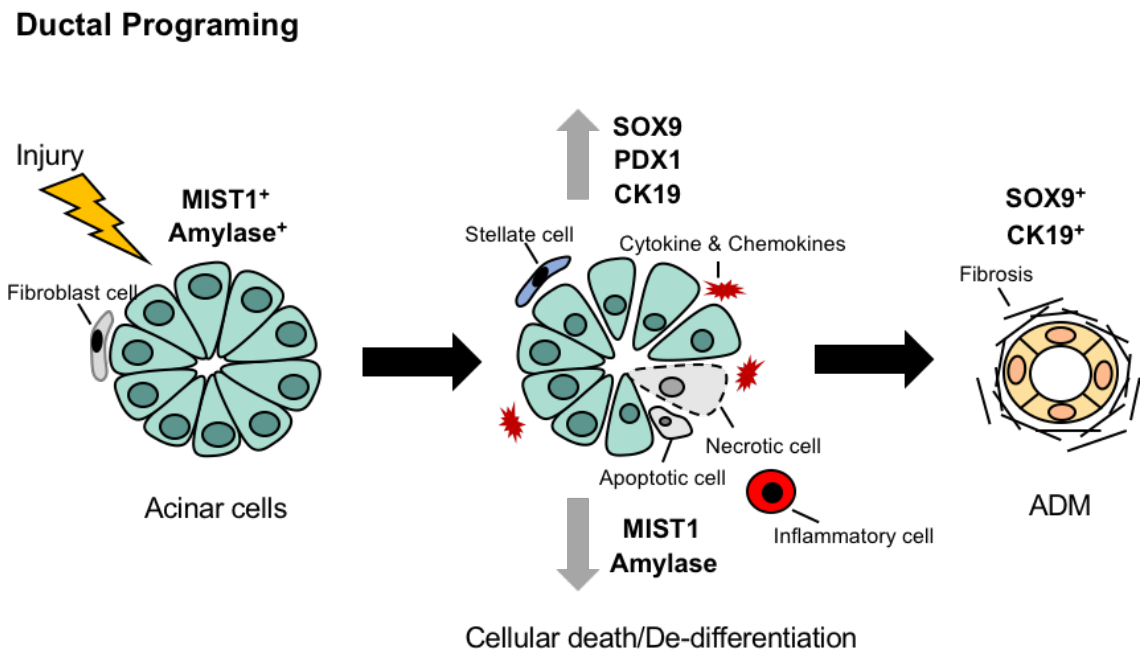

Figure 1.3. Acinar-to-Ductal cell Metaplasia (ADM). Pancreatic injury results in acinar cells to undergo cellular de-differentiation where transcription factors involved in maintaining mature acinar cells are downregulated and transcription factors involved in promoting ductal gene expression are upregulated. This results in ADM lesions that express *Sox9* and *Ck19,* which are markers of ADM. This process is necessary for acinar cell regeneration and re-differentiation once injury is ceased.

1.6 The unfolded protein response pathway

The UPR signaling pathway plays a pivotal role in the lumen of the ER to prevent accumulation of misfolded proteins and maintains a homeostatic protein load within the cell (Ron & Walter, 2007; Kadowaki & Nishitoh, 2013). The concentration of misfolded proteins can increase due to factors such as genetic mutations, nutritional deprivation of the cell, hypoxic conditions, changes in pH and temperature (Bernales et al., 2006; Maas & Diehl, 2015). The UPR responds to the demand of misfolded proteins by increasing the recruitment of chaperone proteins to misfolded proteins thereby promoting proper folding or degradation (Liu & Kaufman, 2003; Ron & Walter, 2007; Kadowaki & Nishitoh, 2013). Chaperone proteins such as BiP (member of the heat shock protein HSP70 family), protein disulfide isomerase and glucose-regulated protein 94 (GRP94) are all responsible for facilitating proper folding of proteins (Ron & Walter, 2007). If the misfolded protein load still persists, the UPR will quickly attempt to reduce overall global protein translation or target proteins for degradation by ER-associated degradation (ERAD). If high misfolded proteins concentration still persists, the UPR will trigger cellular apoptosis (Liu & Kaufman, 2003; Ron & Walter, 2007; Kadowaki & Nishitoh, 2013). The UPR mechanistically decides the appropriate response by activating three UPR signalling branches according to the concentration of misfolded proteins within the cell.

1.6.1 Signal transducers of the UPR pathway

The UPR consists of three signalling branches: double-stranded RNA-activated protein kinase (PKR)–like ER kinase (PERK), inositol requiring enzyme 1 (IRE1) and activating transcription factor 6 (ATF6). The two branches that respond immediately to the deregulation of UPR homeostasis are the PERK and IRE1 branches (Liu & Kaufman, 2003; Ron & Walter, 2007; Kadowaki & Nishitoh, 2013). PERK is activated as a result of RER transmembrane oligomerization and autophosphorylation. This leads to the dissociation of chaperone proteins from PERK and the phosphorylation of the α subunit of translation initiation factor 2 (eIF2α). Phosphorylation of eIF2α results in inactivation

and inhibition of global mRNA translation, thus reducing protein load in the RER (Ron & Walter, 2007). However, proteins that have a small 5' open reading frame are preferentially translated when the ratio of phosphorylated eIF2α exceeds the active form (Ron & Walter, 2007). One such protein is ATF4. ATF4 targets downstream genes such as transcription factor C/EBP homologous protein (CHOP) and growth arrest and DNA damage inducible 34 (GADD34) (Ron & Walter, 2007). GADD34 encodes protein phosphatases that counteract eIF2α phosphorylation (Ron & Walter, 2007) while CHOP induces apoptotic cell death. In addition, ATF4 expression induces activating transcription factor 3 (*Atf3*) gene expression.

The second branch of the UPR, IRE1, is highly conserved and activated immediately along with PERK (Liu & Kaufman, 2003). IRE1 is activated as a result of conformational changes from oligomerization in the ER membrane (Liu & Kaufman, 2003). The activated form of IRE1 cleaves X-box binding protein 1 (XBP1) giving rise to the spliced variant of XBP1 (sXBP1) (Liu & Kaufman, 2003; Ron & Walter, 2007). Spliced XBP1 regulates genes that promote ERAD activity (Liu & Kaufman, 2003; Ron & Walter, 2007). The last branch that is activated is the highly conserved ATF6 pathway (Ron & Walter, 2007). ATF6 relocates to the Golgi apparatus where it is proteolytically cleaved. The cleaved form translocates to the nucleus where it activates genes that give rise to chaperone proteins (Ron & Walter, 2007).

1.6.2 The role of the UPR in pancreatic injury

Unlike other cell types, the UPR pathway is active under physiological conditions in pancreatic acinar cells (Iwawaki et al., 2010), likely due to the high protein turnover rate in acinar cells (Iwawaki et al., 2010). Deleting *Xbp1* causes lethality shortly after birth in mice as a result of abnormal embryonic pancreatic development (Lee et al., 2005). Interestingly, with the exception of the pancreas and salivary glands, other organs remain unaffected in the absence of XBP1 (Lee et al., 2005). Further, ablation of PERK mice results in pancreatic atrophy after birth along with abnormalities in other organ systems (Iida et al., 2007). This highlights that the UPR plays a crucial role in normal pancreatic

function and development compared to other organs. In pathological conditions, such as pancreatitis, inhibiting one branch of the UPR pathway (IRE1) results in the sustained activation of the PERK branch suggesting that compensatory mechanisms between the branches do exist (Lugea et al., 2011). However, ablating *Chop* results in less severe pancreatitis in experimental models (Suyama et al., 2008), suggesting that the UPR pathway can promote pathology in addition to having a physiological role in the pancreas. To develop additional therapies and detection capabilities for PDAC and pancreatitis, better understanding of downstream effectors of the UPR pathway is required.

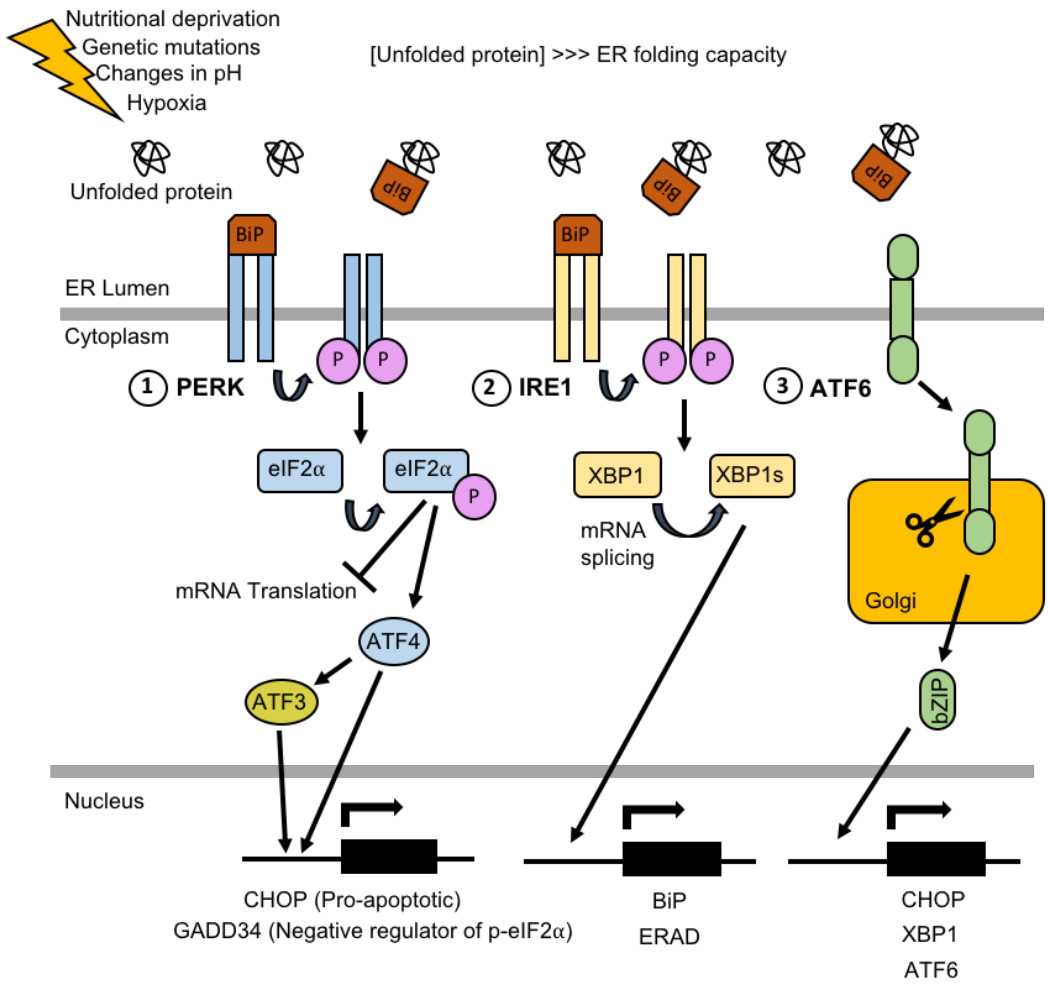

Figure 1.4. The Unfolded Protein Response pathway (UPR). The UPR pathway is activated in response to increasing misfolded protein load that exceeds its capacity to correctly fold. The UPR has three signalling branches that help correct misfolded proteins and reduce protein load. The three signalling branches in the UPR includes the double-stranded RNA-activated protein kinase (PKR)–like ER kinase (PERK), inositol requiring enzyme 1 (IRE1) and activating transcription factor 6 (ATF6). Overall, the three pathways result in reduced overall protein translation elevating protein load in the ER and the transcription of genes that are components of the UPR ERAD pathway.

1.6.3 Role of Activating Transcription Factor 3 in the UPR

ATF3 is a stress response protein downstream of ATF4 within the PERK branch of the UPR (Jiang et al., 2004; Brooks et al., 2014; Rohini et al., 2018). ATF3 expression is rapidly induced by cellular stress with maximal expression seen 4 hours into cerulein treatment (48-fold higher compared to non-injured cells) in pancreatic cells as evident by mRNA and protein expression (Fazio et al., 2017). The *Atf3* gene encodes a 181 amino acid protein with a molecular mass of 21 kDa (Rohini et al., 2018). ATF3 belongs to the family of activating transcription factor/cAMP responsive element binding (ATF/CREB) proteins (Rohini et al., 2018). ATF/CREB proteins are classified as basic leucine zipper (bZIP) transcription factors that can induce or repress transcriptional activity depending on ATF3's binding partner and the gene being targeted (Rohini et al., 2018; Li et al., 2018). Normally truncated forms of ATF3 do exist (ATFΔZip; 135 amino acids), which lack the functional bZIP DNA binding element domain (Jiang et al., 2004; Brooks et al., 2014; Rohini et al., 2018). ATFΔZip has the ability to bind other transcription factors with a bZIP binding element and influence gene expression (Jiang et al., 2004; Brooks et al., 2014; Rohini et al., 2018).

In the conical UPR pathway, PERK activation under cellular stress (Bernales et al., 2006; Maas & Diehl, 2015) signals ATF4 to bind C/EBP-ATF response element (CARE) on the ATF3 promoter inducing transcription (Hai et al., 1999; Eferl & Wagner, 2003). ATF3 along with ATF4 induces *Chop* and *Gadd34* transcription (Jiang et al., 2004; Han & Kaufman, 2017). Overexpression of ATF3 can partially bypass the requirement of PERK activation for the induction of GADD34 as a result of cellular stress (Jiang et al., 2004) indicating that ATF3 can function indirectly to induce gene expression in the absence of PERK activation. Additionally, ATF3 can be activated through the IRE1 branch of the UPR pathway (Liang et al., 1996; Jiang et al., 2004). Phosphorylation of ATF2 and cJUN as a result of cellular stress mediated by IRE1 can activate ATF3 expression downstream (Liang et al., 1996; Jiang et al., 2004). Finally, the ATF6 branch of the UPR pathway is capable of activating ATF3 by binding CARE on the ATF3 promoter (Kowalik et al., 2007). These findings suggest ATF3 is a central mediator of the pathological response to

UPR activation. Therefore, ATF3's role in physiological and stress induced conditions its transcriptional complexes and targets needs to be better understood.

1.6.4 Transcriptional complexes and targets of ATF3

ATF3 can form a wide array of complexes either as a homodimer or a heterodimer (Rohini et al., 2018). ATF3 homodimer or in a complex with other proteins is rapid in inducing or repressing gene transcription upon various stress signals depending on the target gene (Rohini et al., 2018). The expression of ATF3 alone is capable of repressing *Nrf2* expression, which is responsible for regulating genes involved in the regulation of free-radical oxygen species (ROS) (Brown et al., 2008). ATF3 represses *Nrf2* gene transcription by directly binding antioxidant response elements (ARE) in the *Nrf2* promoter (Brown et al., 2008). Furthermore, *Nrf2* repression is significantly more enhanced by TGF-β mediated ATF3 activation (Brown et al., 2008). Secondly, ATF3 can complex with p53 and repress expression of matrix metallopeptidase 2 (MMP2) (Yan et al., 2002). MMP2 is involved in enzymatically cleaving components of the ECM and molecules involved in signal transduction (Yan et al., 2002; Mo et al., 2010). ATF3 also has the ability of complexing with mutated p53 and repressing its oncogenic effects (Mo et al., 2010). Additionally, ATF3 can complex with ATF4 and induce the expression of phorbol-12-myristate-13-acetate-induced protein 1 (PMAIP1) independent of p53 induced PMAIP1 activity to promote apoptotic cell death (Wang et al., 2009).

Along with transcriptional regulation, there is also a role for ATF3 in epigenetic regulation of chromatin remodelling and gene expression (Li et al., 2016; Cui et al., 2015). ATF3 complexed with histone deacetylase 6 (HDAC6) is associated with an increase in chromatin remodelling (Li et al., 2016). Moreover, ATF3 stabilizes and enhances histone acetyltransferase (HAT) activity, which is involved in transferring acetyl groups to lysine residues on histones (Cui et al., 2015).

1.6.5 Role of ATF3 in physiology and pathology

Once induced, ATF3 can affect several signaling pathways including SMAD, ERK, c-Jun N-terminal kinase (JNK), p38 and NF-κB (Hoetzenecker et al., 2012; Anido et al., 2010; Wang & Yan, 2016; Guo et al., 2015). These signalling pathways are primarily utilized by ATF3 to relieve stress by DNA damage repair and cell cycle regulation (Je et al., 2014). In addition, ATF3 can also bind NF-κB and repress the expression of cytokines (IL-6, TLR-4) that are activated and secreted as a result of NF-κB signalling (Dawn et al., 2004; Gilchrist et al., 2006). Further, ATF3 is vital for the migration of neutrophils to areas of injury to mitigate damage in lung tissue (Boespflug et al., 2014). In contrast, in skin tissue, ATF3 is critical for negatively regulating cancer-associated fibroblasts (CAFs) to prevent the excessive deposition of ECM proteins that would otherwise promote carcinogenesis (Kim et al., 2017).

Under pathological conditions ATF3 acts to promote carcinogenesis or cell death in a cell type dependent manner (Thompson et al., 2009; Yin et al., 2010; Wu et al., 2010; Ishiguro et al., 2000). Conflicting roles for ATF3 have been reported for metastatic prostate cancer (Wang et al., 2015; Bandyopadhyay et al., 2006). In mouse models, knock-down of ATF3 promotes more aggressive metastatic prostate cancer (Wang et al., 2015). In contrast, the high expression of ATF3 by androgen stimulation in cell-based models results in the down-regulation of the anti-metastatic gene (Drg1: developmentally regulated GTP binding protein 1) (Bandyopadhyay et al., 2006). Similarly, in breast cancer cell lines and tumours derived from human patient samples, the overexpression of ATF3, as a result of TGF-β signalling, reduces patient survival and promotes tumour development and metastasis (Massagué et al., 2000). Further, ATF3 promotes the expression of runt-related transcription factor 2 (Runx2) in breast cancers allowing for metastasis to the bone marrow (Vishal et al., 2017). Alternatively, in colon and colorectal cancers, ATF3 overexpression reduces cell survival by exerting anti-tumorigenic effects (Song et al., 2016; Kim et al., 2015). In pancreatic cancer, ATF3's role has not yet been examined to date.

1.7 Rationale, hypothesis & objectives

Rationale: PDAC is the most common form of pancreatic cancer with a very low survival rate (James et al. 2018; Koikawa et al. 2018). In addition to oncogenic KRAS activation other genetic and environmental factors are needed for full PDAC progression (Bryant et al., 2014; O'Hagan & Heyer, 2011; James et al., 2018). In a previous study our lab showed ATF3 was upregulated within hours of inducing acute pancreatitis. That study found ATF3 directly regulated the ADM process by recruiting histone deacetylase 5 (HDAC5) to the *Mist1* promoter to repress gene activation (Fazio et al., 2017). In addition, ATF3 was shown to directly bind the *Sox9* promoter to induce gene activation and promote ADM development. It is understood that persistent ADM increases the likelihood of neoplastic transformation which can progress to full blown PDAC (Kopp et al., 2012). Further, the study identified pathways (RAS, MAPK and Wnt signalling) linked to pancreatitis severity that could potentially lead to carcinogenesis (Fazio et al., 2017). Although, this study found a novel role for ATF3 in acute injury, acute pancreatitis is reversible and remains to be a poor predictor of PDAC (Yadav & Lowenfels, 2006). Recurrent forms of pancreatitis that have the potential of developing into CP remains to be the best predictor and susceptibility factor for PDAC development (Yadav & Lowenfels, 2006; Fagenholz et al., 2007; Krishna et al., 2017; Lew et al., 2017). To our knowledge the role of ATF3 has not been studied in recurrent forms of injury nor in the context of oncogenic KRAS, which has the capability of giving rise to PDAC.

Hypothesis: *I hypothesize that* ATF3 *is required for persistent acinar-to-ductal cell metaplasia (ADM) and* pancreatic intraepithelial neoplasia *(PanIN) in recurrent pancreatitis and PDAC*

Objectives:

1. Determine if the absence of ATF3 affects the severity of recurrent pancreatitis.
2. Determine the requirement of ATF3 for the initiation of oncogenic KRAS-induced PDAC.

This thesis will investigate a novel role for ATF3 in recurrent pancreatitis. It will allow me to determine if ATF3 has a role in recurrent pancreatitis susceptibility or affect on pancreatic tissue regeneration. Additionally, this thesis will allow me to determine if oncogenic KRAS bypasses the need for ATF3 in PDAC progression.

CHAPTER 2

2 METHODS

2.1 Mouse Models

All experiments carried out with mice were approved and handled according to regulations by the Animal Care and Use Committee at the University of Western Ontario (protocol #2017-001). Male and female C57/bl6 mice carrying a germline deletion for *Atf3* (*Atf3*$^{-/-}$) as described by Hartman et al., 2004 were used for recurrent pancreatitis studies and compared to C57/bl6 wild-type mice (*Atf3*$^{+/+}$) at ages ranging from two-to-four months. In addition, *Atf3*$^{-/-}$ mice were bred with mice carrying *CreERT* targeted to a *Ptf1a* allele (*Ptf1a*$^{creERT/+}$). *Ptf1a* is an acinar cell-specific gene and *creERT* allows inducible deletion through the cre-LoxP system when tamoxifen is present. *Atf3*$^{-/-}$ *Ptf1a*$^{creERT/+}$ mice were crossed to mice carrying a constitutively active *Kras* gene (KRAS^{G12D}) preceded by *loxP* sites flanking a stop codon (*loxP-stop-loxP*; *LSL*) and targeted to the *Kras* allele (*Kras*$^{LSL\text{-}G12D/+}$). Mice lacking *Atf3* with *Ptf1a*$^{creERT/+}$ and *Kras*$^{LSL\text{-}G12D/+}$ (*Atf3*$^{-/-}$*; Ptf1a*$^{creERT/+}$*; Kras*$^{LSL\text{-}G12D/+}$) were experimentally treated and compared to *Atf3*$^{+/+}$ (*Atf3*$^{+/+}$*; Ptf1a*$^{creERT/+}$*; Kras*$^{LSL\text{-}G12D/+}$) mice. Mice lacking oncogenic *Kras* with *Ptf1a*$^{CreERT/+}$ in the presence (*Atf3*$^{+/+}$*; Ptf1a*$^{CreERT/+}$) or absence of *Atf3* (*Atf3*$^{-/-}$*; Ptf1a*$^{CreERT/+}$) were used as controls to determine if loss of one *Ptf1a* allele affected pancreatic morphology and function. A yellow fluorescent protein (*Yfp*) knocked into the *Rosa26R* (*Rosa26R*$^{YFP/+}$) allele was also bred into this line for lineage tracing origin of lesions. Genotypes were confirmed before and after experimentation using the primers indicated in **Table 2.1**.

2.2 Cerulein Induced Pancreatitis (CIP)

Mice were given normal chow and water *ad libitum* throughout the experiment. To induce recurrent pancreatitis, *Atf3*$^{-/-}$ and *Atf3*$^{+/+}$ mice received intraperitoneal injections of ceruelin (250 µg/kg body weight; Sigma; Cat. #17650-98-5; St. Louis, MO) or 0.9% saline (control) at 9 AM and 3 PM daily (n = 5-6 per genotype/treatment for both time points). Cerulein is a CCK analog (Aghdassi et al., 2011). Mice were weighed daily to determine changes in body weight. 14 days after initiating pancreatitis, cerulein injections were stopped. Mice were euthanized one or seven days after the last set of injections. Pancreatic weight (g) was determined post mortem and compared to total body weight.

Table 2.1: DNA primers used for genotyping mice

Gene	Forward	Reverse	Common
Atf3	5' - TGAAGAAGGTAAACA CACCGTG	5' - ATCAGCCAGCCTCTGTT CCAC	5' - AGAGCTTCAGCAATG GTTTGC
LSL-Kras^{G12D}	5' - GTCTTTCCCCAGCACA GTGC	5' - CTCTTGCCTACGCCACC AGCTC	5' - AGCTAGCCACCATGG CTTGAGTAAGTCTGCA
P48^{CreERT}	5' - TCGCGATTATCTTCTA TATCTTCAG	5' - GCTCGACCAGTTTAGTT ACCC	
Rosa26R	5' - GGAGCGGGAGAAATG GATATG	5' - GCGAAGAGTTTGTCCTC AACC	5' - AAAGTCGCTCTGAGTT GTTAT
Yfp	5' - ACATGGTCCTGCTGGA GTTC	5' - GCGATGCAATTTCCTCA TTT	

To activate *creERT* and promote *Kras*^{G12D} expression mice received an oral gavage of tamoxifen (5 mg/day; Sigma-Aldrich; Cat. #10540-29-1) for 5 days. This produces cre-recombination efficiency >95% (Roy et al., 2016). Mice were allowed to rest for 7 days to recover from the tamoxifen treatment. On days 13 and 15 mice were administered

cerulein (I.P. injection; 50 μg/kg) 8 times over 7 hours (n = 3-10 per genotype/treatment at both time points). Mice were weighed to monitor overall health. If body weight dropped below 15% of their starting weight, mice were sacrificed. Mice were sacrificed either two or five weeks after cerulein administration and pancreatic tissue collected and weighed.

2.3 Tissue Fixation & Histology

Pancreatic tissue from the head and tail of the pancreas was harvested, rinsed in PBS and fixed in 4% formaldehyde in PBS overnight at 4°C. Tissue samples were washed in PBS for 24 h at 4°C post fixation, then dehydrated and embedded in paraffin. Tissue was sectioned at 5 μm using a HM325 Rotary Microtome (ThermoFisher Scientific) and sections rehydrated prior to staining protocols.

To assess histologically and identify differences in pancreatic tissue architecture, sections were stained with H&E and analyzed. Early neoplastic lesions (ADM) were classified based on flat cuboidal tubular complexes surrounded by fibrosis and inflammation. Progressive lesions (PanINs) were graded based on nuclear irregularities, mucinous epithelium, and dense areas of fibrosis and inflammation surrounding PanIN lesions. In addition, specific ductal and transcription markers were further used to identity lesions from healthy tissue.

To assess fibrosis, paraffin sections were stained using a standard Mason's Trichrome stain (ab150686; Abcam Inc.). The area staining blue (fibrosis) was identified and quantified using ImageJ as a percent of total tissue area. Secondly, mucin accumulation was visualized using an Alcian Blue stain kit (ab150662; Abcam Inc.). The kit targets all variants of the mucin protein. The total area of blue staining was taken as a percentage of the whole tissue area.

In all cases, 10-15 images were taken for each sample and from multiple sections that were at least 200 μm apart using an Aperio CS2 Digital Scanner and Aperio ImageScope

software (Leica Biosystems Imaging Inc, San Diego, CA, USA) and Leica Microscope DM5500B (Leica Microsystems, Wetzlar, Germany) with LAS V4.4 software.

To assess recombination efficiency through YFP detection, tissue was fixed in 4% methanol-free paraformaldehyde for 2 h and incubated at 4°C. Following PBS washes post fixation, samples were incubated in 30% sucrose overnight at 4°C. Pancreatic tissue was embedded in cryomatrix (ThermoFisher Scientific) and stored at -80°C for sectioning. Frozen blocks were allowed to climatize to the cryostat chamber and sectioned to 6 µm using a Shandon cryostat (ThermoFisher Scientific). YFP expression was determined by fixing sections with 4% paraformaldehyde. YFP expression was determined natively without the use of immunostaining. The percent of YFP expression was determine by calculating the total area positive for YFP over the total tissue area. Images (8-10 per tissue) were obtained with a Leica Microscope DM5500B DFC365 FX camera and used for analysis and quantification.

2.4 Immunohistochemistry & Immunofluorescence

Immunohistochemistry (IHC) was performed on paraffin embedded sections using a Vectastain ABC HRP kit. Sections were rehydrated and then incubated in PBS for 5 minutes before being immersed in working solution (0.1 M Citric Acid Monohydrate, 0.1 M sodium citrate dehydrate in dH_2O). For antigen retrieval, sections were heated in a rice cooker for 45 minutes and cooled to room temperature, then immersed in H_2O_2 in methanol for 10 minutes to reduce endogenous peroxidase activity. Sections were permeabilized with 0.2% Triton-X in PBS for 12 minutes at RT, washed with 0.2% Tween-20 in PBS, then blocked in 5% sheep serum in PBS for 1 hour at room temperature. Blocking solution was removed and samples covered in primary antibody diluted in 5% sheep serum in PBS and incubated overnight at 4°C. Primary antibodies used included PDX1 (1:1000; Abcam Inc. Cambridge, MA), amylase (1:600; Abcam Inc.), CK19 (1:500; Abcam Inc.) and MIST1 (1:500; Pin et al., 2000). The next day, sections were washed in PBS 4X for 5 minutes, then incubated in biotinylated mouse anti-rabbit IgG secondary antibody (1:1000 dilution in 5% sheep serum) for 30 minutes at

room temperature. Secondary antibody was removed, and sections washed with PBS 4X. Sections were incubated in AB reagent for 30 minutes at room temperature. AB reagent was washed off and ImmPACT DAB Peroxidase (HRP) substrate (Vector Laboratories, Cat. #PK-4001/SK-4105) used for detection of HRP. DAB substrate was left on sections until reaction was complete based on visualization with a light microscope. To stop the DAB reaction, sections were immersed in dH_2O. Slides were counterstained with hematoxylin for 7 seconds and washed with dH_2O for 1 minute. Counterstained slides were dehydrated in increasing ethanol concentration before being incubated in xylene. Slides were covered with permount and coverslip and imaged using Leica Microscope DM5500B (Leica Microsystems) and LAS V4.4 software.

Immunofluorescence analysis (IF) was performed on paraffin embedded tissue sections similar to the IHC. The same IHC protocol was followed with the exception of the H_2O_2 in methanol step. Primary antibodies used included: SOX9 (rabbit, 1:250; Millipore Sigma), Ki67 (rabbit, 1:250; Abcam Inc.) and F4/80 (rat, 1:200; Abcam Inc.). Slides were washed 4 times for 10 minutes and immersed in secondary antibody conjugated to a TRITC (1:300; Jackson ImmunoResearch, West Grove, PA) or FITC (1:300; Jackson ImmunoResearch) fluorophore protein for 1 hour at room temperature. Secondary antibody was removed, and sections washed 4X times with PBS and then in DAPI (diluted 1:1000 in PBS; Thermo Fisher Scientific) for 5 minutes at room temperature. DAPI was removed, slides mounted with Vectashield Permafluor mountant (Thermo Fisher Scientific) and imaged using Leica DFC365 FX camera on the Leica DM5500B microscope. Images were taken on Leica LAS V4.4 software.

2.5 Protein Isolation & Immunoblots

Pancreatic tissue was taken from the middle portion of the pancreas and flash frozen in liquid nitrogen and stored at -80°C. Samples were homogenized in protein isolation buffer on ice. Protein isolation buffer consisted of 5 mM $MgCl_2$, 50 mM Tris pH 7.2, 10 mM DTT, 1 mM $CaCl_2$, 1% NP-40, RNAse A (50 µg/ml), DNAse (100 units/ml), 1 mM PMSF, 30 mM NaF, 2 mM Na_3VO_4 and 5 µg/ml of each protease inhibitors: leupeptin,

aprotinin and pepstatin. Samples were kept on ice and sonicated for 20 seconds and centrifuged at 5000 x g for 5 minutes at 4°C. The supernatant was collected, and the pellet discarded. Protein concentration was determined using Bradford Assay dye (BioRad, Mississauga, ON) as per manufacturer's instructions.

Loading dye was added to either 2 μg (for amylase analysis) or 40 μg of protein (SOX9, pERK and αSMA) and incubated at 95°C for 5 minutes. Denatured protein samples were resolved by a 12% SDS-PAGE at 200 volts and transferred to PVDF membrane (200 mV, 90 minutes). Following transfer, blots were incubated in 5% NFDM for 1 hour at room temperature. Blots were washed once in TBS, then incubated in primary antibodies diluted in 0.1% TBST with 5% BSA. Primary antibodies included rabbit anti-phosphorylated ERK (diluted 1:500) and rabbit anti-total ERK (1:500) (Cell Signaling Technology, Danvers, MA). In some instances, primary antibody was incubated in 5% NFDM overnight at 4°C (rabbit anti-amylase [1;1000]; rabbit anti-SOX9 [1:500]; rabbit anti-αSMA [1:500]), in which case TBS washes after blocking were omitted. Following primary antibody incubation, blots were washed 4 x 5 minutes with TBS, then incubated in secondary antibody (anti-rabbit HRP, diluted 1:10,000 in 5% NFDM; Jackson Labs) for 1 hour at room temperature. Blots were washed 4 times with TBS, then incubated in Western ECL (Bio-Rad) substrate for 1 minute before being imaged on a VersaDoc system with Quantity One analysis software (Bio-Rad). Blots were quantified using densitometry on ImageJ and normalized to tERK expression.

2.6 Statistical Analysis

Data was analyzed using a Student's t-test (unpaired, two-tailed), one-way ANOVA or two-way ANOVA with a Tukey's post hoc test on GraphPad Prism 6 software. Statistics used for weight loss over time was a repeated measures two-way ANOVA with a Tukey's post hoc test. Data is shown with individual samples and error bars representing the mean ± standard error (SE). P value <0.05 was considered significant.

CHAPTER 3

3 RESULTS

3.1 The absence of ATF3 reduces ADM and improves tissue regeneration in mice undergoing recurrent pancreatic injury

To determine if ATF3 was required for change in cell differentiation in response to pancreatic injury, a cohort of wild type and *Atf3*$^{-/-}$ mice were subjected to recurrent pancreatitis (RP) using CIP for two-weeks (14 days). Pancreatic tissue was collected on days one and seven following cessation of cerulein treatment to assess tissue damage and regeneration **(Figure 3.1A)**. The percent change in body weight in WT and *Atf3*$^{-/-}$ mice after undergoing RP showed no significant difference between WT and *Atf3*$^{-/-}$ genotypes. However, both genotypes undergoing RP showed significant weight loss compared to saline treated genotypes **(Figure 3.1B)**. Upon dissection one day after cerulein cessation, WT and *Atf3*$^{-/-}$ mice had significantly smaller pancreata compared to saline treated mice **(Figure 3.2A)**. However, no difference in percent pancreatic weight relative to body weight was seen between WT and *Atf3*$^{-/-}$ CIP treated mice at this time point. Seven days after post RP recovery, CIP-treated *Atf3*$^{-/-}$ mice had a significantly higher percent P.W./B.W. ratio compared to CIP-treated WT mice **(Figure 3.2A)**. In fact, percent *Atf3*$^{-/-}$ CIP P.W./B.W. ratios were statistically similar to saline treated *Atf3*$^{-/-}$ pancreatic weight seven days after the cessation of cerulein treatment. In contrast, WT CIP treated pancreata remained small compared to WT saline treated mice after recovery.

To determine the extent of injury in WT and *Atf3*$^{-/-}$ mice, pancreatic tissue sections were assessed by histological staining. H&E staining of pancreatic tissue from WT and *Atf3*$^{-/-}$ CIP-treated mice revealed significantly more putative ADM (based on cuboidal morphology of cells) compared to saline treated mice one- and seven-day following CIP **(Figure 3.2B and C)**. No significant differences in the number of putative ADM per unit area was seen between WT and *Atf3*$^{-/-}$ CIP treated mice on day one; however,

significantly fewer putative ADM was observed in CIP-treated *Atf3*$^{-/-}$ mice compared to CIP-treated WT mice seven days into recovery **(Figure 3.2C)**. Next, the severity of fibrosis was determined using Mason's Trichrome stain. No significant differences in fibrosis area was seen between the genotypes one or seven days after CIP treatment **(Figure 3.3)**, although overall fibrosis was reduced by day seven compared to day one in both genotypes.

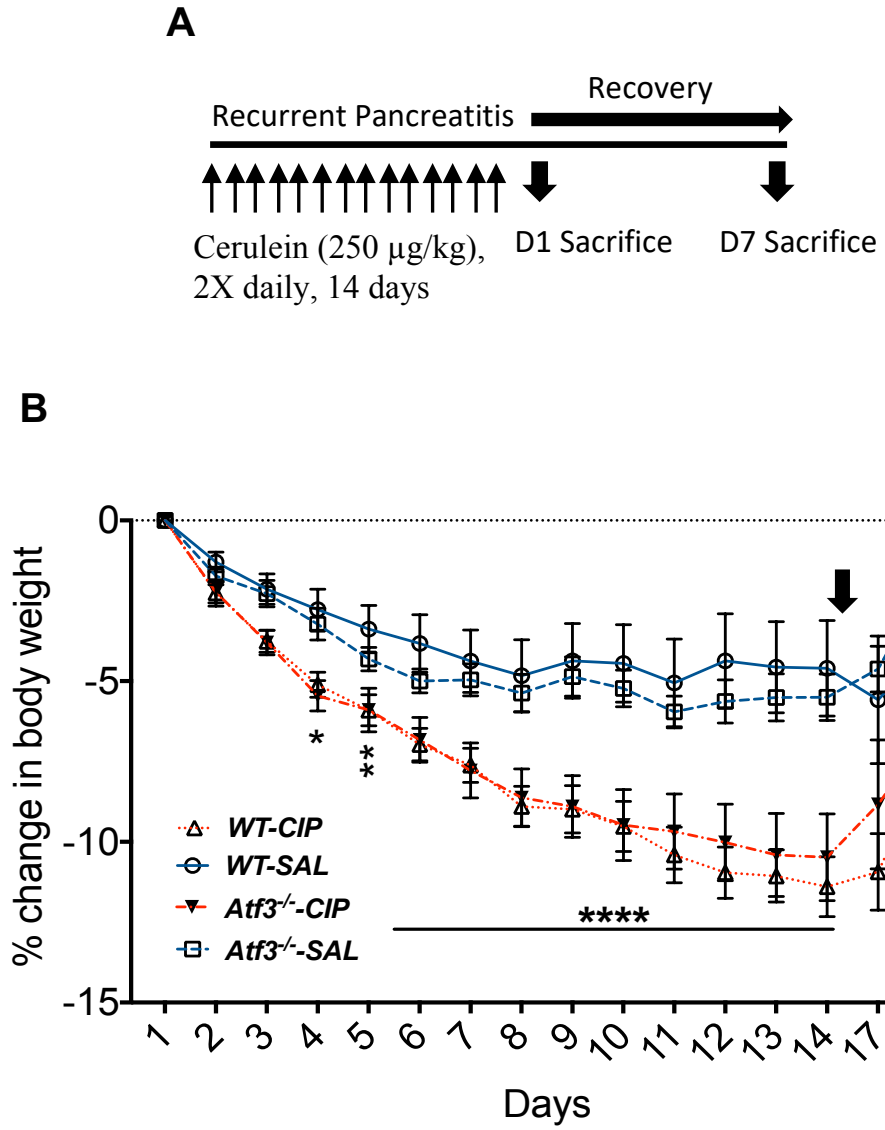
A
Recurrent Pancreatitis
Recovery
Cerulein (250 µg/kg),
2X daily, 14 days
D1 Sacrifice
D7 Sacrifice
B
% change in body weight
0
-5
-10
-15
WT-CIP
WT-SAL
Atf3-/--CIP
Atf3-/--SAL
*
**
****
1
2
3
4
5
6
7
8
9
10
11
12
13
14
17
21
Days

Figure 3.1. *Atf3*$^{-/-}$ mice show no significant difference in body weight compared to WT mice undergoing RP. (A) A schematic timeline showing the treatment regimen used and the dates when mice were sacrificed. **(B)** Both WT and *Atf3*$^{-/-}$ mice (n = 11-21) that received cerulein lost significant body weight compared to mice that received saline (*P<0.05, **P<0.005, ****P<0.0001) starting from day 4 to day 14. However, no significant difference in body weight was seen between the genotypes in the cerulein treated group (P>0.05). The black arrows indicate when mice were sacrificed. The error bars represent mean ± SE; A repeated measures Two-way ANOVA with a Tukey's post hoc test was performed.

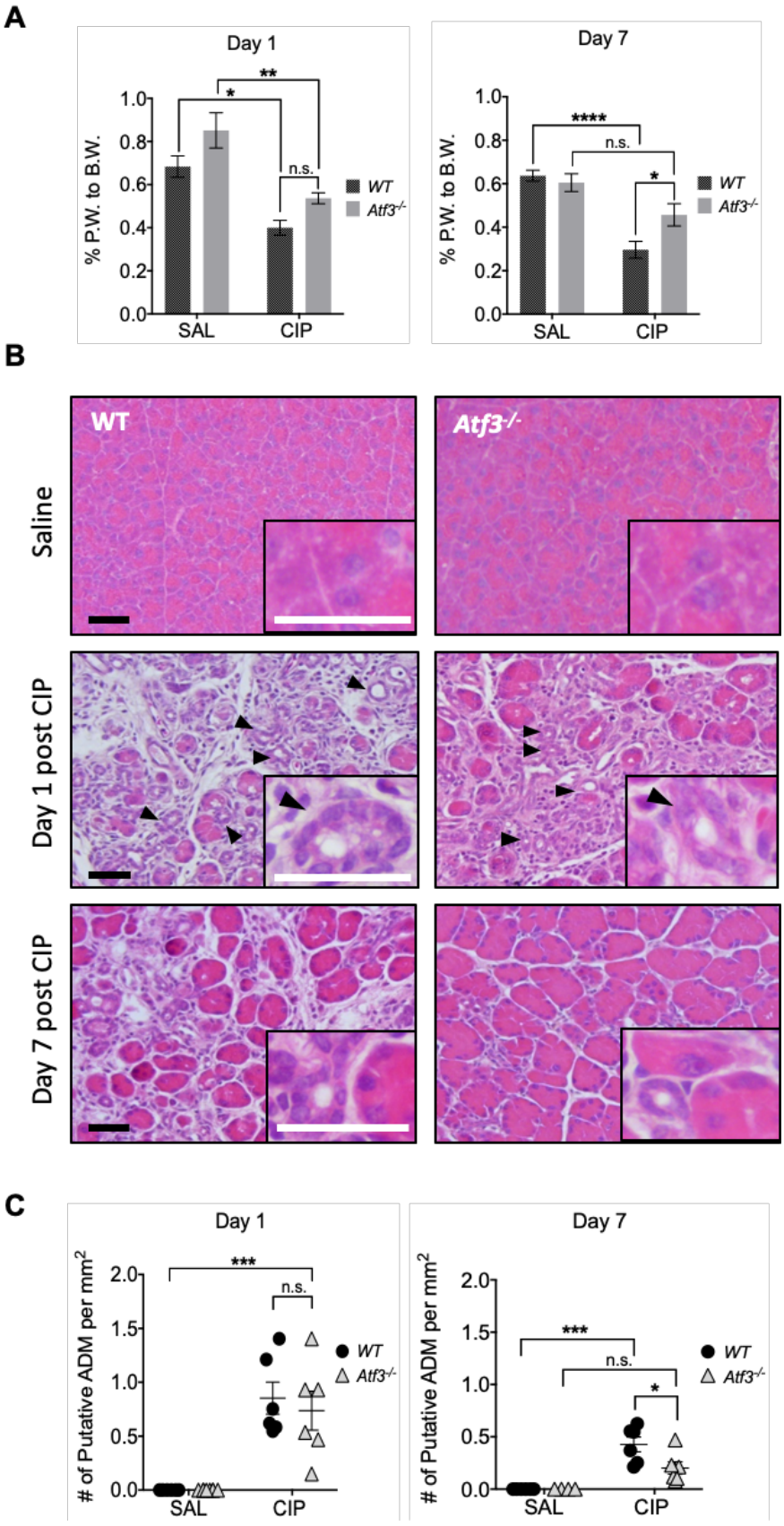
A
Day 1
Day 7
% P.W. to B.W.
1.0
0.8
0.6
0.4
0.2
0.0
*
**
n.s.
****
SAL
CIP
WT
Atf3-/-
B
WT
Atf3-/-
Saline
Day 1 post CIP
Day 7 post CIP
C
Day 1
Day 7
# of Putative ADM per mm2
2.0
1.5
1.0
0.5
0.0
***
n.s.
*
SAL
CIP
WT
Atf3-/-

Figure 3.2. *Atf3*$^{-/-}$ mice show pancreatic tissue regeneration and a lower putative ADM count after the cessation of RP. **(A)** Percent pancreatic weight relative to body weight. On day one post RP, there was a significant decrease in pancreatic weight in both genotypes treated with cerulein compared to the genotypes receiving saline (WT; *P<0.05, *Atf3*$^{-/-}$; **P<0.005; n = 6-7). No significant difference in pancreatic weight was seen between the genotypes in the cerulein treated group after the immediate cessation of RP. Following seven days of RP cessation, *Atf3*$^{-/-}$ mice showed a significant increase in pancreatic weight compared to WT mice (*P<0.05). However, WT CIP pancreata remained small compared to WT saline treated tissue (****P<0.0001) while tissue lacking ATF3 was comparable in pancreatic weight to *Atf3*$^{-/-}$ saline treated tissue (P>0.05; n = 4-6; % mean ± SE shown). **(B)** Representative H&E shows loss of healthy acinar tissue in both genotypes and a significant increase in putative ADM one day after RP in both genotypes, black arrowhead points to putative ADM. **(C)** There was significantly less putative ADM in *Atf3*$^{-/-}$ mice after seven days of RP compared to WT mice in the CIP group (*P<0.05; n = 4-6; mean ± SE shown). The black bar represents 200 μm while the white bar represents 50 μm. A two-way ANOVA with a Tukey's post hoc test was performed.

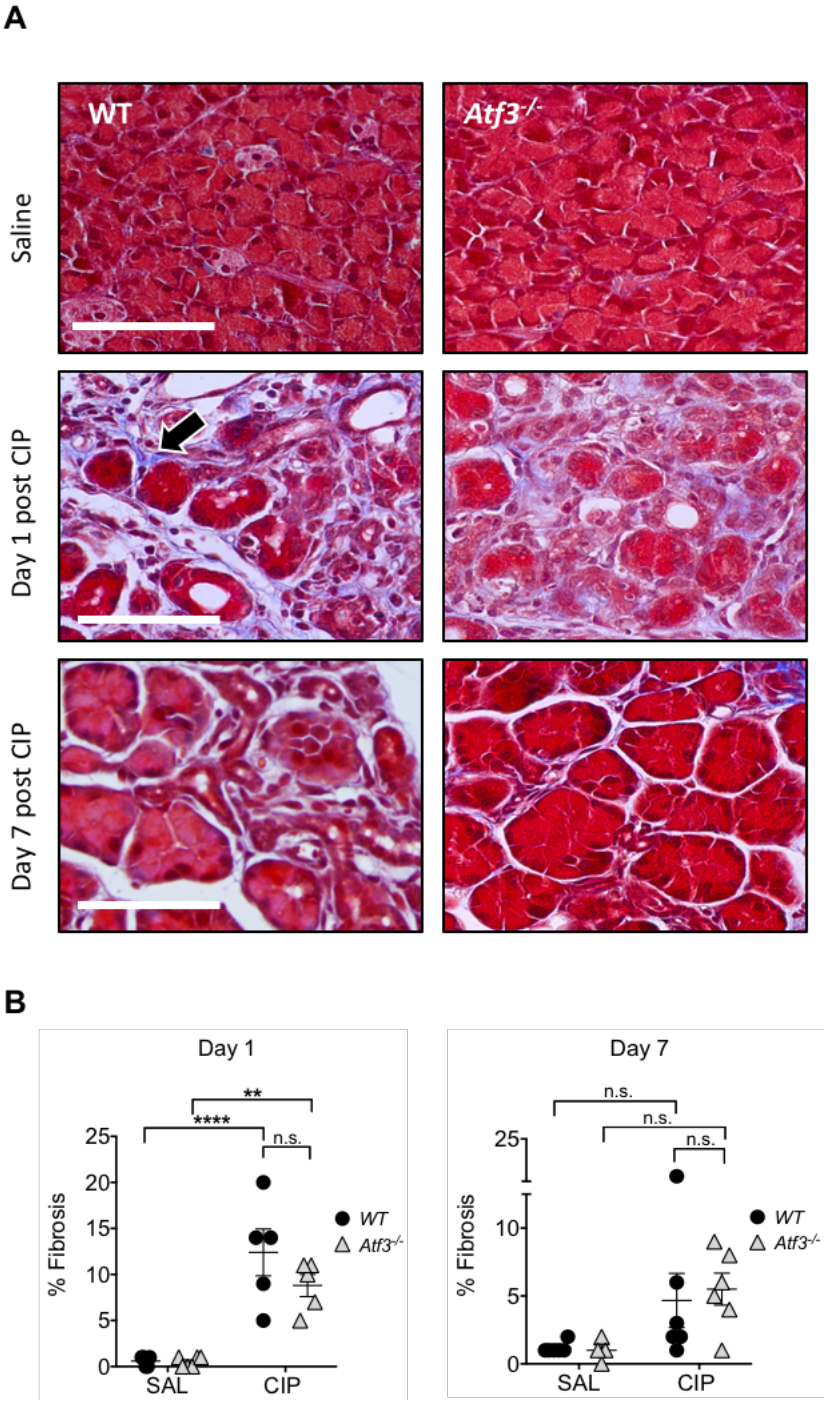
A
WT
Atf3-/-
Saline
Day 1 post CIP
Day 7 post CIP
B
Day 1
**
****
n.s.
% Fibrosis
25
20
15
10
5
0
SAL
CIP
WT
Atf3-/-
Day 7
n.s.
n.s.
n.s.
% Fibrosis
25
10
5
0
SAL
CIP
WT
Atf3-/-

Figure 3.3. The absence of ATF3 does not alter fibrosis. (A) Representative images showing Mason's Trichrome stain used to detect collagen as a measure of fibrosis (black arrow points to collagen deposits; n = 4-6). **(B)** RP induced significant fibrosis one-day post injury cessation in both genotypes compared to saline treated mice (*Atf3*$^{-/-}$; **P<0.005, WT; ****P<0.0001). No significant difference in fibrosis was seen between WT and *Atf3*$^{-/-}$ CIP treated mice on day one post CIP. Following seven days of recovery, percent fibrosis was comparable between saline and CIP treated groups. The white bars represent 50 µm. % mean ± SE shown. A two-way ANOVA with a Tukey's post hoc test was performed.

Histological (H&E) analysis suggested *Atf3*$^{-/-}$ mice have greater tissue regeneration in response to recovery post RP. This was further supported by molecular markers of ADM. Immunohistochemistry staining for CK19, a marker of ductal cells, showed significantly more CK19^{+} cells in WT mice compared to *Atf3*$^{-/-}$ mice both one **(Figure 3.4A and B)** and seven days following CIP treatment. Analysis for amylase, a marker of acinar cells, showed no difference one day post recovery, but was significantly higher in *Atf3*$^{-/-}$ mice compared to WT mice after seven days of recovery based on IHC **(Figure 3.4C)** and immunoblotting **(Figure 3.4D and E)**. The expression of amylase protein was 2.4 ± 1.76-fold higher in *Atf3*$^{-/-}$ tissue compared to WT tissue after seven days of recovery post RP **(Figure 3.4E)**.

To better understand the ADM process in RP and recovery, specific transcription factors involved in the ADM development program were examined by IHC and IF. MIST1 is a transcription factor that is needed to maintain the mature acinar cell phenotype (Pin, et al., 2001). IHC revealed significantly more MIST1^{+} nuclei (black arrowhead) in *Atf3*$^{-/-}$ tissue compared to WT tissue one day following cessation of RP **(Figure 3.5A and B)**. In addition, many putative ADM lesions in *Atf3*$^{-/-}$ tissue expressed MIST1 (white arrowhead) while putative ADM lesions seen in WT tissue were found to be MIST1 negative. Seven days following recovery, no significant differences in MIST1 expression was seen between cerulein treated *Atf3*$^{-/-}$ and WT mice **(Figure 3.5A and B)**. To determine if transcription factors involved in ADM formation and maintenance was affected in the absence of ATF3 we evaluated SOX9 and PDX1 expression (Kopp et al., 2011; Roy et al., 2016). Immunoblotting for SOX9 showed no detectable protein expression in *Atf3*$^{-/-}$ tissue one or seven days following CIP **(Figure 3.5C)**. IF analysis confirmed significantly fewer SOX9^{+} cells at both time points **(Figure 3.5 D and E)**. Similar to SOX9 expression, PDX1 was expressed in significantly fewer ADM and acinar cells in *Atf3*$^{-/-}$ tissue compared to WT tissue **(Figure 3.5 F and G)**.

To determine if cellular proliferation was also affected in the absence of ATF3, Ki67 immunofluorescence was performed (**Figure 3.6**). The percent Ki67^{+} cells were significantly higher in *Atf3*$^{-/-}$ tissue one day after the cessation of RP compared to WT

mice that underwent RP (**Figure 3.6B).** Following seven days of recovery there was a significant reduction in proliferation in *Atf3*$^{-/-}$ tissue compared to WT tissue.

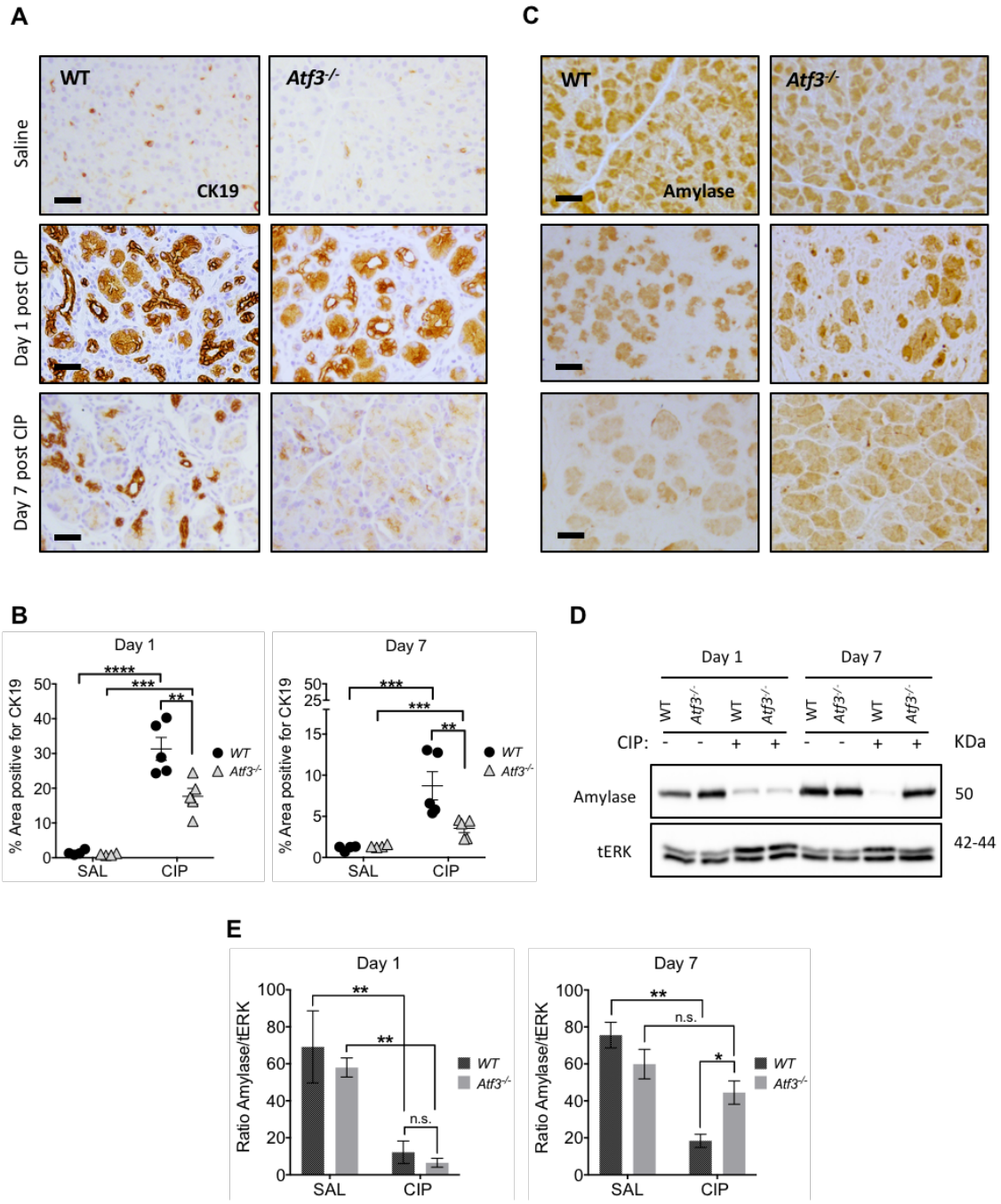
A
WT
Atf3-/-
CK19
Saline
Day 1 post CIP
Day 7 post CIP
C
Amylase
B
Day 1
Day 7
% Area positive for CK19
SAL
CIP
WT
Atf3-/-
D
CIP:
KDa
Amylase
tERK
50
42-44
E
Ratio Amylase/tERK
n.s.

Figure 3.4. *Atf3*$^{-/-}$ tissue shows reduced duct marker staining and increased digestive enzyme accumulation. (A) IHC for the duct marker CK19 shows a reduction in cytoplasmic staining in the absence of ATF3 compared to WT tissue at both days one and seven post CIP. **(B)** Quantification of representative IHC images for CK19 confirms a significant reduction in percent area staining for CK19 in *Atf3*$^{-/-}$ tissue compared to WT tissue at both experimental time points (**P<0.005; n = 4-5; % mean ± SE; a two-way ANOVA with a Tukey's post hoc test was performed). **(C)** Representative IHC for amylase shows enzyme accumulation seven days following recovery in *Atf3*$^{-/-}$ tissue compared to WT tissue. **(D)** Representative Western blot shows increased amylase protein accumulation in the *Atf3*$^{-/-}$ tissue compared to WT tissue following seven days of recovery. **(E)** Relative protein expression was quantified using densitometry and normalized to tERK expression. Significantly more amylase accumulation was observed in the absence of ATF3 compared with WT tissue on day seven following RP (*Atf3*$^{-/-}$; *P<0.05; n = 4-6; mean ± SE; a two-way ANOVA with a Tukey's post hoc test was performed).

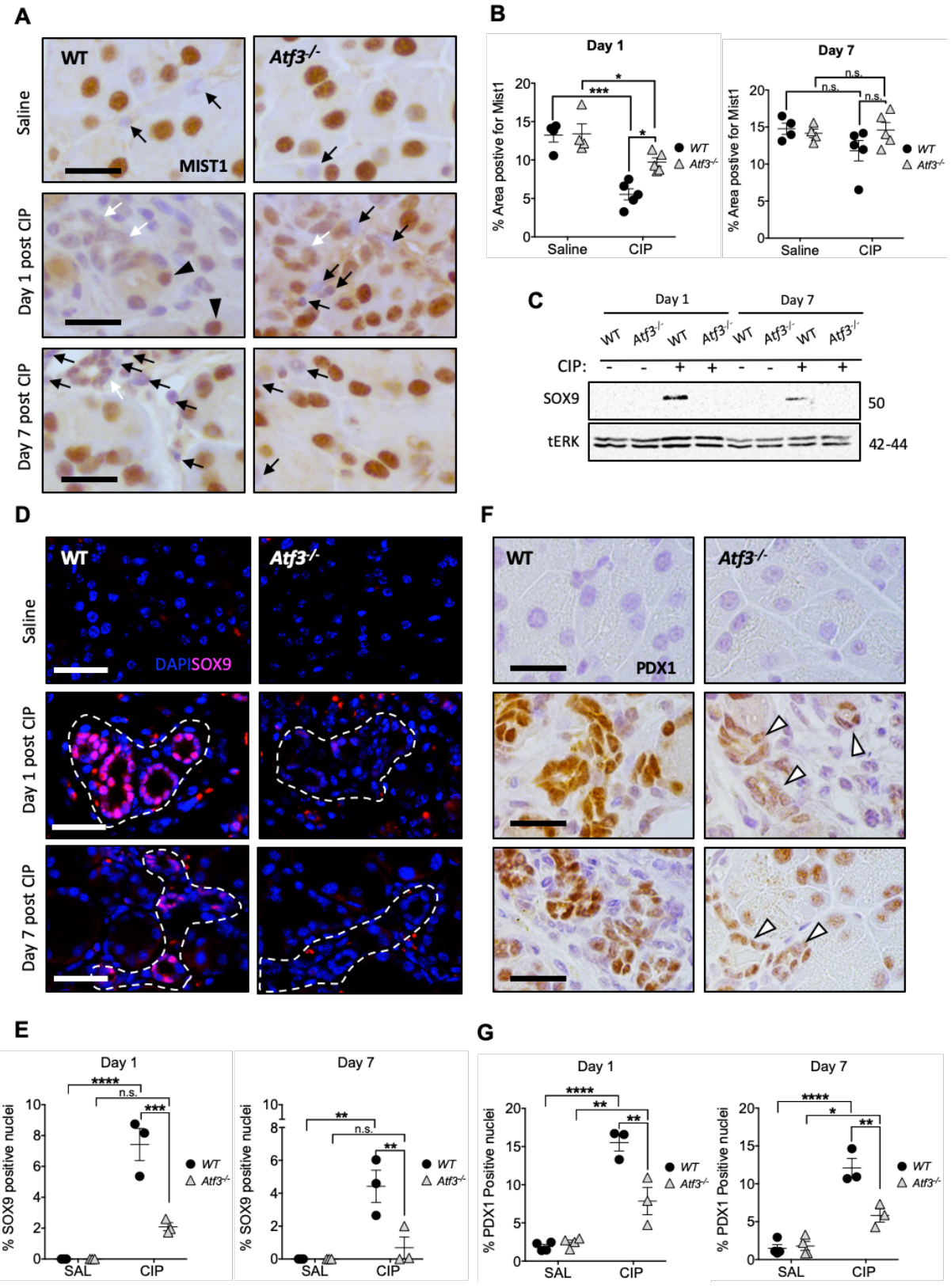
A
WT
Atf3-/-
Saline
Day 1 post CIP
Day 7 post CIP
MIST1
B
Day 1
Day 7
% Area postive for Mist1
WT
Atf3-/-
Saline
CIP
n.s.
C
Day 1
Day 7
CIP:
SOX9
tERK
50
42-44
D
DAPI SOX9
F
PDX1
E
% SOX9 positive nuclei
SAL
G
% PDX1 Positive nuclei

Figure 3.5. ATF3 affects the expression of transcription factors involved in ADM during RP. **(A)** The expression of MIST1 (IHC) was maintained one-day post cessation of injury in *Atf3*$^{-/-}$ tissue compared to WT. The expression of MIST1 in both WT and *Atf3*$^{-/-}$ cerulein treated tissue was comparable to the saline treated genotypes by day seven post recovery. Black arrows point to MIST1 negative nuclei. White arrows point to putative ADM. Black arrowheads point to MIST1 positive nuclei. **(B)** Quantification of MIST1 supported this finding (day one: *Atf3*$^{-/-}$; *P<0.05, WT; ***P<0.005, day seven: P>0.05, n = 4-5; % mean ± SE; a two-way ANOVA with a Tukey's post hoc test was performed). **(C)** Representative Western blot shows no SOX9 protein expression in *Atf3*$^{-/-}$ tissue at both experimental time points compared to WT tissue. **(D)** Representative IF images confirm findings seen in Western blot and show fewer SOX9 positive nuclei in *Atf3*$^{-/-}$ tissue at both time points (outlined by white dashes). **(E)** Quantification of representative IF images confirm a reduction in the percent of nuclei positive for SOX9 in the absence of ATF3 at both time points (**P<0.005; ***P<0.0005; n = 3; % mean ± SE; a two-way ANOVA with a Tukey's post hoc test was performed). Similarly, the percent of nuclear PDX1 staining was significantly reduced in the *Atf3*$^{-/-}$ tissue at both time points (**F, G**; **P<0.005; n = 3; % mean ± SE; a two-way ANOVA with a Tukey's post hoc test was performed). White arrowheads point to PDX1 positive nuclei, both black and white bars represent 50 μm.

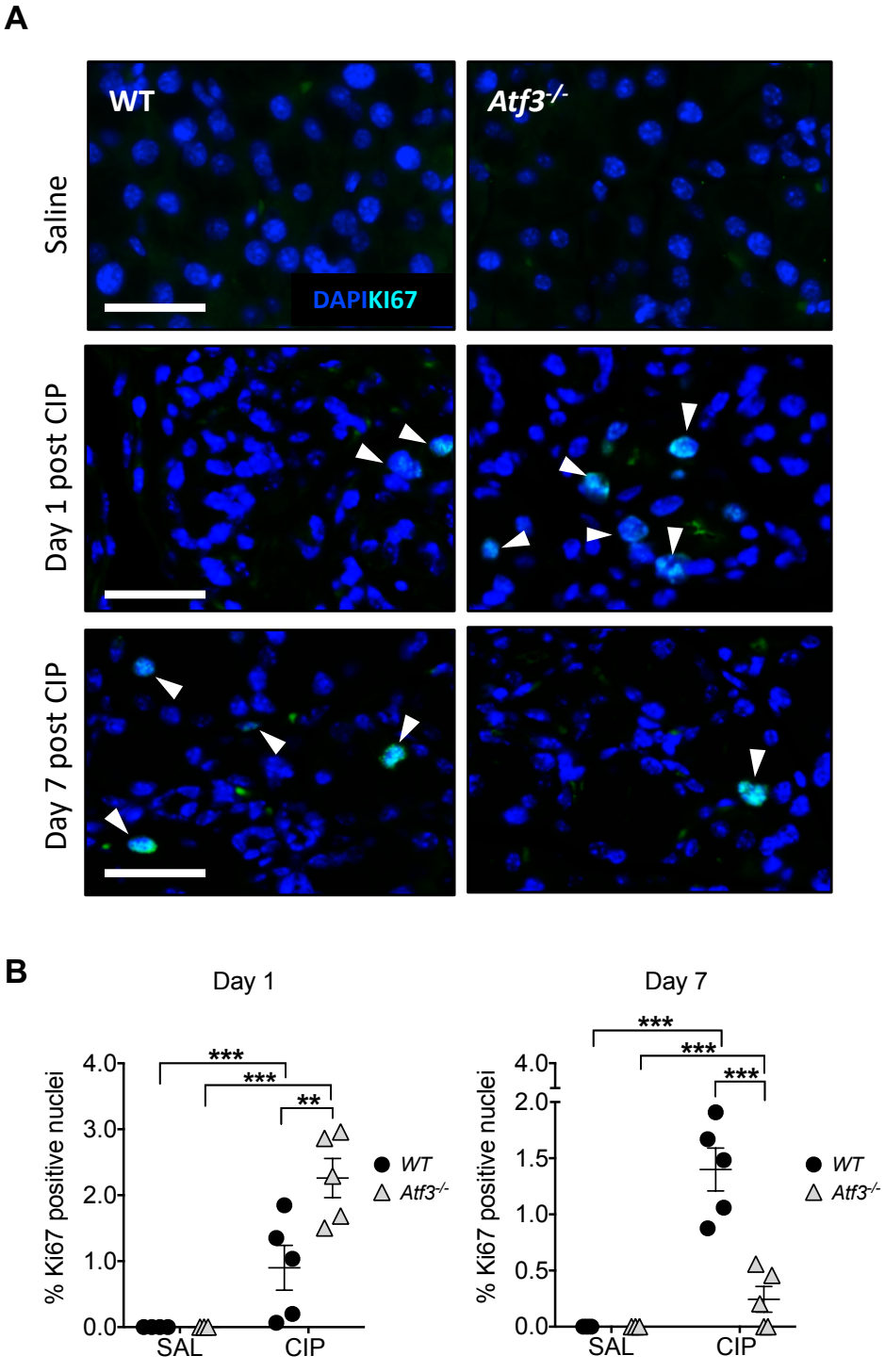
A
WT
Atf3-/-
Saline
DAPIKI67
Day 1 post CIP
Day 7 post CIP
B
Day 1
Day 7
% Ki67 positive nuclei
4.0
3.0
2.0
1.0
0.0
***
***
**
SAL
CIP
WT
Atf3-/-
2.0
1.5
1.0
0.5

Figure 3.6. Proliferation is altered during RP in the absence of ATF3. (A) Representative IF images show significantly more percent positive nuclei for Ki67 in the absence of ATF3 one-day post CIP. After seven days of post CIP recovery the percent of nuclear staining was reduced in the absence of ATF3. White arrowheads represent Ki67 positive nuclei. **(B)** There was a significant increase in the number of positive nuclei for Ki67 in *Atf3*$^{-/-}$ tissue on day one compared to WT tissue (**P<0.005). On day seven, the percent of Ki67 positive nuclei was significantly reduced in the absence of ATF3 compared to WT tissue (***P<0.0005; n=4-5). Error bars represent mean ± SE; a two-way ANOVA with a Tukey's post hoc test was performed). White bars represent 50 μm.

3.2 Mice lacking ATF3 show reduced high grade PanIN lesions following the activation of oncogenic KRAS

My analysis of *Atf3*$^{-/-}$ mice indicated that ATF3 is required for ADM in recurrent pancreatitis suggesting it may also be required for ADM associated with initial stages of PDAC. However, it is possible that oncogenic KRAS can bypass this requirement. To answer this question *Atf3*$^{-/-}$ mice allowing for inducible activation of constitutive KRAS were used following the induction of cerulein-induced pancreatitis (*Atf3*$^{-/-}$*; Ptf1a*$^{creERT/+}$*; Kras*$^{LSL\text{-}G12D/+}$) **(Figure 3.7A)**. CreERT driven by *Ptf1a* was activated specifically in acinar cells by tamoxifen administration which led to oncogenic *Kras* activation. Following oncogenic *Kras* activation, mice underwent acute CIP to induce *Atf3* expression. Tissue was collected at weeks two and five post injury **(Figure 3.7B)**. The reporter gene YFP was also bred into *Atf3*$^{-/-}$*; Ptf1a*$^{creERT/+}$*; Kras*$^{LSL\text{-}G12D/+}$ line and indicated extensive cre-recombination (97.98 ± 0.17% creERT-efficiency) had taken place in acinar cells following treatment with tamoxifen **(Figure 3.7C)**. During TX treatment and acute CIP, mice were weighed daily. All saline-treated mice, regardless of ATF3 expression or oncogenic KRAS activity gained body weight over the experimental time period **(Figure 3.8A)**. However, *Atf3*$^{-/-}$*; Ptf1a*$^{creERT/+}$*; Kras*$^{LSL\text{-}G12D/+}$ mice that underwent CIP had a significant reduction in body weight compared to *Atf3*$^{+/+}$*; Ptf1a*$^{creERT/+}$*; Kras*$^{LSL\text{-}G12D/+}$ and control *Atf3*$^{+/+}$*; Ptf1a*$^{CreERT/+}$ and *Atf3*$^{-/-}$*; Ptf1a*$^{CreERT/+}$ mice treated with cerulein. *Atf3*$^{+/+}$*; Ptf1a*$^{creERT/+}$*; Kras*$^{LSL\text{-}G12D/+}$ mice had significantly reduced body weight on days 43 and 50 compared to *Atf3*$^{+/+}$*; Ptf1a*$^{creERT/+}$ and *Atf3*$^{-/-}$*; Ptf1a*$^{CreERT/+}$ mice.

Mice were sacrificed two- and five-weeks post-CIP and pancreatic tissue was collected for histological and biochemical analysis. Upon dissection, the pancreas was visually examined to determine if any visible changes occurred gross morphologically between genotypes and treatment groups. Multiple fibrotic nodules were present only in *Atf3*$^{+/+}$*; Ptf1a*$^{creERT/+}$*; Kras*$^{LSL\text{-}G12D/+}$ pancreatic tissue treated with ceruelin at both time points, while *Atf3*$^{-/-}$*; Ptf1a*$^{creERT/+}$*; Kras*$^{LSL\text{-}G12D/+}$ mice had pancreata that appeared visually small with no nodules were present **(Figure 3.8C)**. To quantify visual difference in pancreatic

size, the pancreas was weighed and measured as percent weight relative to body weight **(Figure 3.8D)**. No significant differences in pancreatic weight was observed between saline-treated genotypes at either experimental time point. However, *Atf3*$^{+/+}$; *Ptf1a*$^{creERT/+}$; *Kras*$^{LSL\text{-}G12D/+}$ mice treated with ceruelin had significantly increased pancreatic weight as a ratio to total body weight when compared to other saline and cerulein treated groups at week two post CIP. At week five, *Atf3*$^{-/-}$; *Ptf1a*$^{creERT/+}$; *Kras*$^{LSL\text{-}G12D/+}$ pancreatic tissue was significantly smaller compared to genotypes in both treatment groups at week two and remained small up to week five. Overall, *Atf3*$^{-/-}$; *Ptf1a*$^{creERT/+}$; *Kras*$^{LSL\text{-}G12D/+}$ mice lost significant body weight and showed an atrophied pancreas at both experimental time points.

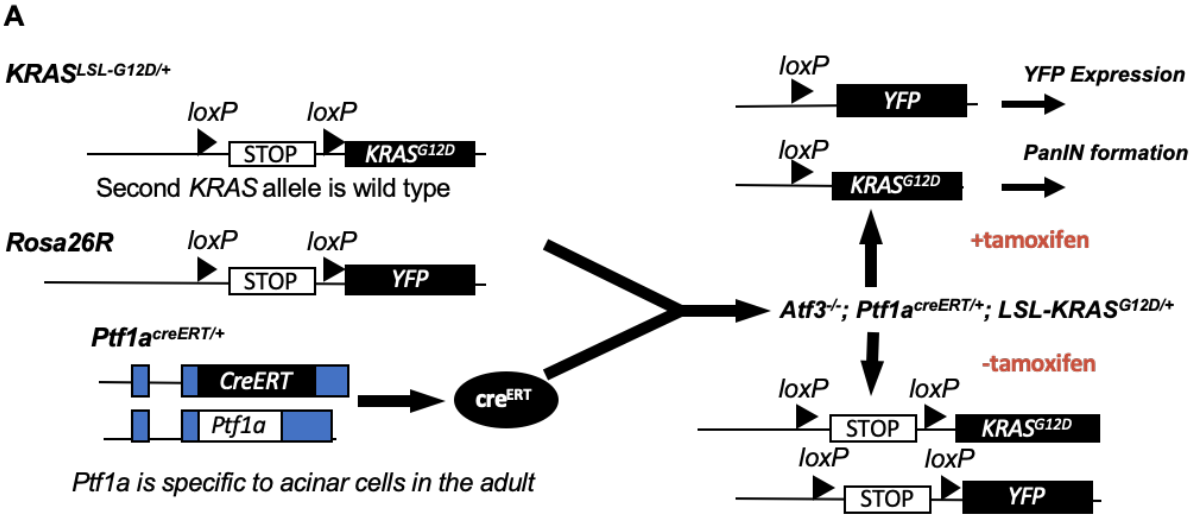
A
KRASLSL-G12D/+
loxP
loxP
STOP
KRASG12D
Second KRAS allele is wild type
Rosa26R
loxP
loxP
STOP
YFP
Ptf1acreERT/+
CreERT
Ptf1a
creERT
Ptf1a is specific to acinar cells in the adult
loxP
YFP
YFP Expression
loxP
KRASG12D
PanIN formation
+tamoxifen
Atf3-/-; Ptf1acreERT/+; LSL-KRASG12D/+
-tamoxifen
loxP
loxP
STOP
KRASG12D
loxP
loxP
STOP
YFP

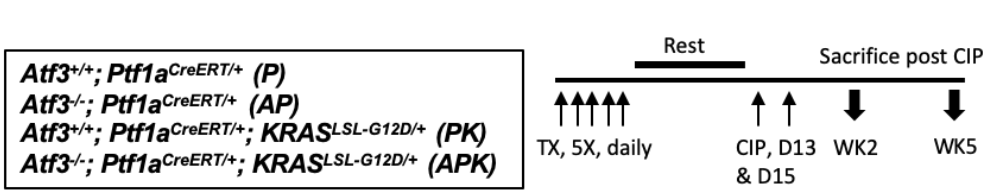
B
Atf3+/+; Ptf1aCreERT/+ (P)
Atf3-/-; Ptf1aCreERT/+ (AP)
Atf3+/+; Ptf1aCreERT/+; KRASLSL-G12D/+ (PK)
Atf3-/-; Ptf1aCreERT/+; KRASLSL-G12D/+ (APK)
Rest
Sacrifice post CIP
TX, 5X, daily
CIP, D13 & D15
WK2
WK5

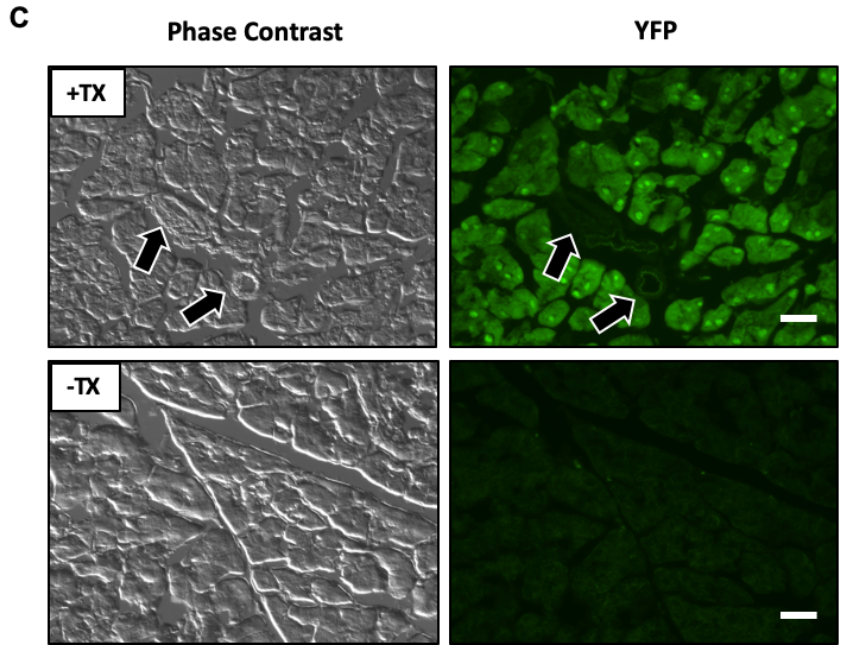
C
Phase Contrast
YFP
+TX
-TX

Figure 3.7. KRAS-(*G12D*) is specifically activated in acinar cells of *Atf3*$^{-/-}$; *Ptf1a*$^{creERT/+}$; *Kras*$^{LSL\text{-}G12D/+}$ mice. **(A)** Schematic of mouse model used for experimentation. **(B)** Different mouse lines used for experimentation along with the timeline used in this experiment. **(C)** Fluorescence images of YFP show expression specially in acinar cells following cre-recombination induced by tamoxifen administration. The black arrows point to YFP negative blood vessels. The white magnification bars represent 100 μm.

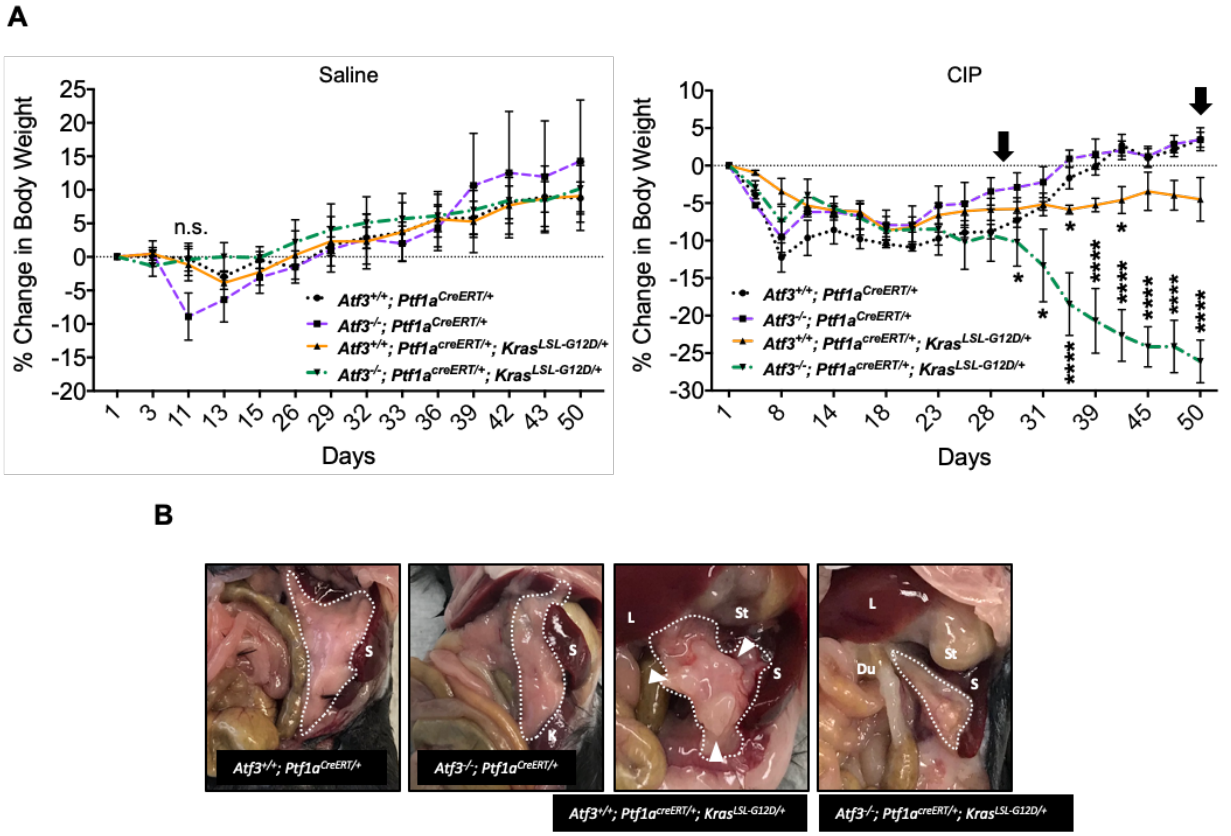
A
Saline
% Change in Body Weight
Days
n.s.
Atf3+/+; Ptf1aCreERT/+
Atf3-/-; Ptf1aCreERT/+
Atf3+/+; Ptf1acreERT/+; KrasLSL-G12D/+
Atf3-/-; Ptf1acreERT/+; KrasLSL-G12D/+
CIP
B
Atf3+/+; Ptf1aCreERT/+
Atf3-/-; Ptf1aCreERT/+
Atf3+/+; Ptf1acreERT/+; KrasLSL-G12D/+
Atf3-/-; Ptf1acreERT/+; KrasLSL-G12D/+
S
L
St
Du
C
Week 2
Week 5
% P.W. to B.W.
n.s.
SAL
CIP
Atf3+/+; Ptf1aCreERT/+
Atf3-/-; Ptf1aCreERT/+
Atf3+/+; Ptf1acreERT/+; KrasLSL-G12D/+
Atf3-/-; Ptf1acreERT/+; KrasLSL-G12D/+

Figure 3.8. *Atf3$^{-/-}$; Ptf1a$^{creERT/+}$; Kras$^{LSL-G12D/+}$* mice lose body weight and show an atrophied pancreas. (A) Percent change in body weight shows no difference between the four genotypes treated with saline (n = 4-5; % mean ± SE). Significant body weight loss is observed in *Atf3$^{-/-}$; Ptf1a$^{creERT/+}$; Kras$^{LSL-G12D/+}$* mice compared to *Atf3$^{+/+}$; Ptf1a$^{creERT/+}$; Kras$^{LSL-G12D/+}$* and control *Atf3$^{+/+}$; Ptf1a$^{creERT/+}$* and *Atf3$^{-/-}$; Ptf1a$^{creERT/+}$* mice that underwent pancreatitis (*P<0.05; ****P<0.0001; n = 5-6; % mean ± SE; a repeated measures Two-way ANOVA with a Tukey's post hoc test was performed), black arrows point to sacrifice time points. **(B)** Representative images of pancreatic gross morphology (pancreas highlighted by the dotted white line; S = spleen, L = liver, K = kidney, St = stomach and Du = duodenum) and their associated genotypes at week two. *Atf3$^{+/+}$; Ptf1a$^{creERT/+}$; Kras$^{LSL-G12D/+}$* mice showed nodular spots on the pancreas (white arrowheads), while *Atf3$^{-/-}$; Ptf1a$^{creERT/+}$; Kras$^{LSL-G12D/+}$*genotypes had smaller pancreata compared to control mice lacking oncogenic KRAS. **(C)** Quantification of pancreatic weight as a percent relative to body weight. Week two post CIP, *Atf3$^{+/+}$; Ptf1a$^{creERT/+}$; Kras$^{LSL-G12D/+}$* mice show a significant increase in pancreatic weight compared to *Atf3$^{+/+}$; Ptf1a$^{creERT/+}$; Kras$^{LSL-G12D/+}$* mice treated with saline (****P<0.0001). By week five, *Atf3$^{+/+}$; Ptf1a$^{creERT/+}$; Kras$^{LSL-G12D/+}$* genotypes treated with CIP were comparable genotypes treated with saline. *Atf3$^{-/-}$; Ptf1a$^{creERT/+}$; Kras$^{LSL-G12D/+}$* pancreata was significantly small compared to mice in both saline and CIP treated groups at week two (****P<0.0001). The pancreas of *Atf3$^{-/-}$; Ptf1a$^{creERT/+}$; Kras$^{LSL-G12D/+}$* mice remained small by week five post CIP (*P<0.005, n = 3-5; error bars represent % mean ± SE). Three *Atf3$^{+/+}$; Ptf1a$^{creERT/+}$; Kras$^{LSL-G12D/+}$* mice and one *Atf3$^{-/-}$; Ptf1a$^{creERT/+}$; Kras$^{LSL-G12D/+}$* mouse died during experimentation.

I next determined if the gross morphological size differences observed was explained by histological differences. Pancreatic tissue was analyzed using H&E stain to determine lesion grade (See **Appendix 2** for classification of lesions). Samples for each genotype were grouped based on highest grade lesion present per tissue area. In the saline treated groups, the absence of oncogenic KRAS resulted in no damage both in the presence or absence of ATF3 within two weeks of CIP **(Figure 3.9)**. Saline-treated *Atf3*$^{+/+}$*; Ptf1a*$^{creERT/+}$*; Kras*$^{LSL\text{-}G12D/+}$ mice showed greater incidences of focal PanIN1 lesions compared to incidences of focal ADM seen in *Atf3*$^{-/-}$*; Ptf1a*$^{creERT/+}$*; Kras*$^{LSL\text{-}G12D/+}$ mice by week two post CIP **(Table 3.1)**. By week five, saline-treated *Atf3*$^{+/+}$*; Ptf1a*$^{creERT/+}$*; Kras*$^{LSL\text{-}G12D/+}$ tissue persistently showed more PanIN1 and PanIN2 lesions compared to *Atf3*$^{-/-}$*; Ptf1a*$^{creERT/+}$*; Kras*$^{LSL\text{-}G12D/+}$, which varied from being normal to having focal regions that showed PanIN2 lesions. Alternatively, *Atf3*$^{-/-}$*; Ptf1a*$^{creERT/+}$*; Kras*$^{LSL\text{-}G12D/+}$ and *Atf3*$^{+/+}$*; Ptf1a*$^{creERT/+}$*; Kras*$^{LSL\text{-}G12D/+}$ mice treated with cerulein showed higher grade PanIN3 lesions within two weeks of CIP **(Figure 3.10A)**. However, by week five, *Atf3*$^{-/-}$*; Ptf1a*$^{creERT/+}$*; Kras*$^{LSL\text{-}G12D/+}$ tissue showed predominately lower grade PanIN1 and 2 lesions compared to the PanIN3 and PDAC lesions scored in *Atf3*$^{+/+}$*; Ptf1a*$^{creERT/+}$*; Kras*$^{LSL\text{-}G12D/+}$ tissue **(Table 3.2)**. This finding was further supported by significantly more mucin accumulation seen in lesions in *Atf3*$^{+/+}$*; Ptf1a*$^{creERT/+}$*; Kras*$^{LSL\text{-}G12D/+}$ tissue compared to *Atf3*$^{-/-}$*; Ptf1a*$^{creERT/+}$*; Kras*$^{LSL\text{-}G12D/+}$ mice based on Alcian blue accumulation **(Figure 3.10B and C)**. In summary, histological lesion scores showed reduced incidences of high grade PanIN lesions in *Atf3*$^{-/-}$*; Ptf1a*$^{creERT/+}$*; Kras*$^{LSL\text{-}G12D/+}$ tissue compared to *Atf3*$^{+/+}$*; Ptf1a*$^{creERT/+}$*; Kras*$^{LSL\text{-}G12D/+}$ tissue post five weeks after CIP.

The findings from the histological lesion scores were surprising given the gross morphological assessment showed small pancreatic tissue with no nodules in *Atf3*$^{-/-}$*; Ptf1a*$^{creERT/+}$*; Kras*$^{LSL\text{-}G12D/+}$ mice compared to *Atf3*$^{+/+}$*; Ptf1a*$^{creERT/+}$*; Kras*$^{LSL\text{-}G12D/+}$ mice. One possibility is that the lesions are the result of duct expansion in *Atf3*$^{-/-}$*; Ptf1a*$^{creERT/+}$*; Kras*$^{LSL\text{-}G12D/+}$ mice and acinar transformation in *Atf3*$^{+/+}$*; Ptf1a*$^{creERT/+}$*; Kras*$^{LSL\text{-}G12D/+}$ mice. To determine if the PanIN lesions are derived from acinar tissue, I performed lineage tracing analysis and showed PanIN lesions were of acinar cell origin in both genotypes **(Figure 3.11A)**. However, the percent of YFP^{+} lesions in *Atf3*$^{-/-}$*; Ptf1a*$^{creERT/+}$*;*

Kras$^{LSL\text{-}G12D/+}$ tissue was significantly lower (22.76 ± 4.91%) compared to *Atf3*$^{+/+}$; *Ptf1a*$^{creERT/+}$; *Kras*$^{LSL\text{-}G12D/+}$ tissue (45.84 ± 7.73%) **(Figure 3.11B)**. Duct-like cells that did not express YFP were more frequently seen in *Atf3*$^{-/-}$; *Ptf1a*$^{creERT/+}$; *Kras*$^{LSL\text{-}G12D/+}$ tissue (black arrowhead) suggesting these cells were not derived from acinar tissue. IHC analysis done for a duct cell-specific marker cytokeratin 19 (CK19) (**Figure 3.11A and B**) indicated the amount of accumulated lesions was significantly lower in *Atf3*$^{-/-}$; *Ptf1a*$^{creERT/+}$; *Kras*$^{LSL\text{-}G12D/+}$ tissue compared to *Atf3*$^{+/+}$; *Ptf1a*$^{creERT/+}$; *Kras*$^{LSL\text{-}G12D/+}$ at both time points (**Figure 3.11C**). It is also possible that acinar cells are transforming in *Atf3*$^{-/-}$; *Ptf1a*$^{creERT/+}$; *Kras*$^{LSL\text{-}G12D/+}$ mice but not proliferating; *Atf3*$^{-/-}$; *Ptf1a*$^{creERT/+}$; *Kras*$^{LSL\text{-}G12D/+}$ tissue showed significantly fewer proliferative cells based on Ki67 staining compared to *Atf3*$^{+/+}$; *Ptf1a*$^{creERT/+}$; *Kras*$^{LSL\text{-}G12D/+}$ tissue at week two post injury (**Figure 3.11D** and **E**). Surprisingly, by week five, proliferation in *Atf3*$^{-/-}$; *Ptf1a*$^{creERT/+}$; *Kras*$^{LSL\text{-}G12D/+}$ tissue was negligible and statistically comparable to saline treated genotypes. These results showed *Atf3*$^{-/-}$; *Ptf1a*$^{creERT/+}$; *Kras*$^{LSL\text{-}G12D/+}$ tissue had reduced YFP^{+} lesions, lower duct cell accumulation along with reduced proliferation compared to *Atf3*$^{+/+}$; *Ptf1a*$^{creERT/+}$; *Kras*$^{LSL\text{-}G12D/+}$ tissue.

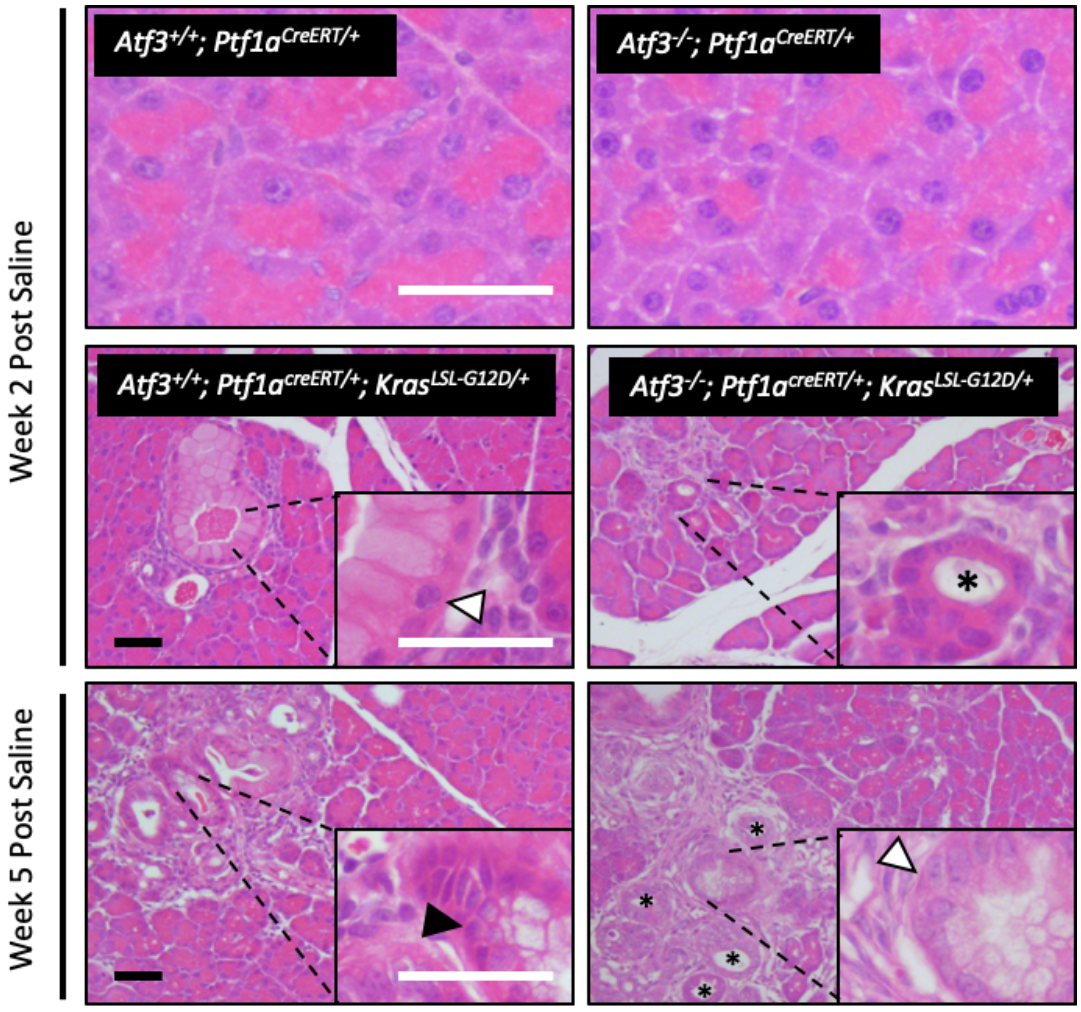
Atf3+/+; Ptf1aCreERT/+
Atf3-/-; Ptf1aCreERT/+
Atf3+/+; Ptf1acreERT/+; KrasLSL-G12D/+
Atf3-/-; Ptf1acreERT/+; KrasLSL-G12D/+
Week 2 Post Saline
Week 5 Post Saline

Figure 3.9. The absence of ATF3 reduces high grade PanIN lesions in mice expressing oncogenic KRAS. Representative H&E images shown. Two weeks after the induction of pancreatitis *Atf3*$^{+/+}$*; Ptf1a*$^{creERT/+}$*; Kras*$^{LSL\text{-}G12D/+}$ pancreata showed more incidences of higher grade PanIN1 lesions (white arrowhead) compared to ADM (represented by the asterisk symbol) seen in *Atf3*$^{-/-}$*; Ptf1a*$^{creERT/+}$*; Kras*$^{LSL\text{-}G12D/+}$ mice. Five weeks post CIP, the incidence of PanIN2 (black arrowhead) lesions were more frequent in *Atf3*$^{+/+}$*; Ptf1a*$^{creERT/+}$*; Kras*$^{LSL\text{-}G12D/+}$ mice compared to *Atf3*$^{-/-}$*; Ptf1a*$^{creERT/+}$*; Kras*$^{LSL\text{-}G12D/+}$ mice. Black bars represent 200 μm; white bars represent 50 μm.

Table 3.1. Histological lesion scores for mice treated with saline in the presence or absence of ATF3 with or without KRAS-(*G12D*) activation

	Atf3$^{+/+}$; *Ptf1a*$^{CreERT/+}$		*Atf3*$^{-/-}$; *Ptf1a*$^{CreERT/+}$		*Atf3*$^{+/+}$; *Ptf1a*$^{creERT/+}$; *Kras*$^{LSL-G12D/+}$		*Atf3*$^{-/-}$; *Ptf1a*$^{creERT/+}$; *Kras*$^{LSL-G12D/+}$	
	WK2 (4)	*WK5 (3)*	*WK2 (3)*	*WK5 (2)*	*WK2 (3)*	*WK5 (3)*	*WK2 (3)*	*WK5 (3)*
Normal	4	2	3	2	1	0	1	1
ADM	0	1	0	0	0	0	1	0
PanIN1	0	0	0	0	2	2	1	1
PanIN2	0	0	0	0	0	1	0	1
PanIN3	0	0	0	0	0	0	0	0
PDAC	0	0	0	0	0	0	0	0

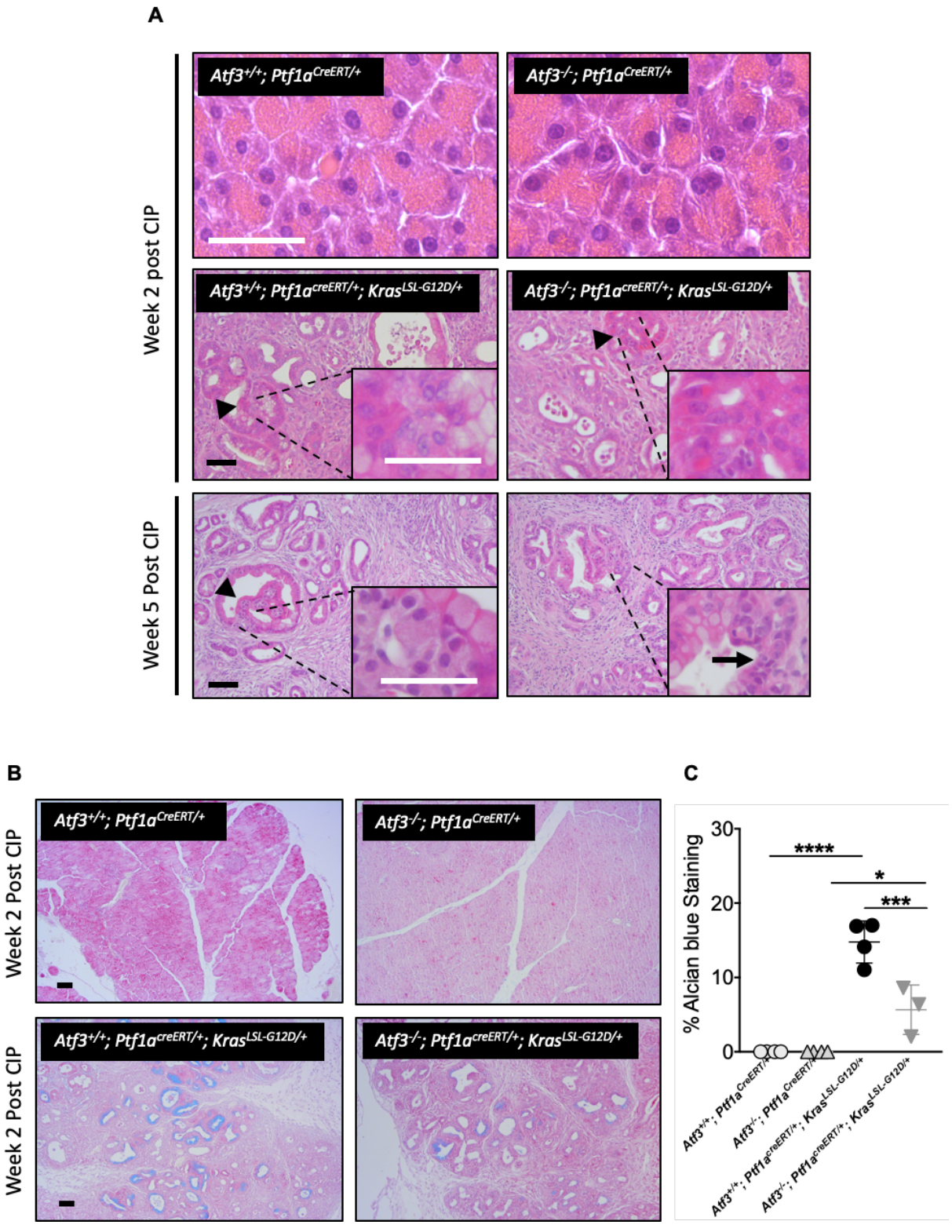
A
Atf3+/+; Ptf1aCreERT/+
Atf3-/-; Ptf1aCreERT/+
Atf3+/+; Ptf1acreERT/+; KrasLSL-G12D/+
Atf3-/-; Ptf1acreERT/+; KrasLSL-G12D/+
Week 2 post CIP
Week 5 Post CIP
B
Atf3+/+; Ptf1aCreERT/+
Atf3-/-; Ptf1aCreERT/+
Atf3+/+; Ptf1acreERT/+; KrasLSL-G12D/+
Atf3-/-; Ptf1acreERT/+; KrasLSL-G12D/+
Week 2 Post CIP
Week 2 Post CIP
C
% Alcian blue Staining
30
20
10
0
****
*
***
Atf3+/+; Ptf1aCreERT/+
Atf3-/-; Ptf1aCreERT/+
Atf3+/+; Ptf1acreERT/+; KrasLSL-G12D/+
Atf3-/-; Ptf1acreERT/+; KrasLSL-G12D/+

Figure 3.10. ***Atf3*$^{-/-}$*; Ptf1a*$^{creERT/+}$*; Kras*$^{LSL\text{-}G12D/+}$ **mice treated with cerulein show reduced incidence of high-grade lesions later at week five post CIP. (A)** Representative H&E images show both *Atf3*$^{+/+}$*; Ptf1a*$^{creERT/+}$*; Kras*$^{LSL\text{-}G12D/+}$ and *Atf3*$^{-/-}$*; Ptf1a*$^{creERT/+}$*; Kras*$^{LSL\text{-}G12D/+}$ with high grade PanIN3 lesions (indicated by the black arrowheads) at two weeks post CIP treatment. At week five post CIP, *Atf3*$^{-/-}$*; Ptf1a*$^{creERT/+}$*; Kras*$^{LSL\text{-}G12D/+}$ mice show lower incidences of high grade PanIN3 lesions and no PDAC compared to *Atf3*$^{+/+}$*; Ptf1a*$^{creERT/+}$*; Kras*$^{LSL\text{-}G12D/+}$ mice. Black arrow points to lower grade PanIN2 lesion. White scale bar represents 50 μm; black scale bars represents 200 μm. **(B)** Representative images of Alcian blue showed a higher percent area stained for mucin in the *Atf3*$^{+/+}$*; Ptf1a*$^{creERT/+}$*; Kras*$^{LSL\text{-}G12D/+}$ mice compared to *Atf3*$^{-/-}$*; Ptf1a*$^{creERT/+}$*; Kras*$^{LSL\text{-}G12D/+}$ mice. Black scale bars represent 400 μm. **(C)** The quantification of percent area stained Alcian blue showed a 3-fold decrease in *Atf3*$^{-/-}$*; Ptf1a*$^{creERT/+}$*; Kras*$^{LSL\text{-}G12D/+}$ tissue at week two post CIP (***$P<0.001$; % mean ± SE; n = 3-4; a One-way ANOVA with a Tukey's post hoc test was performed).

Table 3.2. Histological lesion scores for mice treated with cerulein in the presence or absence of ATF3 with or without KRAS-(*G12D*) activation

	Atf3$^{+/+}$; *Ptf1a*$^{CreERT/+}$		*Atf3*$^{-/-}$; *Ptf1a*$^{CreERT/+}$		*Atf3*$^{+/+}$; *Ptf1a*$^{creERT/+}$; *Kras*$^{LSL-G12D/+}$		*Atf3*$^{-/-}$; *Ptf1a*$^{creERT/+}$; *Kras*$^{LSL-G12D/+}$	
	WK2 (2)	*WK5 (2)*	*WK2 (3)*	*WK5 (1)*	*WK2 (12)*	*WK5 (7)*	*WK2 (6)*	*WK5 (8)*
Normal	0	2	2	0	0	0	0	0
ADM	2	0	0	1	0	0	0	0
PanIN1	0	0	1	0	0	0	2	1
PanIN2	0	0	0	0	2	2	0	5
PanIN3	0	0	0	0	9	4	4	2
PDAC	0	0	0	0	1	1	0	0
Death*	0	0	0	0	0	3	1	0

*Death occurred during experimentation closest to the approaching sacrifice date as indicated above. Three *PK* mice died within 10 days before reaching the sacrifice date on week 5. One *APK* mouse died 4 days before reaching sacrifice date on week 2.

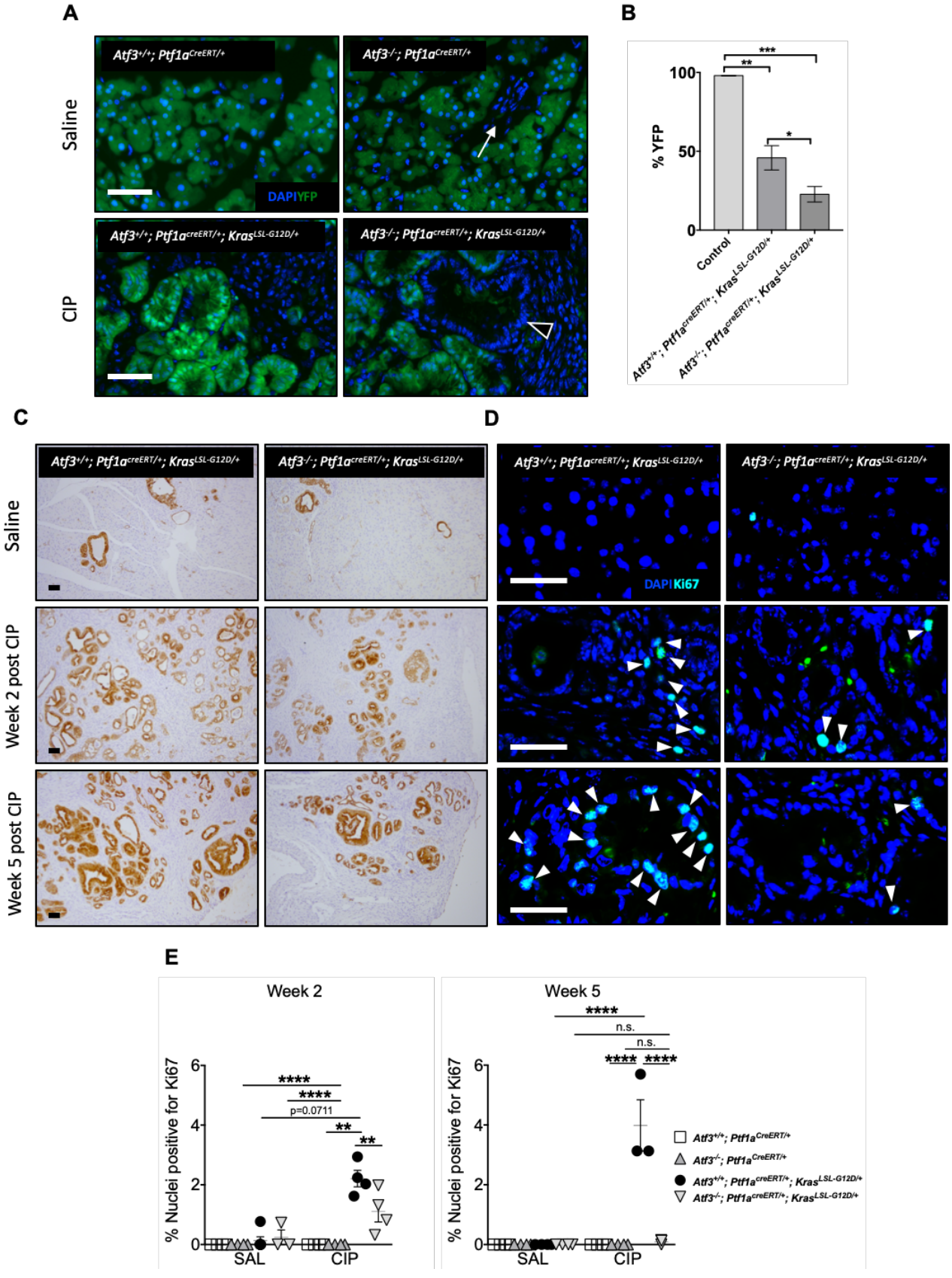
A
Saline
CIP
Atf3+/+; Ptf1aCreERT/+
Atf3-/-; Ptf1aCreERT/+
Atf3+/+; Ptf1acreERT/+; KrasLSL-G12D/+
Atf3-/-; Ptf1acreERT/+; KrasLSL-G12D/+
DAPIYFP
B
% YFP
100
50
0
***
**
*
Control
Atf3+/+; Ptf1acreERT/+; KrasLSL-G12D/+
Atf3-/-; Ptf1acreERT/+; KrasLSL-G12D/+
C
D
Saline
Week 2 post CIP
Week 5 post CIP
DAPIKi67
E
Week 2
Week 5
% Nuclei positive for Ki67
SAL
CIP
****
p=0.0711
**
n.s.
Atf3+/+; Ptf1aCreERT/+
Atf3-/-; Ptf1aCreERT/+
Atf3+/+; Ptf1acreERT/+; KrasLSL-G12D/+
Atf3-/-; Ptf1acreERT/+; KrasLSL-G12D/+

Figure 3.11. *Atf3$^{-/-}$; Ptf1a$^{creERT/+}$; Kras$^{LSL-G12D/+}$* mice show significantly less lesion accumulation and fewer proliferative cells. **(A)** The YFP reporter shows specific recombination in pancreatic acinar cells (white arrow points to an islet). Upon pancreatic injury, lesions in both *Atf3$^{+/+}$; Ptf1a$^{creERT/+}$; Kras$^{LSL-G12D/+}$* and *Atf3$^{-/-}$; Ptf1a$^{creERT/+}$; Kras$^{LSL-G12D/+}$* tissue expressed YFP (black arrowhead points to ductal structure not expressing YFP). Magnification bars represent 50 μm. **(B)** The quantification of YFP expression as a percent area of the tissue cross section showed 97.98 ± 0.17% cre-recombination efficiency in both *Atf3$^{+/+}$; Ptf1a$^{creERT/+}$* and *Atf3$^{-/-}$; Ptf1a$^{creERT/+}$* mice that received saline. There was a significant reduction in YFP expression in *Atf3$^{-/-}$; Ptf1a$^{creERT/+}$; Kras$^{LSL-G12D/+}$* tissue compared to *Atf3$^{+/+}$; Ptf1a$^{creERT/+}$; Kras$^{LSL-G12D/+}$* tissue (*P<0.05; % mean ± SE; n = 3; a One-way ANOVA with a Tukey's post hoc test was performed). **(C)** Representative IHC images show fewer CK19^{+} lesions in *Atf3$^{-/-}$; Ptf1a$^{creERT/+}$; Kras$^{LSL-G12D/+}$* mice both at weeks two and five post CIP. Magnification bars represent 500 μm. **(D)** Representative IF images for Ki67 show a significant decrease in the percent of Ki67^{+} nuclei in *Atf3$^{-/-}$; Ptf1a$^{creERT/+}$; Kras$^{LSL-G12D/+}$* tissue compared to *Atf3$^{+/+}$; Ptf1a$^{creERT/+}$; Kras$^{LSL-G12D/+}$* at both time points. White arrowheads indicate Ki67^{+} nuclei. Magnification bars represent 100 μm. **(E)** Quantification of Ki67 at both time points **P<0.001, ****P<0.0001; error bars represent % mean ± SE; n = 3-4; Two-way ANOVA with a Tukey's post hoc test was performed).

To determine if the decreased amount of duct-like tissue is reflective of reduced ADM, I next examined pancreatic cell-specific markers, and transcription and signalling factors involved in ADM. Immunoblots for amylase, a marker of acinar cells, showed no detectable accumulation in *Atf3*$^{+/+}$*; Ptf1a*$^{creERT/+}$*; Kras*$^{LSL\text{-}G12D/+}$ and *Atf3*$^{-/-}$*; Ptf1a*$^{creERT/+}$*; Kras*$^{LSL\text{-}G12D/+}$ tissue post CIP treatment **(Figure 12A)** suggesting acinar tissue is completely lost in both genotypes compared to genotypes treated with saline. In contrast, immunoblots revealed less SOX9 accumulation in *Atf3*$^{-/-}$*; Ptf1a*$^{creERT/+}$*; Kras*$^{LSL\text{-}G12D/+}$ pancreatic tissue at two and five weeks post pancreatic injury. SOX9 protein expression was 7.99 ± 1.24-fold lower in *Atf3*$^{-/-}$*; Ptf1a*$^{creERT/+}$*; Kras*$^{LSL\text{-}G12D/+}$ tissue compared to *Atf3*$^{+/+}$*; Ptf1a*$^{creERT/+}$*; Kras*$^{LSL\text{-}G12D/+}$ tissue at week two post CIP and 2.58 ± 1.41-fold lower at five weeks post CIP **(Figure 12C)**. Next, I examined MAPK signalling downstream effector pERK by performing immunoblot analysis. Reduced pERK accumulation was observed in *Atf3*$^{-/-}$*; Ptf1a*$^{creERT/+}$*; Kras*$^{LSL\text{-}G12D/+}$ tissue at two (2.21 ± 0.66-fold less pERK) and five weeks (2.42 ± 0.25-fold less pERK) after injury compared to *Atf3*$^{+/+}$*; Ptf1a*$^{creERT/+}$*; Kras*$^{LSL\text{-}G12D/+}$ tissue **(Figure 12D)**. Further, contrary to the SOX9 immunoblots, IF analysis for SOX9 showed no difference in the number of SOX9^{+} nuclei in *Atf3*$^{+/+}$*; Ptf1a*$^{creERT/+}$*; Kras*$^{LSL\text{-}G12D/+}$ and *Atf3*$^{-/-}$*; Ptf1a*$^{creERT/+}$*; Kras*$^{LSL\text{-}G12D/+}$ tissue at week two post CIP **(Figure 12E and F)**. Although there may be no difference in the number of nuclei staining for SOX9 between the two genotypes, it is however possible that the amount of lesions based on SOX9 accumulation is lower in *Atf3*$^{-/-}$*; Ptf1a*$^{creERT/+}$*; Kras*$^{LSL\text{-}G12D/+}$ tissue at week two. Conversely, by week five post CIP-treatment, significantly fewer SOX9^{+} nuclei were observed in *Atf3*$^{-/-}$*; Ptf1a*$^{creERT/+}$*; Kras*$^{LSL\text{-}G12D/+}$ tissue compared to *Atf3*$^{+/+}$*; Ptf1a*$^{creERT/+}$*; Kras*$^{LSL\text{-}G12D/+}$ tissue. Combined, these results suggest that the absence of ATF3 in the presence of oncogenic KRAS reduces the expression of markers involved in ADM and PanIN lesion development.

Since several non-acinar cell types contribute to the pancreatic pathology observed in PDAC, including stromal cells and immune cells, I determined if the absence of ATF3 leads to altered accumulation of these cells in *Atf3*$^{-/-}$*; Ptf1a*$^{creERT/+}$*; Kras*$^{LSL\text{-}G12D/+}$ mice. Fibrosis, as determined by Mason's Trichrome stain, was significantly more pronounced two weeks post injury in *Atf3*$^{-/-}$*; Ptf1a*$^{creERT/+}$*; Kras*$^{LSL\text{-}G12D/+}$ tissue compared to *Atf3*$^{+/+}$*;*

Ptf1a$^{creERT/+}$*; Kras*$^{LSL\text{-}G12D/+}$ tissue **(Figure 13A and B)**. However, immunoblots for smooth muscle actin-α, a marker of activated stellate cells, showed no significant difference between *Atf3*$^{+/+}$*; Ptf1a*$^{creERT/+}$*; Kras*$^{LSL\text{-}G12D/+}$ and *Atf3*$^{-/-}$*; Ptf1a*$^{creERT/+}$*; Kras*$^{LSL\text{-}G12D/+}$ tissue at either time point post injury **(Figure 13C and D)**. By five weeks post CIP-treatment there was no significant difference in fibrosis between and *Atf3*$^{+/+}$*; Ptf1a*$^{creERT/+}$*; Kras*$^{LSL\text{-}G12D/+}$ and *Atf3*$^{-/-}$*; Ptf1a*$^{creERT/+}$*; Kras*$^{LSL\text{-}G12D/+}$ tissue. This suggests that stellate cell function, but not accumulation, may be affected by the absence of ATF3. Next, to profile the immune system in the absence of ATF3, macrophage infiltration was assessed by IF for F4/80 (macrophage marker). My findings showed significantly fewer macrophages in *Atf3*$^{-/-}$*; Ptf1a*$^{creERT/+}$*; Kras*$^{LSL\text{-}G12D/+}$ tissue five weeks after injury **(Figure 14A and B)**. These results suggest that the loss of ATF3 in the context of oncogenic KRAS may have a role in both acinar and non-acinar cells.

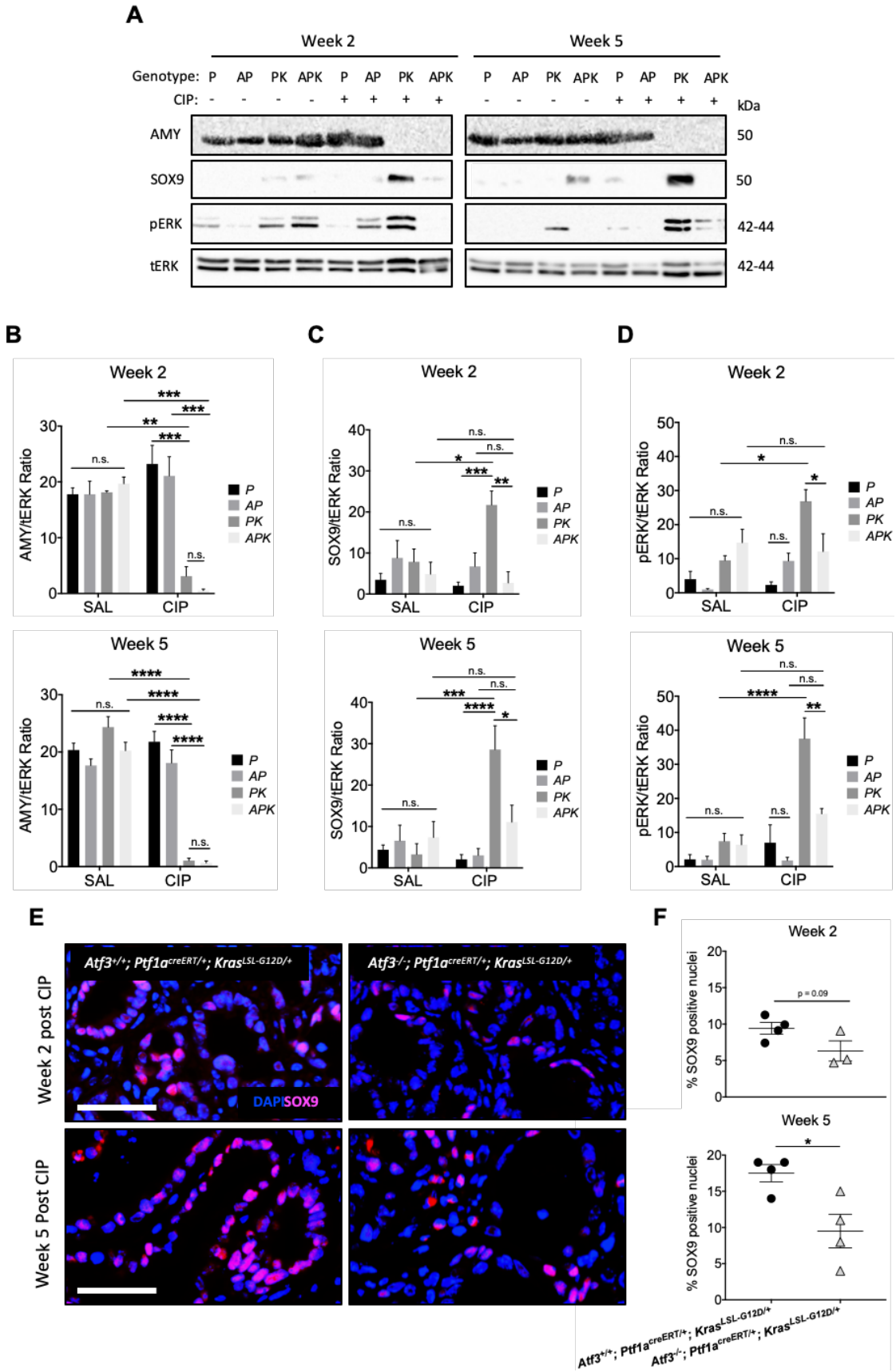
A
Week 2
Week 5
Genotype: P AP PK APK P AP PK APK P AP PK APK P AP PK APK
CIP: - - - - + + + + - - - - + + + +
kDa
AMY
SOX9
pERK
tERK
50
50
42-44
42-44
B
C
D
Week 2
Week 5
AMY/tERK Ratio
SOX9/tERK Ratio
pERK/tERK Ratio
P
AP
PK
APK
SAL
CIP
n.s.
E
F
Atf3+/+; Ptf1acreERT/+; KrasLSL-G12D/+
Atf3-/-; Ptf1acreERT/+; KrasLSL-G12D/+
Week 2 post CIP
Week 5 Post CIP
DAPI SOX9
% SOX9 positive nuclei
p = 0.09

Figure 3.12. SOX9 expression and pERK accumulation are significantly reduced in *Atf3$^{-/-}$; Ptf1a$^{creERT/+}$; Kras$^{LSL-G12D/+}$* pancreatic tissue. (A) Amylase was not detectable in either *Atf3$^{+/+}$; Ptf1a$^{creERT/+}$; Kras$^{LSL-G12D/+}$* and *Atf3$^{-/-}$; Ptf1a$^{creERT/+}$; Kras$^{LSL-G12D/+}$* tissue after injury compared to saline-control tissues. **(B)** Quantification of amylase confirmed no significant difference between *Atf3$^{+/+}$; Ptf1a$^{creERT/+}$; Kras$^{LSL-G12D/+}$* and *Atf3$^{-/-}$; Ptf1a$^{creERT/+}$; Kras$^{LSL-G12D/+}$* tissue post injury (% mean ± SE; n = 3-6; P>0.05). Representative Western blots show reduced to no detectable SOX9 and pERK expression in *Atf3$^{-/-}$; Ptf1a$^{creERT/+}$; Kras$^{LSL-G12D/+}$* tissue compared to *Atf3$^{+/+}$; Ptf1a$^{creERT/+}$; Kras$^{LSL-G12D/+}$* at two- and five-weeks post CIP. Quantification of SOX9 and pERK **(C and D)** confirmed significantly lower protein levels in *Atf3$^{-/-}$; Ptf1a$^{creERT/+}$; Kras$^{LSL-G12D/+}$* tissue at both time points compared to controls (*Atf3$^{-/-}$; Ptf1a$^{creERT/+}$; Kras$^{LSL-G12D/+}$*; *P<0.05, **P<0.001; n = 3-6; Two-way ANOVA with a Tukey's post hoc test was performed). **(E)** Shows representative IF images of SOX9 expression in both *Atf3$^{+/+}$; Ptf1a$^{creERT/+}$; Kras$^{LSL-G12D/+}$* and *Atf3$^{-/-}$; Ptf1a$^{creERT/+}$; Kras$^{LSL-G12D/+}$* genotypes at weeks two and five post CIP. Magnification bars represent 50 μm. **(F)** Quantification of SOX9 positive nuclei showed no significant difference within two weeks post CIP between *Atf3$^{+/+}$; Ptf1a$^{creERT/+}$; Kras$^{LSL-G12D/+}$* and *Atf3$^{-/-}$; Ptf1a$^{creERT/+}$; Kras$^{LSL-G12D/+}$* tissue (p=0.09). However, five weeks post CIP, significantly fewer SOX9^{+} nuclei were observed in *Atf3$^{-/-}$; Ptf1a$^{creERT/+}$; Kras$^{LSL-G12D/+}$* tissue compared to *Atf3$^{+/+}$; Ptf1a$^{creERT/+}$; Kras$^{LSL-G12D/+}$* tissue (*P<0.05; n = 3-4; Student's t-test, unpaired, two-tailed analysis performed).

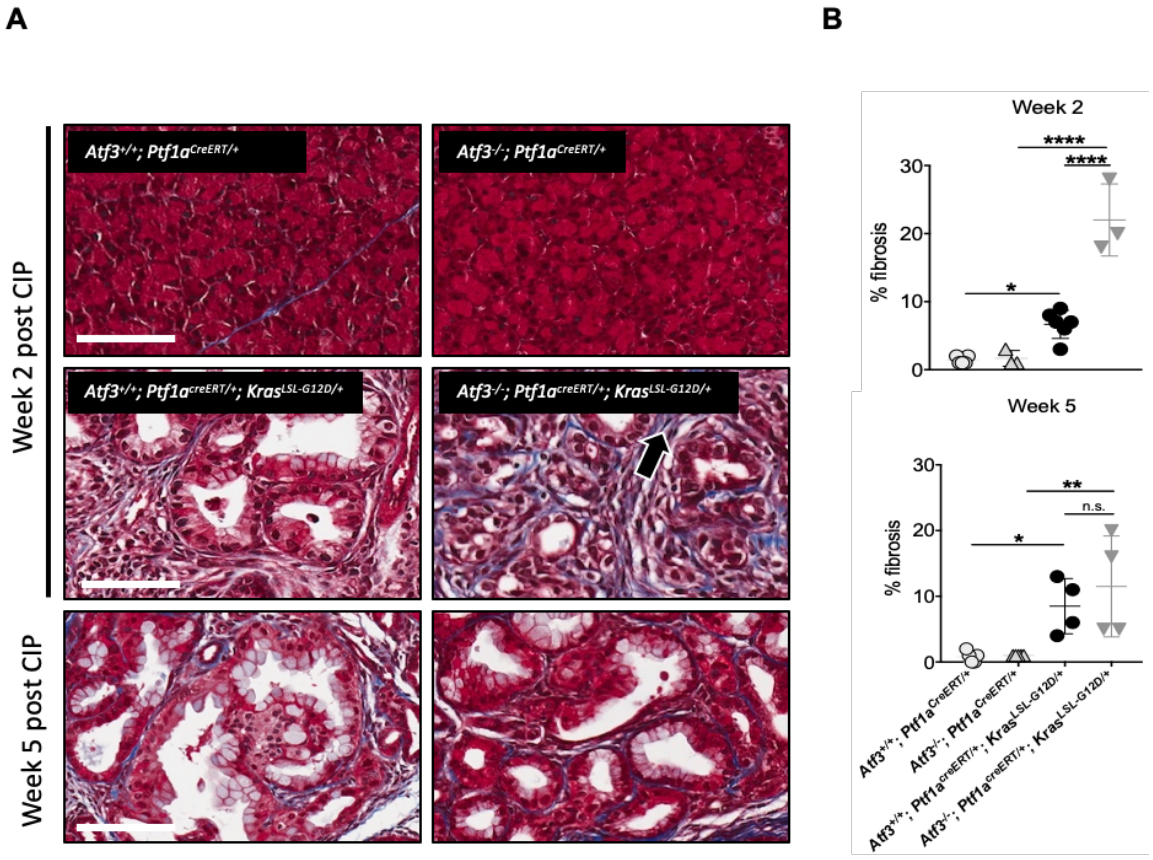
A
B
Week 2 post CIP
Week 5 post CIP
Atf3+/+; Ptf1aCreERT/+
Atf3-/-; Ptf1aCreERT/+
Atf3+/+; Ptf1acreERT/+; KrasLSL-G12D/+
Atf3-/-; Ptf1acreERT/+; KrasLSL-G12D/+
Week 2
Week 5
% fibrosis
****
*
**
n.s.
Atf3+/+; Ptf1aCreERT/+
Atf3-/-; Ptf1aCreERT/+
Atf3+/+; Ptf1acreERT/+; KrasLSL-G12D/+
Atf3-/-; Ptf1acreERT/+; KrasLSL-G12D/+
C
Week 2
Week 5
Genotype: P AP PK APK P AP PK APK P AP PK APK P AP PK APK
CIP: - - - - + + + + - - - - + + + +
kDa
αSMA
42
tERK
42-44
D
Week 2
Week 5
αSMA/tERK ratio
SAL
CIP
P
AP
PK
APK
n.s.

Figure 3.13. *Atf3$^{-/-}$; Ptf1a$^{creERT/+}$; Kras$^{LSL-G12D/+}$* mice display increased fibrosis at two weeks point after pancreatic injury. (A) Representative images for fibrosis in *Atf3$^{-/-}$; Ptf1a$^{creERT/+}$; Kras$^{LSL-G12D/+}$* tissue compared to *Atf3$^{+/+}$; Ptf1a$^{creERT/+}$; Kras$^{LSL-G12D/+}$* two- and five-weeks post-CIP using Mason's Trichrome stain kit (black arrow points to fibrosis), magnification bars represent 50 μm. **(B)** Quantification of fibrosis (% area staining blue) shows significant higher levels in *Atf3$^{-/-}$; Ptf1a$^{creERT/+}$; Kras$^{LSL-G12D/+}$* tissue compared to *Atf3$^{+/+}$; Ptf1a$^{creERT/+}$; Kras$^{LSL-G12D/+}$* at two weeks post CIP (****P<0.0001; % mean ± SE; n = 3-5). No significant difference was seen at week five post CIP between the two genotypes. A One-way ANOVA, Tukey's post hoc test was performed. **(C)** and **(D)** Western blot for αSMA shows no significant difference between cerulein treated *Atf3$^{+/+}$; Ptf1a$^{creERT/+}$; Kras$^{LSL-G12D/+}$* and *Atf3$^{-/-}$; Ptf1a$^{creERT/+}$; Kras$^{LSL-G12D/+}$* genotypes at both time points (n = 3; mean ± SE; n = 3; A Two-way ANOVA, Tukey's post hoc test was performed).

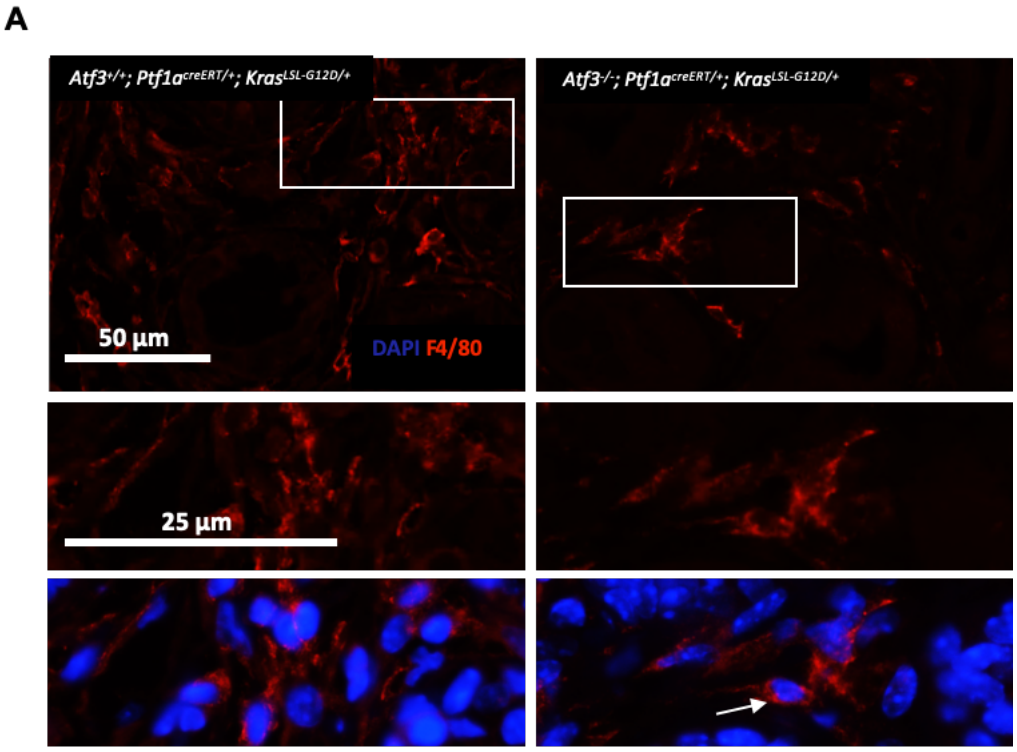
A
Atf3+/+; Ptf1acreERT/+; KrasLSL-G12D/+
Atf3-/-; Ptf1acreERT/+; KrasLSL-G12D/+
50 µm
DAPI F4/80
25 µm

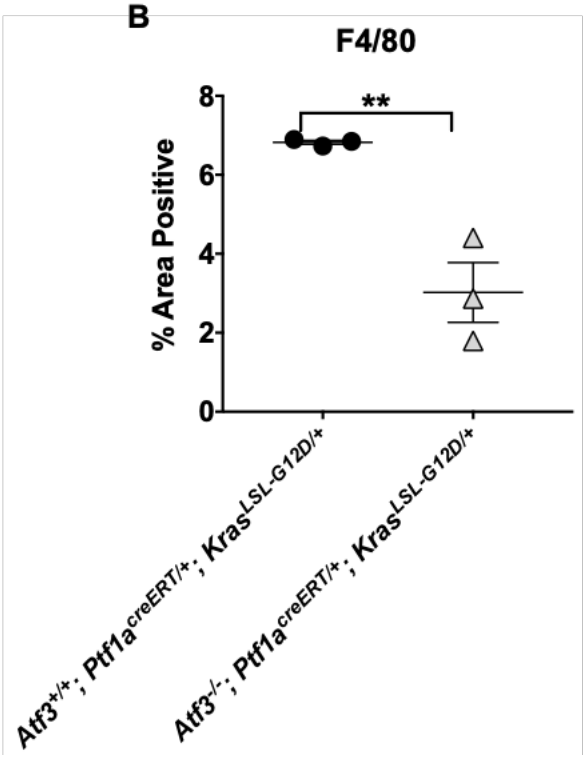
B
F4/80
**
% Area Positive
8
6
4
2
0
Atf3+/+; Ptf1acreERT/+; KrasLSL-G12D/+
Atf3-/-; Ptf1acreERT/+; KrasLSL-G12D/+

Figure 3.14. Macrophage infiltration is significantly reduced in *Atf3*$^{-/-}$*; Ptf1a*$^{creERT/+}$*; Kras*$^{LSL\text{-}G12D/+}$ tissue compared to *Atf3*$^{+/+}$*; Ptf1a*$^{creERT/+}$*; Kras*$^{LSL\text{-}G12D/+}$. (A and B) Representative IF images show significantly fewer macrophages in *Atf3*$^{-/-}$*; Ptf1a*$^{creERT/+}$*; Kras*$^{LSL\text{-}G12D/+}$ tissue compared to *Atf3*$^{+/+}$*; Ptf1a*$^{creERT/+}$*; Kras*$^{LSL\text{-}G12D/+}$ five weeks post-injury (**P<0.005, % mean ± SE; n = 3). White arrow points to F4/80 staining, which is a surface marker. Student's t-test, unpaired, two-tailed analysis performed.

CHAPTER 4

4 DISCUSSION

4.1 General Overview of Findings

In this study, ATF3 was identified to play a critical role in recurrent pancreatic (RP) injury and progression to PDAC. The lack of ATF3 expression in pancreatic tissue during recovery post-RP resulted in increased tissue regeneration. Further, in the context of oncogenic KRAS, the loss of ATF3 resulted in smaller pancreata and less high grade PanIN lesions. Molecular markers for pancreatic lesions supported a requirement for ATF3 for complete and persistent ADM. Ultimately, these results suggest the potential for directly targeting and inhibiting ATF3 in the pancreas to reduce injury and reduce high grade PanIN lesions, which could potentially develop into PDAC.

4.2 General Discussion

4.2.1 Role of ATF3 in RP tissue regeneration

To understand PDAC initiation and progression, it is critical to understand the development of early precancerous lesions such as ADM. A previous study done in our lab examined and characterized ATF3's role, but only in acute pancreatitis (Fazio et al., 2017), which is not a predictor of PDAC (Yadav & Lowenfels, 2006). The study showed that loss of ATF3 was detrimental to the pancreas early in injury, however, significantly more pancreatic tissue regeneration along with reduced ADM was seen 72-hours post injury in the absence of ATF3. The work presented in this thesis utilized similar methodologies to examine ATF3's role in RP, which is a significant risk factor for PDAC (Guda et al., 2018; Yadav & Lowenfels, 2013). My findings demonstrated no difference in overall lesion formation (fibrosis, inflammation, and ADM) after the immediate

cessation of RP, suggesting that the lack of ATF3 may not affect early susceptibility to injury based on H&E analysis alone. However, the lack of ATF3 did improve tissue regeneration in RP based on findings seen seven days after cessation of RP. These findings support our previous work on ATF3 in the context of acute pancreatitis. Therefore, it is possible that the lack of ATF3 is playing a vital role by increasing the regenerative capacity of progenitor-like cells allowing for re-differentiation of ADM to acinar cells both in acute injury and RP during the regenerative phase. It is also possible that ATF3 is further signalling cells to a ductal cell fate, thus, preventing the increased re-differentiation of duct cells back to acinar cells during recovery. This raises the question of how ATF3 is capable of maintaining the ADM program making possible for further lesion progression and increasing susceptibility for PDAC development.

4.2.2 Regulation of intrinsic signalling factors in RP

During pancreatic injury, intrinsic factors that normally function to maintain the acinar cell phenotype are down-regulated and factors that promote the development of ADM are up-regulated (Park et al., 2011; Miyatsuka, 2006; Shi et al., 2013; Liou et al., 2013). Subsequently, the cells de-differentiate and take on a progenitor-like state which act to propagate and re-differentiate back to acinar cells in the absence of injury to cope for tissue loss (Liou et al., 2013; Houbracken et al. 2011). This thesis examined the requirement of ATF3 for changes in the expression of transcription factors involved in ADM. While no histological differences were observed in *Atf3*$^{-/-}$ mice immediately after cessation of injury; IF analysis supported a model in which ATF3 is required for repressing MIST1 expression during RP injury. The exact mechanism by which ATF3 represses MIST1 during RP injury was not examined directly, our laboratory's previous work indicated the *Mist1* gene is directly regulated by ATF3. Utilizing chromatin immunoprecipitation followed by Next Generation Sequencing (ChIP-Seq) the study showed ATF3 repressed *Mist1* by recruiting inhibitory histone deacetylase 5 (HDAC5) to the *Mist1* promoter (Fazio et al., 2017). It is possible that as long as ATF3 expression is maintained, HDAC5 remains bound to the MIST1 promoter, repressing its activity. In addition, along with MIST1 repression, there is a potential that ATF3 represses other

transcription factors involved in maintaining acinar cell identity, such as *Nr5a2* and *Rbpjl*. Further, it is also likely that after the immediate cessation of injury, the pool of cells that lack ATF3 and maintain MIST1 expression have not fully differentiated into a duct fate and have greater proliferative potential to cope for the loss of acinar cells. This theory would support the Ki67 results that show high proliferative capacity in *Atf3*$^{-/-}$ tissue compared to WT tissue immediately one-day after the cessation of injury.

Increased expression of both SOX9 and PDX1 are correlated with ADM (Stanger & Hebrok, 2013; Pinho et al., 2011; Rooman & Real, 2012). In addition, SOX9 and PDX1 are required for the maintence of ADM morphology along with the regulation of duct specific genes such as *Ck19* (Carrière et al., 2011). My findings suggest that in the absence of ATF3 both SOX9 and PDX1 expression are reduced compared to WT mice. This was further supported by reduced CK19 accumulation (marker of duct cells) in *Atf3*$^{-/-}$ tissue compared to WT tissue as seen by IHC analysis. Although, SOX9, PDX1 and CK19 expression is reduced in the absence of ATF3, there still appears to be duct-like structures that resemble ADM in the pancreas as seen by both H&E and IHC analysis. It is possible that other ADM promoting factors are compensating for the decreased expression of SOX9 (the main transcription factor involved in ADM development) in the absence of ATF3. Studies show that injury alone can induce ADM development to some extent in *Sox9*-deficient acinar cells, although *Sox9* overexpression is known to greatly promote ADM (Delous et al., 2012; Manfroid et al., 2012). It is also possible that hepatocyte nuclear factor 6 (HNF6) compensates for the absence of SOX9 allowing ADM development, although, less efficiently (Prévot et al., 2012; Manfroid et al., 2012). The expression of SOX9 and HNF6 work in synergy to promote ADM development and the expression of *Hnf6* is not maintained in more progressive lesions (PanIN lesions) while SOX9 is maintained (Prévot et al., 2012; Manfroid et al., 2012). Given the reduced accumulation of CK19, it does appear that ADM is significantly impaired in the absence of ATF3. It is possible that putative ADM is not derived from acinar cells (i.e. they are physiological ducts).

4.2.3 Regulation of extrinsic signalling factors in RP

The molecular program of ADM is widely studied whether it be through intrinsic or extrinsic signalling pathways (Bryant et al., 2014; O'Hagan & Heyer, 2011; Liu & Kaufman, 2003; Ron & Walter, 2007). However, the mechanism by which ADM programming is triggered as a result of pancreatic insult is still not well understood. One postulated mechanism of ADM development by extrinsic signalling involves the release of the cytokine TNF-α by macrophages, which can infiltrate the parenchymal tissue as result of inflammation and damage (Clark et al., 2007). TNF-α can bind EGFR, stimulate over-activation of MAPK signalling, and induce the formation of ADM both in culture and mouse models (Liou et al., 2015; Liou et al., 2016). Although not examined in the context of RP, ATF3 may play a role in macrophage infiltration and EGFR signalling during RP. Our previous study examining acute pancreatitis showed genes linked to the EGFR signalling pathway were indeed downregulated in the absence of ATF3. Hedgehog signalling is another factor involved in promoting ADM development. Damaged acinar cells through Hedgehog paracrine signalling activate fibroblast cells into stellate cells (Yauch et al., 2008; Bailey et al., 2008). My results showed ATF3 does not affect overall pancreatic fibrosis based on the amount of collagen deposits seen in the ECM post injury and recovery. However, it is possible that ATF3 has a specific role in pancreatic stellate cells. There are a number of studies that suggest ATF3 regulates fibrosis in other systems (Mallano et al., 2016; Kim et al., 2017). In contrast, there remains a bigger role for ATF3 signalling in acinar cells compared to cells of the stroma. Indeed, a previous study in our lab showed a 60-fold increase in ATF3 expression in acinar cells within four hours of acute pancreatitis (Fazio et al. 2017). As a result, this thesis focused heavily on intrinsic factors in acinar cells involved in triggering ADM.

4.2.4 Role of ATF3 in the presence of oncogenic KRAS

Next, I wanted determined whether the loss of ATF3 would reduce or prevent ADM in the presence of oncogenic KRAS. To do this, oncogenic KRAS was activated specifically in adult acinar cells followed by the induction of acute pancreatic injury. Pancreatic injury resulted in both *Atf3*$^{+/+}$*; Ptf1a*$^{creERT/+}$*; Kras*$^{LSL\text{-}G12D/+}$ and *Atf3*$^{-/-}$*; Ptf1a*$^{creERT/+}$*; Kras*$^{LSL\text{-}G12D/+}$ mice losing body weight compared *to Atf3*$^{+/+}$*; Ptf1a*$^{creERT/+}$ and *Atf3*$^{-/-}$*; Ptf1a*$^{creERT/+}$ mice within five weeks after injury. Surprisingly, *Atf3*$^{-/-}$*; Ptf1a*$^{creERT/+}$*; Kras*$^{LSL\text{-}G12D/+}$ mice lost significantly more body weight compared to *Atf3*$^{+/+}$*; Ptf1a*$^{creERT/+}$*; Kras*$^{LSL\text{-}G12D/+}$ mice, suggesting that overall health had been compromised. Studies demonstrate KRAS^{G12D} activation along with pancreatitis is sufficient to induce PDAC within five months (Guerra et al., 2007). Surprisingly, this thesis showed gross morphological characteristics (based on nodules and fibrosis) of PDAC and confirmed through histological grading that PDAC occurred in *Atf3*$^{+/+}$*; Ptf1a*$^{creERT/+}$*; Kras*$^{LSL\text{-}G12D/+}$ mice alone within two weeks of acute pancreatitis after oncogenic KRAS activation. It is possible that PDAC incidences are occurring earlier as a result of widespread cre-recombination, thus greater degree of KRAS^{G12D} activation seen in acinar cells (97.98 ± 0.17% Cre-efficiency).

Gross morphologically *Atf3*$^{-/-}$*; Ptf1a*$^{creERT/+}$*; Kras*$^{LSL\text{-}G12D/+}$ pancreata appeared small in size, which suggests that the loss in body weight is likely correlated to the loss of healthy pancreatic tissue. It is unlikely that the size differences of the pancreas seen between *Atf3*$^{+/+}$*; Ptf1a*$^{creERT/+}$*; Kras*$^{LSL\text{-}G12D/+}$ and *Atf3*$^{-/-}$*; Ptf1a*$^{creERT/+}$*; Kras*$^{LSL\text{-}G12D/+}$ mice is due to differences in water weight alone (edema), as the tissue histologically showed no signs of epithelial cell swelling in both *Atf3*$^{+/+}$*; Ptf1a*$^{creERT/+}$*; Kras*$^{LSL\text{-}G12D/+}$ and *Atf3*$^{-/-}$*; Ptf1a*$^{creERT/+}$*; Kras*$^{LSL\text{-}G12D/+}$ mice. It is possible that there may be differences in stromal fluid turgor pressure that could be resulting in the differences seen in tissue size. Analyzing dry tissue weight would help address this question in the future. More likely, the differences seen in pancreatic size may be explained by differences in lesion grade and accumulation. To address this, tissue samples were analyzed and graded histologically.

Interestingly, my results based on H&E indicated no overt differences in lesion grade between *Atf3*$^{+/+}$*; Ptf1a*$^{creERT/+}$*; Kras*$^{LSL\text{-}G12D/+}$ and *Atf3*$^{-/-}$*; Ptf1a*$^{creERT/+}$*; Kras*$^{LSL\text{-}G12D/+}$ pancreatic tissue within two weeks of pancreatic injury. However, by five weeks of injury, *Atf3*$^{-/-}$*; Ptf1a*$^{creERT/+}$*; Kras*$^{LSL\text{-}G12D/+}$ tissue showed lower incidences of high grade PanIN3 lesions and no incidences of PDAC compared to *Atf3*$^{+/+}$*; Ptf1a*$^{creERT/+}$*; Kras*$^{LSL\text{-}G12D/+}$ tissue. In accordance with other studies (Chen et al., 2018; Bailey et al., 2014; Rooman & Real, 2012) we showed through lineage tracing that PanIN lesions were indeed arising from acinar cells in both *Atf3*$^{+/+}$*; Ptf1a*$^{creERT/+}$*; Kras*$^{LSL\text{-}G12D/+}$ and *Atf3*$^{-/-}$*; Ptf1a*$^{creERT/+}$*; Kras*$^{LSL\text{-}G12D/+}$ tissue and not resident duct cells. Further, studies indicate that mucins (MUC1 and MUC4 proteins primarily) are atypically expressed in PDAC and is strongly correlated with tumour size, dysplasia and high grade PanIN lesions (Suh et al., 2017). Similarly, my work showed a high degree of mucin accumulation in *Atf3*$^{+/+}$*; Ptf1a*$^{creERT/+}$*; Kras*$^{LSL\text{-}G12D/+}$ tissue within five weeks of injury based on Alcian blue analysis that targets all acidic mucins. In contrast, *Atf3*$^{-/-}$*; Ptf1a*$^{creERT/+}$*; Kras*$^{LSL\text{-}G12D/+}$ tissue had lower levels of mucin compared to *Atf3*$^{+/+}$*; Ptf1a*$^{creERT/+}$*; Kras*$^{LSL\text{-}G12D/+}$ tissue. These findings support histological findings that indicate a reduction in high-grade lesions in *Atf3*$^{-/-}$*; Ptf1a*$^{creERT/+}$*; Kras*$^{LSL\text{-}G12D/+}$ tissue. Although, similar incidences of high grade PanIN lesions were seen early on in *Atf3*$^{-/-}$*; Ptf1a*$^{creERT/+}$*; Kras*$^{LSL\text{-}G12D/+}$ tissue, it is possible that further progression to PDAC does not occur in *Atf3*$^{-/-}$*; Ptf1a*$^{creERT/+}$*; Kras*$^{LSL\text{-}G12D/+}$ mice, or that there is an increase in apoptotic cell death that leads to loss of PanIN3 lesions within the span of five weeks after injury. This would potentially explain the gross morphological size differences seen between the genotypes. In either event more epithelial tissue is still lost in *Atf3*$^{-/-}$*; Ptf1a*$^{creERT/+}$*; Kras*$^{LSL\text{-}G12D/+}$ mice.

It is possible that the reduction in epithelial cells as marked by YFP and CK19 staining is one factor that resulted in an atrophied pancreas seen in *Atf3*$^{-/-}$*; Ptf1a*$^{creERT/+}$*; Kras*$^{LSL\text{-}G12D/+}$ tissue. It is also possible that epithelial cells exhibit reduced proliferation, which is supported by reduced Ki67^{+} cells in *Atf3*$^{-/-}$*; Ptf1a*$^{creERT/+}$*; Kras*$^{LSL\text{-}G12D/+}$ tissue. To further expand on these two key findings, it would be important to co-stain for CK19 and YFP to determine if ducts derived from non-acinar cells within the pancreas expand upon

pancreatic injury. My analysis identified large duct-like lesions that do not express YFP in *Atf3*$^{-/-}$*; Ptf1a*$^{creERT/+}$*; Kras*$^{LSL\text{-}G12D/+}$ tissue, which would support this theory. Finally, it is possible that high-grade lesions within *Atf3*$^{-/-}$*; Ptf1a*$^{creERT/+}$*; Kras*$^{LSL\text{-}G12D/+}$ tissue cannot be maintained and undergo apoptotic cell death by week five post injury. This would support the low lesion accumulation seen at week five and the remaining non-acinar lineage lesions seen in *Atf3*$^{-/-}$*; Ptf1a*$^{creERT/+}$*; Kras*$^{LSL\text{-}G12D/+}$ tissue that are likely just duct cells. In the future, makers of cell death need to be examined to factor in this possibility.

4.2.5 Regulation of factors by ATF3 in KRAS^{G12D} background

My findings demonstrate that along with reduced CK19 accumulation there is reduced SOX9 and pERK accumulation in *Atf3*$^{-/-}$*; Ptf1a*$^{creERT/+}$*; Kras*$^{LSL\text{-}G12D/+}$mice. The downstream mediators of the MAPK signalling pathway are often targeted to attenuate ADM and PanIN lesion progression in PDAC (Engelman et al., 2008; Castellano et al., 2013). The exact point in which ATF3 regulates the MAPK signalling pathway is hard to delineate. Currently, no antibody specific for oncogenic KRAS exists to show that oncogenic KRAS activity is directly affected by ATF3 expression (Nussinov et al., 2018). Although, potential mechanisms can be postulated for MAPK and SOX9 expression by ATF3 based on other studies. For example, in non-small-cell lung carcinoma (NSCLC) ATF3 is known to regulate MEK and pERK to promote carcinogenesis (Bar et al., 2011). It is possible that ATF3 similarly could be regulating upstream mediators such as MEK and RAF along with pERK in PDAC. In future studies, upstream mediators will be examined to address this question. Interestingly, a study done by Chen et al., 2015 found that depletion of Nuclear Factor of Activated T cells c1 (NFATc1) caused a loss of SOX9 expression even upon EGFR activation. Further, the study found that NFATc1 was recruited to the *Sox9* promoter in response to EGFR activation. It could be possible that ATF3 is upregulating pERK expression to induce EGFR mediated NFATc1 activation along with directly binding the *Sox9* promoter. The exploration of NFATc1 expression in the context of ATF3 in a KRAS^{G12D} background may provide us with a potential mechanistic axis for ADM regulation. In contrast, it is also likely that ATF3 may be influencing its effects in a non-acinar cell manner to

promote PDAC. To address this point, cells of the microenvironment were examined in in the context of oncogenic KRAS.

Since this thesis utilized a global knockout for *Atf3*, we cannot discern acinar from non-acinar roles of ATF3. This is important since ATF3 affects cancer progression in other systems (Gardian et al., 2012; Kurahara et al., 2011; Helm et al., 2014). The lack of *Atf3* expression globally provides the comparative possibility of examining other cell types that may be contributing to PDAC progression. My findings showed that there was more fibrosis within two weeks of injury in $Atf3^{-/-}; Ptf1a^{creERT/+}; Kras^{LSL\text{-}G12D/+}$ tissue and was found to be comparable by five weeks of injury to $Atf3^{+/+}; Ptf1a^{creERT/+}; Kras^{LSL\text{-}G12D/+}$ tissue. Interestingly, α-SMA protein expression was found to not differ between the genotypes at both time points. It is unlikely that stellate cells as marked by α-SMA alone is capable of remodelling the ECM. Rather, it is likely a complex interaction between macrophages and stellate cells that results in significant degree of fibrosis seen in PDAC (Shi et al., 2014). Although, precise macrophage-stellate interactions were not studied, my results showed less macrophage infiltration in $Atf3^{-/-}; Ptf1a^{creERT/+}; Kras^{LSL\text{-}G12D/+}$ tissue within five weeks of injury. Tumor-associated macrophages (TAMs) promote cancer fibrosis by secreting factors that activate fibroblast-mediated extracellular matrix remodeling (Clark et al., 2007). Interesting, it is possible that early into injury, TAMS infiltrate the $Atf3^{-/-}; Ptf1a^{creERT/+}; Kras^{LSL\text{-}G12D/+}$ ECM and promote fibrosis, but over time undergo cellular death or infiltration is prevented in the absence of ATF3 later in pancreatic injury. It is difficult to draw mechanistic conclusions without precisely knocking out ATF3 in stellate cells and macrophages. Future studies will examine ATF3's role in a cell specific manner.

In summary, the findings in this study support a role for ATF3 in pancreatic injury. In the context of RP, it was shown that the lack of ATF3 maintains factors involved in promoting acinar cell maturation in addition to repressing factors involved in promoting ADM. As a result, the lack of ATF3 promoted significant tissue regeneration. In the context of oncogenic KRAS, the lack of ATF3 similarly repressed factors involved in ADM and prevented further high grade PanIN3 lesion development. Interestingly, the

pancreas atrophied in size likely due to the lack of lesion accumulation or potentially due to cellular death in addition to less lesion accumulation. A proposed schematic model of the findings can be seen in (**Figure 4.1**).

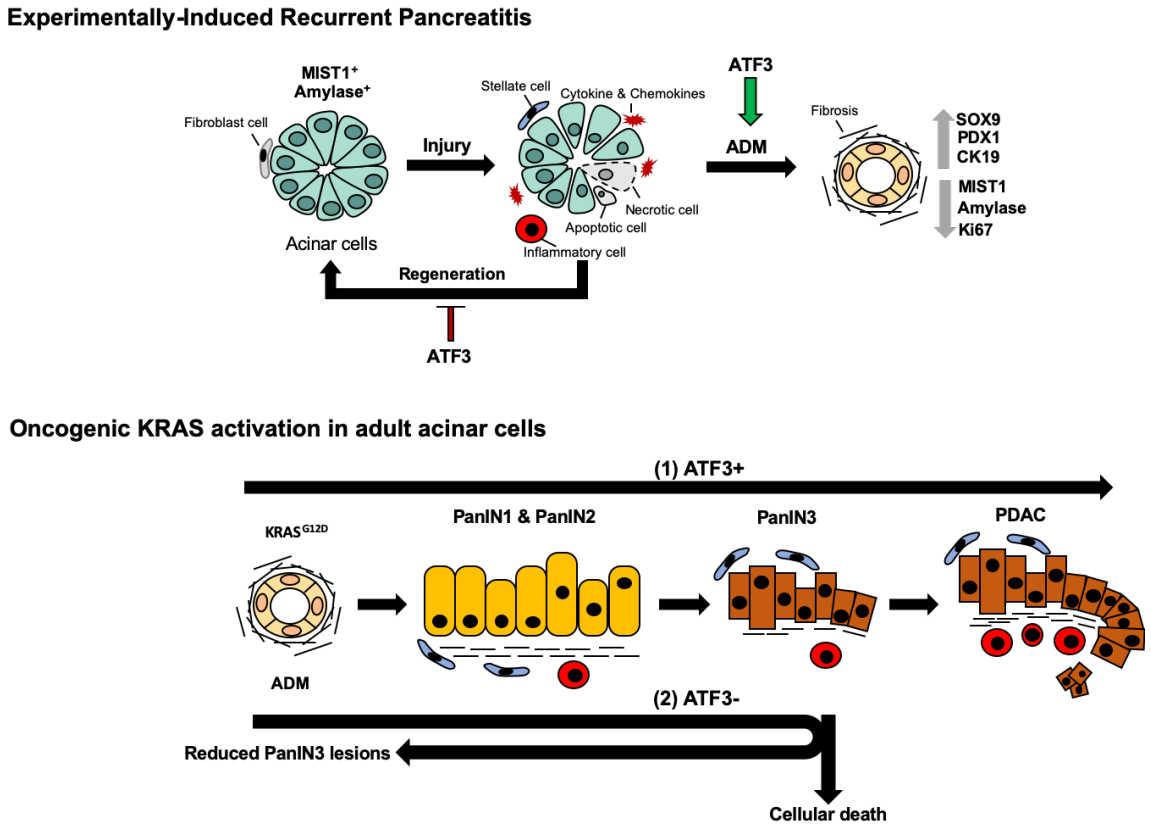

Figure 4.1. Purposed model for ATF3 in experimental RP and its role in the context of oncogenic KRAS. In this model, the lack of ATF3 allows for increased tissue regeneration in experimentally induced RP. Once oncogenic KRAS is activated the lack of ATF3 reduces high grade PanIN3 lesions and has an affect on the fibroinflammatory profile of the tissue within five weeks of post CIP.

4.3 Limitations & Future directions

The limitations for this study in the context of RP as alluded before includes the lack of immune profiling in addition to the lack of EGFR signalling pathway analysis. It would have been interesting to determine if the lack of ATF3 altered macrophage infiltration early into damage or during recovery. Secondly, the examination of the EGFR signalling pathway would have highlighted potential mechanisms between the ATF3-pERK-SOX9 axis in promoting ADM development and progression. In the context of oncogenic KRAS, this study would have benefited if cellular death was examined to rule out the possibility of apoptotic cellular death accounting for the atrophied pancreatic size seen in *Atf3*$^{-/-}$*; Ptf1a*$^{creERT/+}$*; Kras*$^{LSL\text{-}G12D/+}$ pancreata.

In future studies, to further determine if ATF3 binding of promoters persists throughout RP, it could be beneficial to run ChIP-seq for acinar cells isolated from each time point. This would help answer if ATF3 is still bound and is altering transcription or if other transcription factors takeover and ATF3 becomes dispensable. To tease out intracellular mechanisms that promote ADM, the investigation of transcription factors involved in this pathway could be examined ex-vivo in culture. This would better solidify current in-vivo findings.

This study showed that oncogenic KRAS alone in the presence or absence of ATF3 promotes focal lesions within 5 weeks of injury. In future long-term studies, it would be interesting to determine if *Atf3*$^{-/-}$*; Ptf1a*$^{creERT/+}$*; Kras*$^{LSL\text{-}G12D/+}$ tissue with oncogenic KRAS activation but without injury limits PanIN progression compared to *Atf3*$^{+/+}$*; Ptf1a*$^{creERT/+}$*; Kras*$^{LSL\text{-}G12D/+}$ mice alone. In addition, lower doses of tamoxifen may be administered to induce focal recombination of oncogenic KRAS activation and determine if lesions prevented from developing into high grade lesions when injury is induced in the absence of ATF3. Also, it is difficult to delineate the cell-specific contributions of ATF3 due to *Atf3* being globally knockout. To tease out a potential mechanism, *Atf3* can be ablated in a cell specific manner in future studies.

CHAPTER 5

5 REFERENCES

Abdulla, A., Awla, D., Thorlacius, H., & Regnér, S. (2011). Role of neutrophils in the activation of trypsinogen in severe acute pancreatitis. Journal of Leukocyte Biology, 90(5), 975–982.

Ahn, D. H., Krishna, K., Blazer, M., Reardon, J., Wei, L., Wu, C., … Bekaii-Saab, T. (2017). A modified regimen of biweekly gemcitabine and nab-paclitaxel in patients with metastatic pancreatic cancer is both tolerable and effective: a retrospective analysis. Therapeutic Advances in Medical Oncology, 9(2), 75–82.

Anido, J., Sáez-Borderías, A., Gonzàlez-Juncà, A., Rodón, L., Folch, G., Carmona, M. A., … Seoane, J. (2010). TGF-β Receptor Inhibitors Target the CD44high/Id1high Glioma-Initiating Cell Population in Human Glioblastoma. Cancer Cell, 18(6), 655–668.

Archer, H., Jura, N., Keller, J., Jacobson, M., & Bar-Sagi, D. (2006). A mouse model of hereditary pancreatitis generated by transgenic expression of R122H trypsinogen. Gastroenterology, 131(6), 1844–55.

Ardito, C. M., Grüner, B. M., Takeuchi, K. K., Lubeseder-Martellato, C., Teichmann, N., Mazur, P. K., … Siveke, J. T. (2012). EGF receptor is required for KRAS-induced pancreatic tumorigenesis. Cancer Cell, 22(3), 304–17.

Athwal, T., Huang, W., Mukherjee, R., Latawiec, D., Chvanov, M., Clarke, R., … Vlatković, N. (2014). Expression of human cationic trypsinogen (PRSS1) in murine acinar cells promotes pancreatitis and apoptotic cell death. Cell Death & Disease, 5(4), e1165.

Bailey, J. M., DelGiorno, K. E., & Crawford, H. C. (2014). The secret origins and surprising fates of pancreas tumors. Carcinogenesis, 35(7), 1436–40.

Bailey, J. M., Swanson, B. J., Hamada, T., Eggers, J. P., Singh, P. K., Caffery, T., … Hollingsworth, M. A. (2008). Sonic hedgehog promotes desmoplasia in pancreatic cancer. Clinical Cancer Research: An Official Journal of the American Association for Cancer Research, 14(19), 5995–6004.

Bandyopadhyay, S., Wang, Y., Zhan, R., Pai, S. K., Watabe, M., Iiizumi, M., … Watabe, K. (2006). The Tumor Metastasis Suppressor Gene Drg-1 Down-regulates the Expression of Activating Transcription Factor 3 in Prostate Cancer. Cancer Research, 66(24), 11983–11990.

Bar, J., Gorn-hundermann, I., Reid, S., O'Brien, A., Niknejad, N., Goss, G. D., & Dimitroulakos, J. (2011). Activating transcription factor 3 (ATF3) as a potential biomarker of platinum sensitivity in non-small cell lung cancer (NSCLC). Journal of Clinical Oncology, 29(15_suppl), e21012–e21012.

Basturk, O., Hong, S.-M., Wood, L. D., Adsay, N. V., Albores-Saavedra, J., Biankin, A. V, … Baltimore Consensus Meeting. (2015). A Revised Classification System and Recommendations From the Baltimore Consensus Meeting for Neoplastic Precursor Lesions in the Pancreas. The American Journal of Surgical Pathology, 39(12), 1730–41.

Baumann, B., Wagner, M., Aleksic, T., von Wichert, G., Weber, C. K., Adler, G., & Wirth, T. (2007). Constitutive IKK2 activation in acinar cells is sufficient to induce pancreatitis in vivo. The Journal of Clinical Investigation, 117(6), 1502–13.

Bayne, L. J., Beatty, G. L., Jhala, N., Clark, C. E., Rhim, A. D., Stanger, B. Z., & Vonderheide, R. H. (2012). Tumor-Derived Granulocyte-Macrophage Colony-

Stimulating Factor Regulates Myeloid Inflammation and T Cell Immunity in Pancreatic Cancer. Cancer Cell, 21(6), 822–835.

Beatty, G. L., Chiorean, E. G., Fishman, M. P., Saboury, B., Teitelbaum, U. R., Sun, W., … Vonderheide, R. H. (2011). CD40 Agonists Alter Tumor Stroma and Show Efficacy Against Pancreatic Carcinoma in Mice and Humans. Science, 331(6024), 1612–1616.

Bernales, S., Papa, F. R., & Walter, P. (2006). Intracellular Signaling by the Unfolded Protein Response. Annual Review of Cell and Developmental Biology, 22(1), 487–508.

Boespflug, N. D., Kumar, S., McAlees, J. W., Phelan, J. D., Grimes, H. L., Hoebe, K., … Karp, C. L. (2014). ATF3 is a novel regulator of mouse neutrophil migration. Blood, 123(13), 2084–93.

Bos, J. L. (1989). ras oncogenes in human cancer: a review. Cancer Research, 49(17), 4682–9.

Brady, M., Bhatia, M., Christmas, S., Boyd, M. T., Neoptolemos, J. P., & Slavin, J. (2002). Expression of the chemokines MCP-1/JE and cytokine-induced neutrophil chemoattractant in early acute pancreatitis. Pancreas, 25(3), 260–9.

Breast Cancer Linkage Consortium, T. (1999). Cancer Risks in BRCA2 Mutation Carriers. JNCI Journal of the National Cancer Institute, 91(15), 1310–1316.

Brooks, A. C., Guo, Y., Singh, M., McCracken, J., Xuan, Y.-T., Srivastava, S., … Bhatnagar, A. (2014). Endoplasmic reticulum stress-dependent activation of ATF3 mediates the late phase of ischemic preconditioning. Journal of Molecular and Cellular Cardiology, 76, 138–47.

Brown, S. L., Sekhar, K. R., Rachakonda, G., Sasi, S., & Freeman, M. L. (2008). Activating Transcription Factor 3 Is a Novel Repressor of the Nuclear Factor Erythroid-

Derived 2 Related Factor 2 (Nrf2) Regulated Stress Pathway. Cancer Research, 68(2), 364–368.

Bryant, K. L., Mancias, J. D., Kimmelman, A. C., & Der, C. J. (2014). KRAS: Feeding pancreatic cancer proliferation. Trends in Biochemical Sciences, 39(2), 91–100.

Calle, E. E., Rodriguez, C., Walker-Thurmond, K., & Thun, M. J. (2003). Overweight, Obesity, and Mortality from Cancer in a Prospectively Studied Cohort of U.S. Adults. n engl j med (Vol. 17).

Campos, M. L., Sánchez-Arévalo Lobo, V. J., Rodolosse, A., Gottardi, C. J., Mafficini, A., Beghelli, S., … Real, F. X. (2013). ICAT is a novel Ptf1a interactor that regulates pancreatic acinar differentiation and displays altered expression in tumours. Biochemical Journal, 451(3), 395–405.

Cancer Genome Atlas Research Network. Electronic address: andrew_aguirre@dfci.harvard.edu, T. C. G. A. R., & Cancer Genome Atlas Research Network. (2017). Integrated Genomic Characterization of Pancreatic Ductal Adenocarcinoma. Cancer Cell, 32(2), 185–203.e13.

Carrière, C., Young, A. L., Gunn, J. R., Longnecker, D. S., & Korc, M. (2011). Acute Pancreatitis Accelerates Initiation and Progression to Pancreatic Cancer in Mice Expressing Oncogenic Kras in the Nestin Cell Lineage. PLoS ONE, 6(11), e27725.

Castellano, E., & Downward, J. (2011). RAS Interaction with PI3K: More Than Just Another Effector Pathway. Genes & Cancer, 2(3), 261.

Castellano, E., Sheridan, C., Thin, M. Z., Nye, E., Spencer-Dene, B., Diefenbacher, M. E., … Downward, J. (2013). Requirement for interaction of PI3-kinase p110α with RAS in lung tumor maintenance. Cancer Cell, 24(5), 617–30.

Charnley, R. M. (2003). Hereditary pancreatitis. World Journal of Gastroenterology, 9(1), 1–4.

Chen, N. M., Singh, G., Koenig, A., Liou, G. Y., Storz, P., Zhang, J. S., … Hessmann, E. (2015). NFATc1 Links EGFR Signaling to Induction of Sox9 Transcription and Acinar-Ductal Transdifferentiation in the Pancreas. Gastroenterology, 148(5), 1024–1034.e9.

Chen, Y., Lebleu, V. S., Carstens, J. L., Sugimoto, H., Zheng, X., Malasi, S., … Kalluri, R. (2018). Dual reporter genetic mouse models of pancreatic cancer identify an epithelial-to-mesenchymal transition-independent metastasis program. EMBO Mol Med, 9085.

Clark, C. E., Hingorani, S. R., Mick, R., Combs, C., Tuveson, D. A., & Vonderheide, R. H. (2007). Dynamics of the immune reaction to pancreatic cancer from inception to invasion. Cancer Research, 67(19), 9518–27.

Collins, M. A., Bednar, F., Zhang, Y., Brisset, J.-C., Galbán, S., Galbán, C. J., … Magliano, M. P. di. (2012). Oncogenic Kras is required for both the initiation and maintenance of pancreatic cancer in mice. The Journal of Clinical Investigation, 122(2), 639–653.

Collins, M. A., Brisset, J.-C., Zhang, Y., Bednar, F., Pierre, J., Heist, K. A., … di Magliano, M. P. (2012). Metastatic pancreatic cancer is dependent on oncogenic Kras in mice. PloS One, 7(12), e49707.

Collisson, E. A., Trejo, C. L., Silva, J. M., Gu, S., Korkola, J. E., Heiser, L. M., … McMahon, M. (2012). A central role for RAF→MEK→ERK signaling in the genesis of pancreatic ductal adenocarcinoma. Cancer Discovery, 2(8), 685–93.

Conroy, T., Desseigne, F., Ychou, M., Bouché, O., Guimbaud, R., Bécouarn, Y., … Ducreux, M. (2011). FOLFIRINOX versus Gemcitabine for Metastatic Pancreatic Cancer. New England Journal of Medicine, 364(19), 1817–1825.

Couch, F. J., Johnson, M. R., Rabe, K. G., Brune, K., de Andrade, M., Goggins, M., … Hruban, R. H. (2007). The Prevalence of BRCA2 Mutations in Familial Pancreatic Cancer. Cancer Epidemiology Biomarkers & Prevention, 16(2), 342–346.

Crespo, P., & León, J. (2000). Ras proteins in the control of the cell cycle and cell differentiation. Cellular and Molecular Life Sciences: CMLS, 57(11), 1613–36.

Crockett, S. D., Wani, S., Gardner, T. B., Falck-Ytter, Y., Barkun, A. N., Crockett, S., … Weinberg, D. (2018). American Gastroenterological Association Institute Guideline on Initial Management of Acute Pancreatitis. Gastroenterology, 154(4), 1096–1101.

Cui, H., Guo, M., Xu, D., Ding, Z.-C., Zhou, G., Ding, H.-F., … Yan, C. (2015). ARTICLE The stress-responsive gene ATF3 regulates the histone acetyltransferase Tip60. Nature Communications, 6.

Czakó, L., Takács, T., Varga, I. S., Tiszlavicz, L., Hai, D. Q., Hegyi, P., … Lonovics, J. (1998). Involvement of oxygen-derived free radicals in L-arginine-induced acute pancreatitis. Digestive Diseases and Sciences, 43(8), 1770–7.

DAWN, B., Xuan, Y.-T., Guo, Y., Rezazadeh, A., Stein, A. B., Hunt, G., … Bolli, R. (2004). IL-6 plays an obligatory role in late preconditioning via JAK?STAT signaling and upregulation of iNOS and COX-2. Cardiovascular Research, 64(1), 61–71.

de Latouliere, L., Manni, I., Iacobini, C., Pugliese, G., Grazi, G. L., Perri, P., … Piaggio, G. (2016). A bioluminescent mouse model of proliferation to highlight early stages of pancreatic cancer: A suitable tool for preclinical studies. Annals of Anatomy - Anatomischer Anzeiger, 207, 2–8.

Delous, M., Yin, C., Shin, D., Ninov, N., Debrito Carten, J., Pan, L., … Stainier, D. Y. R. (2012). sox9b Is a Key Regulator of Pancreaticobiliary Ductal System Development. PLoS Genetics, 8(6), e1002754.

Di Magliano, M. P., & Logsdon, C. D. (2013). Roles for KRAS in pancreatic tumor development and progression. Gastroenterology, 144, 1220-9.

Eferl, R., & Wagner, E. F. (2003). AP-1: a double-edged sword in tumorigenesis. Nature Reviews Cancer, 3(11), 859–868.

Engelman, J. A., Chen, L., Tan, X., Crosby, K., Guimaraes, A. R., Upadhyay, R., … Wong, K.-K. (2008). Effective use of PI3K and MEK inhibitors to treat mutant Kras G12D and PIK3CA H1047R murine lung cancers. Nature Medicine, 14(12), 1351–1356.

Eser, S., Reiff, N., Messer, M., Seidler, B., Gottschalk, K., Dobler, M., … Saur, D. (2013). Selective Requirement of PI3K/PDK1 Signaling for Kras Oncogene-Driven Pancreatic Cell Plasticity and Cancer. Cancer Cell, 23(3), 406–420.

Eser, S., Schnieke, A., Schneider, G., & Saur, D. (2014). Oncogenic KRAS signalling in pancreatic cancer. British Journal of Cancer, 111(5), 817–22.

Etemad, B., & Whitcomb, D. C. (2001). Chronic Pancreatitis: Diagnosis, Classification, and New Genetic Developments. Gastroenterology, 120, 682-707.

Fagenholz, P. J., Castillo, C. F.-D., Harris, N. S., Pelletier, A. J., & Camargo, C. A. (2007). Increasing United States Hospital Admissions for Acute Pancreatitis, 1988–2003. Annals of Epidemiology, 17(7), 491.e1-491.e8.

Fazio, E. N., Young, C. C., Toma, J., Levy, M., Berger, K. R., Johnson, C. L., … Pin, C. L. (2017). Activating transcription factor 3 promotes loss of the acinar cell phenotype in response to cerulein-induced pancreatitis in mice. Molecular Biology of the Cell, 28(18), 2347–2359.

Feig, C., Jones, J. O., Kraman, M., Wells, R. J. B., Deonarine, A., Chan, D. S., … Fearon, D. T. (2013). Targeting CXCL12 from FAP-expressing carcinoma-associated fibroblasts synergizes with anti-PD-L1 immunotherapy in pancreatic cancer. Proceedings of the National Academy of Sciences, 110(50), 20212–20217.

Fendrich, V., Esni, F., Garay, M. V. R., Feldmann, G., Habbe, N., Jensen, J. N., … Maitra, A. (2008). Hedgehog signaling is required for effective regeneration of exocrine pancreas. Gastroenterology, 135(2), 621–31.

Ferreira, R. M. M., Sancho, R., Messal, H. A., Nye, E., Spencer-Dene, B., Stone, R. K., … Behrens, A. (2017). Duct- and Acinar-Derived Pancreatic Ductal Adenocarcinomas Show Distinct Tumor Progression and Marker Expression. Cell Reports, 21(4), 966–978.

Fisher, W. E. (2001). Diabetes: risk factor for the development of pancreatic cancer or manifestation of the disease? World Journal of Surgery, 25(4), 503–8.

Furuyama, K., Kawaguchi, Y., Akiyama, H., Horiguchi, M., Kodama, S., Kuhara, T., … Uemoto, S. (2011). Continuous cell supply from a Sox9-expressing progenitor zone in adult liver, exocrine pancreas and intestine. Nature Genetics, 43(1), 34–41.

Gardian, K., Janczewska, S., Olszewski, W. L., & Durlik, M. (2012). Analysis of pancreatic cancer microenvironment: role of macrophage infiltrates and growth factors expression. Journal of Cancer, 3, 285–91.

Ghadirian, P., Boyle, P., Simard, A., Baillargeon, J., Maisonneuve, P., & Perret, C. (n.d.). Reported family aggregation of pancreatic cancer within a population-based case-control study in the francophone community in Montreal, Canada. International Journal of Pancreatology, 10(3–4), 183–196.

Gilchrist, M., Thorsson, V., Li, B., Rust, A. G., Korb, M., Kennedy, K., … Aderem, A. (2006). Systems biology approaches identify ATF3 as a negative regulator of Toll-like receptor 4. Nature, 441(7090), 173–178.

Grimont, A., Pinho, A. V, Cowley, M. J., Augereau, C., Mawson, A., Giry-Laterrière, M., … Jacquemin, P. (2015). SOX9 regulates ERBB signalling in pancreatic cancer development. Gut, 64(11), 1790–9.

Gu, G., Dubauskaite, J., & Melton, D. A. (2002). Direct evidence for the pancreatic lineage: NGN3+ cells are islet progenitors and are distinct from duct progenitors. Development (Cambridge, England), 129(10), 2447–57.

Guda, N. M., Trikudanathan, G., & Freeman, M. L. (2018). Idiopathic recurrent acute pancreatitis. The Lancet. Gastroenterology & Hepatology, 3(10), 720–728.

Guerra, C., Collado, M., Navas, C., Schuhmacher, A. J., Hernández-Porras, I., Cañamero, M., … Barbacid, M. (2011). Pancreatitis-Induced Inflammation Contributes to Pancreatic Cancer by Inhibiting Oncogene-Induced Senescence. Cancer Cell, 19(6), 728–739.

Guerra, C., Schuhmacher, A. J., Cañamero, M., Grippo, P. J., Verdaguer, L., Pérez-Gallego, L., … Barbacid, M. (2007). Chronic pancreatitis is essential for induction of pancreatic ductal adenocarcinoma by K-Ras oncogenes in adult mice. Cancer Cell, 11(3), 291–302.

Guo, N., Meng, C., Bai, W., Wei, Q., Shi, F., Davis, J. S., & Mao, D. (2015). Prostaglandin F2α induces expression of activating transcription factor 3 (ATF3) and activates MAPK signaling in the rat corpus luteum. Acta Histochemica, 117(2), 211–218.

Hai, T., Wolfgang, C. D., Marsee, D. K., Allen, A. E., & Sivaprasad, U. (1999). ATF3 and stress responses. Gene Expression, 7(4–6), 321–35.

Hale, M. A., Kagami, H., Shi, L., Holland, A. M., Elsässer, H.-P., Hammer, R. E., & MacDonald, R. J. (2005). The homeodomain protein PDX1 is required at mid-pancreatic development for the formation of the exocrine pancreas. Developmental Biology, 286(1), 225–237.

Han, J., & Kaufman, R. J. (2017). Physiological/pathological ramifications of transcription factors in the unfolded protein response. Genes & Development, 31(14), 1417–1438.

Hegyi, P., Rakonczay, Z., Sári, R., Góg, C., Lonovics, J., Takács, T., & Czakó, L. (2004). L-arginine-induced experimental pancreatitis. World Journal of Gastroenterology, 10(14), 2003–9.

Helm, O., Held-Feindt, J., Grage-Griebenow, E., Reiling, N., Ungefroren, H., Vogel, I., … Sebens, S. (2014). Tumor-associated macrophages exhibit pro- and anti-inflammatory properties by which they impact on pancreatic tumorigenesis. International Journal of Cancer, 135(4), 843–861.

Hezel, A. F., Kimmelman, A. C., Stanger, B. Z., Bardeesy, N., & Depinho, R. A. (2006). Genetics and biology of pancreatic ductal adenocarcinoma. Genes & Development, 20(10), 1218–49.

Hingorani, S. R., Petricoin, E. F., Maitra, A., Rajapakse, V., King, C., Jacobetz, M. A., … Tuveson, D. A. (2003). Preinvasive and invasive ductal pancreatic cancer and its early detection in the mouse. Cancer Cell, 4(6), 437–50.

Hingorani, S. R., & Tuveson, D. A. (2003). Targeting oncogene dependence and resistance. Cancer Cell, 3(5), 414–417.

Hoetzenecker, W., Echtenacher, B., Guenova, E., Hoetzenecker, K., Woelbing, F., Brück, J., … Röcken, M. (2012). ROS-induced ATF3 causes susceptibility to secondary

infections during sepsis-associated immunosuppression. Nature Medicine, 18(1), 128–134.

Holderfield, M. (2018). Efforts to Develop KRAS Inhibitors. Cold Spring Harbor Perspectives in Medicine, 8(7), a031864.

Houbracken, I., de Waele, E., Lardon, J., Ling, Z., Heimberg, H., Rooman, I., & Bouwens, L. (2011). Lineage Tracing Evidence for Transdifferentiation of Acinar to Duct Cells and Plasticity of Human Pancreas. Gastroenterology, 141(2), 731–741.e4.

Hruban, R. H., Goggins, M., Parsons, J., & Kern, S. E. (2000). Progression model for pancreatic cancer. Clinical Cancer Research: An Official Journal of the American Association for Cancer Research, 6(8), 2969–72.

Hruban, R. H., Maitra, A., & Goggins, M. (2008). Update on pancreatic intraepithelial neoplasia. International Journal of Clinical and Experimental Pathology, 1(4), 306–16.

Hruban, R. H., Petersen, G. M., Ha, P. K., & Kern, S. E. (1998). Genetics of pancreatic cancer. From genes to families. Surgical Oncology Clinics of North America, 7(1), 1–23.

Hyun, J. J., & Lee, H. S. (2014). Experimental Models of Pancreatitis. Clinical Endoscopy, 47(3), 212.

Ishiguro, T., Nagawa, H., Naito, M., & Tsuruo, T. (2000). Inhibitory Effect of ATF3 Antisense Oligonucleotide on Ectopic Growth of HT29 Human Colon Cancer Cells. Japanese Journal of Cancer Research, 91(8), 833–836.

Iwawaki, T., Akai, R., & Kohno, K. (2010). IRE1α Disruption Causes Histological Abnormality of Exocrine Tissues, Increase of Blood Glucose Level, and Decrease of Serum Immunoglobulin Level. PLoS ONE, 5(9), e13052.

Jacobetz, M. A., Chan, D. S., Neesse, A., Bapiro, T. E., Cook, N., Frese, K. K., … Tuveson, D. A. (2013). Hyaluronan impairs vascular function and drug delivery in a mouse model of pancreatic cancer. Gut, 62(1), 112–20.

Jacobs, E. J., Chanock, S. J., Fuchs, C. S., Lacroix, A., McWilliams, R. R., Steplowski, E., … Zeleniuch-Jacquotte, A. (2010). Family history of cancer and risk of pancreatic cancer: a pooled analysis from the Pancreatic Cancer Cohort Consortium (PanScan). International Journal of Cancer, 127(6), 1421–8.

Jakkampudi, A., Jangala, R., Reddy, B. R., Mitnala, S., Reddy, D. N., & Talukdar, R. (2016). NF-κB in acute pancreatitis: Mechanisms and therapeutic potential. Pancreatology, 16(4), 477–488.

Je, Y.-J., Choi, D.-K., Sohn, K.-C., Kim, H.-R., Im, M., Lee, Y., … Seo, Y.-J. (2014). Inhibitory role of Id1 on TGF-β-induced collagen expression in human dermal fibroblasts. Biochemical and Biophysical Research Communications, 444(1), 81–85.

Jiang, H.-Y., Wek, S. A., McGrath, B. C., Lu, D., Hai, T., Harding, H. P., … Wek, R. C. (2004). Activating transcription factor 3 is integral to the eukaryotic initiation factor 2 kinase stress response. Molecular and Cellular Biology, 24(3), 1365–77.

Jiao, L., Berrington de Gonzalez, A., Hartge, P., Pfeiffer, R. M., Park, Y., Freedman, D. M., … Stolzenberg-Solomon, R. Z. (2010). Body mass index, effect modifiers, and risk of pancreatic cancer: a pooled study of seven prospective cohorts. Cancer Causes & Control: CCC, 21(8), 1305–14.

Kadowaki, H., & Nishitoh, H. (2013). Signaling Pathways from the Endoplasmic Reticulum and Their Roles in Disease. Genes, 4(3), 306.

Kalluri, R., & Zeisberg, M. (2006). Fibroblasts in cancer. Nature Reviews Cancer, 6(5), 392–401.

Karimgani, I., Porter, K. A., Langevin, R. E., & Banks, P. A. (1992). Prognostic factors in sterile pancreatic necrosis. Gastroenterology, 103(5), 1636–40.

Karki, A., Humphrey, S. E., Steele, R. E., Hess, D. A., Taparowsky, E. J., & Konieczny, S. F. (2015). Silencing Mist1 Gene Expression Is Essential for Recovery from Acute Pancreatitis. PLOS ONE, 10(12), e0145724.

Kim, D. E., Procopio, M.-G., Ghosh, S., Jo, S.-H., Goruppi, S., Magliozzi, F., … Dotto, G. P. (2017). Convergent roles of ATF3 and CSL in chromatin control of cancer-associated fibroblast activation. Journal of Experimental Medicine, 2349–2368.

Kim, K.-J., Lee, J., Park, Y., & Lee, S.-H. (2015). ATF3 Mediates Anti-Cancer Activity of Trans-10, cis-12-Conjugated Linoleic Acid in Human Colon Cancer Cells. Biomolecules & Therapeutics, 23(2), 134–140.

Kirkbride, M. B. (1912). THE ISLANDS OF LANGERHANS AFTER LIGATION OF THE PANCREATIC DUCTS. The Journal of Experimental Medicine, 15(1), 101.

Kleeff, J., Korc, M., Apte, M., La Vecchia, C., Johnson, C. D., Biankin, A. V., … Neoptolemos, J. P. (2016). Pancreatic cancer. Nature Reviews Disease Primers, 2, 16022.

Klein, A. P. (2012). Genetic susceptibility to pancreatic cancer. Molecular Carcinogenesis, 51(1), 14–24.

Koikawa, K., Ohuchida, K., Ando, Y., Kibe, S., Nakayama, H., Takesue, S., … Nakamura, M. (2018). Basement membrane destruction by pancreatic stellate cells leads to local invasion in pancreatic ductal adenocarcinoma. Cancer Letters, 425, 65–77.

Kopp, J. L., Dubois, C. L., Schaffer, A. E., Hao, E., Shih, H. P., Seymour, P. A., … Sander, M. (2011). Sox9+ ductal cells are multipotent progenitors throughout

development but do not produce new endocrine cells in the normal or injured adult pancreas. Development, 138(4), 653–665.

Kopp, J. L., von Figura, G., Mayes, E., Liu, F.-F., Dubois, C. L., Morris, J. P., … Sander, M. (2012). Identification of Sox9-dependent acinar-to-ductal reprogramming as the principal mechanism for initiation of pancreatic ductal adenocarcinoma. Cancer Cell, 22(6), 737–50.

Kowalik, A. S., Johnson, C. L., Chadi, S. A., Weston, J. Y., Fazio, E. N., & Pin, C. L. (2007). Mice lacking the transcription factor Mist1 exhibit an altered stress response and increased sensitivity to caerulein-induced pancreatitis. American Journal of Physiology-Gastrointestinal and Liver Physiology, 292(4), G1123–G1132.

Krah, N. M., O, J.-P. D. La, Swift, G. H., Hoang, C. Q., Willet, S. G., Pan, F. C., … Murtaugh, L. C. (2015). The acinar differentiation determinant PTF1A inhibits initiation of pancreatic ductal adenocarcinoma. ELife, 4.

Krapp, A., Knöfler, M., Ledermann, B., Bürki, K., Berney, C., Zoerkler, N., … Wellauer, P. K. (1998). The bHLH protein PTF1-p48 is essential for the formation of the exocrine and the correct spatial organization of the endocrine pancreas. Genes and Development, 12(23), 3752–3763.

Krishna, S. G., Kamboj, A. K., Hart, P. A., Hinton, A., & Conwell, D. L. (2017). The Changing Epidemiology of Acute Pancreatitis Hospitalizations. Pancreas, 46(4), 482–488.

Krüger, B., Albrecht, E., & Lerch, M. M. (2000). The Role of Intracellular Calcium Signaling in Premature Protease Activation and the Onset of Pancreatitis. The American Journal of Pathology, 157(1), 43–50.

Kurahara, H., Shinchi, H., Mataki, Y., Maemura, K., Noma, H., Kubo, F., … Takao, S. (2011). Significance of M2-polarized tumor-associated macrophage in pancreatic cancer. The Journal of Surgical Research, 167(2), e211-9.

Lankisch, P. G., Breuer, N., Bruns, A., Weber-Dany, B., Lowenfels, A. B., & Maisonneuve, P. (2009). Natural History of Acute Pancreatitis: A Long-Term Population-Based Study. The American Journal of Gastroenterology, 104(11), 2797–2805.

Lee, A.-H., Chu, G. C., Iwakoshi, N. N., & Glimcher, L. H. (2005). XBP-1 is required for biogenesis of cellular secretory machinery of exocrine glands. The EMBO Journal, 24(24), 4368–4380.

Lee, A. Y. L., Dubois, C. L., Sarai, K., Zarei, S., Schaeffer, D. F., Sander, M., & Kopp, J. L. (2018). Cell of origin affects tumour development and phenotype in pancreatic ductal adenocarcinoma. Gut, gutjnl-2017-314426.

Lerch, M. M., & Gorelick, F. S. (2013). Models of Acute and Chronic Pancreatitis. Gastroenterology, 144(6), 1180-1193.

Lew, D., Afghani, E., & Pandol, S. (2017). Chronic Pancreatitis: Current Status and Challenges for Prevention and Treatment. Digestive Diseases and Sciences, 62(7), 1702–1712.

Li, J., Yang, Z., Chen, Z., Bao, Y., Zhang, H., Fang, X., & Yang, W. (2016). ATF3 suppresses ESCC via downregulation of ID1. Oncology Letters, 12(3), 1642–1648.

Li, N., Wu, X., Holzer, R. G., Lee, J.-H., Todoric, J., Park, E.-J., … Karin, M. (2013). Loss of acinar cell IKKα triggers spontaneous pancreatitis in mice. Journal of Clinical Investigation, 123(5), 2231–2243.

Li, X., Zang, S., Cheng, H., Li, J., & Huang, A. (2018). Overexpression of activating transcription factor 3 exerts suppressive effects in HepG2 cells. Molecular Medicine Reports, 19(2), 869-876.

Liang, G., Wolfgang, C. D., Chen, B. P., Chen, T. H., & Hai, T. (1996). ATF3 gene. Genomic organization, promoter, and regulation. The Journal of Biological Chemistry, 271(3), 1695–701.

Iida, K., Li, Y., McGrath, B. C., Frank, A., & Cavener, D. R. (2007). PERK eIF2 alpha kinase is required to regulate the viability of the exocrine pancreas in mice. BMC Cell Biology, 8, 38.

Liou, G.-Y., Döppler, H., Braun, U. B., Panayiotou, R., Scotti Buzhardt, M., Radisky, D. C., … Storz, P. (2015). Protein kinase D1 drives pancreatic acinar cell reprogramming and progression to intraepithelial neoplasia. Nature Communications, 6(1), 6200.

Liou, G.-Y., Döppler, H., DelGiorno, K. E., Zhang, L., Leitges, M., Crawford, H. C., … Storz, P. (2016). Mutant KRas-Induced Mitochondrial Oxidative Stress in Acinar Cells Upregulates EGFR Signaling to Drive Formation of Pancreatic Precancerous Lesions. Cell Reports, 14(10), 2325–36.

Liou, G.-Y., Döppler, H., Necela, B., Krishna, M., Crawford, H. C., Raimondo, M., & Storz, P. (2013). Macrophage-secreted cytokines drive pancreatic acinar-to-ductal metaplasia through NF-κB and MMPs. The Journal of Cell Biology, 202(3), 563–77.

Liu, C. Y., & Kaufman, R. J. (2003). The unfolded protein response. Journal of Cell Science, 116(Pt 10), 1861–2.

Liu, J., Akanuma, N., Liu, C., Naji, A., Halff, G. A., Washburn, W. K., … Wang, P. (2016). TGF-β1 promotes acinar to ductal metaplasia of human pancreatic acinar cells. Scientific Reports, 6(1), 30904.

Low, G., Panu, A., Millo, N., & Leen, E. (2011). Multimodality Imaging of Neoplastic and Nonneoplastic Solid Lesions of the Pancreas. RadioGraphics, 31(4), 993–1015.

Lu, S., Jang, H., Gu, S., Zhang, J., & Nussinov, R. (2016). Drugging Ras GTPase: a comprehensive mechanistic and signaling structural view. Chemical Society Reviews, 45(18), 4929–52.

Lynch, H. T., Lynch, J. F., & Lanspa, S. J. (2010). Familial pancreatic cancer. Cancers, 2(4), 1861–83.

Maas, N. L., & Diehl, J. A. (2015). Molecular Pathways: The PERKs and Pitfalls of Targeting the Unfolded Protein Response in Cancer. Clinical Cancer Research, 21(4), 675–679.

Macherla, S., Laks, S., Naqash, A., Bulumulle, A., Zervos, E., Muzaffar, M., … Muzaffar, M. (2018). Emerging Role of Immune Checkpoint Blockade in Pancreatic Cancer. International Journal of Molecular Sciences, 19(11), 3505.

Machicado, J. D., & Yadav, D. (2017). Epidemiology of Recurrent Acute and Chronic Pancreatitis: Similarities and Differences. Digestive Diseases and Sciences, 62(7), 1683–1691.

Maisonneuve, P., & Lowenfels, A. B. (2010). Epidemiology of Pancreatic Cancer: An Update. Digestive Diseases, 28(4–5), 645–656.

Makohon-Moore, A., & Iacobuzio-Donahue, C. A. (2016). Pancreatic cancer biology and genetics from an evolutionary perspective. Nature Reviews Cancer, 16(9), 553–565.

Malik, A. M. (2015). Acute pancreatitis. A more common and severe complication of gallstones in males. International Journal of Health Sciences, 9(2), 141–5.

Mallano, T., Palumbo-Zerr, K., Zerr, P., Ramming, A., Zeller, B., Beyer, C., … Distler, J. H. W. (2016). Activating transcription factor 3 regulates canonical TGFβ signalling in systemic sclerosis. Annals of the Rheumatic Diseases, 75(13), 586-92.

Manfroid, I., Ghaye, A., Naye, F., Detry, N., Palm, S., Pan, L., … Peers, B. (2012). Zebrafish sox9b is crucial for hepatopancreatic duct development and pancreatic endocrine cell regeneration. Developmental Biology, 366(2), 268–278.

Marty-Santos, L., & Cleaver, O. (2016). Pdx1 regulates pancreas tubulogenesis and E-cadherin expression. Development, 143(1), 101–112.

Massagué, J., Blain, S. W., & Lo, R. S. (2000). TGFβ Signaling in Growth Control, Cancer, and Heritable Disorders. Cell, 103(2), 295–309.

Masui, T., Swift, G. H., Deering, T., Shen, C., Coats, W. S., Long, Q., … MacDonald, R. J. (2010). Replacement of Rbpj With Rbpjl in the PTF1 Complex Controls the Final Maturation of Pancreatic Acinar Cells. Gastroenterology, 139(1), 270–280.

Mayerle, J., Sendler, M., Hegyi, E., Beyer, G., Lerch, M. M., & Sahin-Tóth, M. (2018). Genetics and Pathophysiology of Pancreatitis. Gastroenterology, 156(7), 1951-1968.

Mitchem, J. B., Brennan, D. J., Knolhoff, B. L., Belt, B. A., Zhu, Y., Sanford, D. E., … DeNardo, D. G. (2013). Targeting tumor-infiltrating macrophages decreases tumor-initiating cells, relieves immunosuppression and improves chemotherapeutic responses. Cancer Research, 73(3), 1128.

Miyatsuka, T. (2006). Persistent expression of PDX-1 in the pancreas causes acinar-to-ductal metaplasia through Stat3 activation. Genes & Development, 20(11), 1435–1440.

Mo, P., Wang, H., Lu, H., Boyd, D. D., & Yan, C. (2010). MDM2 mediates ubiquitination and degradation of activating transcription factor 3. The Journal of Biological Chemistry, 285(35), 26908–15.

Monti, P., Leone, B. E., Marchesi, F., Balzano, G., Zerbi, A., Scaltrini, F., … Piemonti, L. (2003). The CC chemokine MCP-1/CCL2 in pancreatic cancer progression: regulation of expression and potential mechanisms of antimalignant activity. Cancer Research, 63(21), 7451–61.

Mooren, F. C., Hlouschek, V., Finkes, T., Turi, S., Weber, I. A., Singh, J., … Lerch, M. M. (2003). Early Changes in Pancreatic Acinar Cell Calcium Signaling after Pancreatic Duct Obstruction. Journal of Biological Chemistry, 278(11), 9361–9369.

Morris, J. P., Wang, S. C., & Hebrok, M. (2010). KRAS, Hedgehog, Wnt and the twisted developmental biology of pancreatic ductal adenocarcinoma. Nature Reviews Cancer, 10(10), 683–695.

Morton, J. P., Timpson, P., Karim, S. A., Ridgway, R. A., Athineos, D., Doyle, B., … Sansom, O. J. (2010). Mutant p53 drives metastasis and overcomes growth arrest/senescence in pancreatic cancer. Proceedings of the National Academy of Sciences of the United States of America, 107(1), 246–51.

Murdoch, C., Giannoudis, A., Lewis, C. E., Weich, H. A., Mantovani, A., & Marmé, D. (2004). Mechanisms regulating the recruitment of macrophages into hypoxic areas of tumors and other ischemic tissues. Blood, 104(8), 2224–34.

Neesse, A., Michl, P., Frese, K. K., Feig, C., Cook, N., Jacobetz, M. A., … Tuveson, D. A. (2011). Stromal biology and therapy in pancreatic cancer. Gut, 60(6), 861–8.

Neuschwander-Tetri, B. A., Bridle, K. R., Wells, L. D., Marcu, M., & Ramm, G. A. (2000). Repetitive acute pancreatic injury in the mouse induces procollagen alpha1(I)

expression colocalized to pancreatic stellate cells. Laboratory Investigation; a Journal of Technical Methods and Pathology, 80(2), 143–50.

Niederau, C., Ferrell, L. D., & Grendell, J. H. (1985). Caerulein-induced acute necrotizing pancreatitis in mice: protective effects of proglumide, benzotript, and secretin. Gastroenterology, 88(5 Pt 1), 1192–204.

Nøjgaard, C., Becker, U., Matzen, P., Andersen, J. R., Holst, C., & Bendtsen, F. (2011). Progression from acute to chronic pancreatitis: prognostic factors, mortality, and natural course. Pancreas, 40(8), 1195–200.

Nowarski, R., Gagliani, N., Huber, S., & Flavell, R. A. (2013). Innate immune cells in inflammation and cancer. Cancer Immunology Research, 1(2), 77–84.

Nussinov, R., Tsai, C.-J., & Jang, H. (2018). Oncogenic KRas mobility in the membrane and signaling response. Semin. Cancer Biol. 54, 109-113.

O'Hagan, R. C., & Heyer, J. (2011). KRAS Mouse Models: Modeling Cancer Harboring KRAS Mutations. Genes & Cancer, 2(3), 335-43.

Ogami, Y., & Otsuki, M. (1998). Exocrine pancreatic physiology: Overview. Pancreas, 16(3), 265–272.

Ogier, C., Colombo, P. E., Bousquet, C., Canterel-Thouennon, L., Sicard, P., Garambois, V., … Larbouret, C. (2018). Targeting the NRG1/HER3 pathway in tumor cells and cancer-associated fibroblasts with an anti-neuregulin 1 antibody inhibits tumor growth in pre-clinical models of pancreatic cancer. Cancer Letters, 432(June), 227–236.

Olive, K. P., Jacobetz, M. A., Davidson, C. J., Gopinathan, A., McIntyre, D., Honess, D., … Tuveson, D. A. (2009). Inhibition of Hedgehog signaling enhances delivery of

chemotherapy in a mouse model of pancreatic cancer. Science (New York, N.Y.), 324(5933), 1457–61.

Ormanns, S., Haas, M., Remold, A., Kruger, S., Holdenrieder, S., Kirchner, T., … Boeck, S. (2017). The Impact of SMAD4 Loss on Outcome in Patients with Advanced Pancreatic Cancer Treated with Systemic Chemotherapy. International Journal of Molecular Sciences, 18(5).

Park, J. Y., Hong, S.-M., Klimstra, D. S., Goggins, M. G., Maitra, A., & Hruban, R. H. (2011). Pdx1 Expression in Pancreatic Precursor Lesions and Neoplasms. Applied Immunohistochemistry & Molecular Morphology, 19(5), 444–449.

Patel, K. J., Yu, V. P., Lee, H., Corcoran, A., Thistlethwaite, F. C., Evans, M. J., … Venkitaraman, A. R. (1998). Involvement of Brca2 in DNA repair. Molecular Cell, 1(3), 347–57.

Pérez–Mancera, P. A., Guerra, C., Barbacid, M., & Tuveson, D. A. (2012). What We Have Learned About Pancreatic Cancer from Mouse Models. Gastroenterology, 142(5), 1079–1092.

Pin, C. L., Michael Rukstalis, J., Johnson, C., & Konieczny, S. F. (2001). The bHLH transcription factor Mist1 is required to maintain exocrine pancreas cell organization and acinar cell identity. Journal of Cell Biology, 155(4), 519-30.

Pinho, A. V., Rooman, I., Reichert, M., De Medts, N., Bouwens, L., Rustgi, A. K., & Real, F. X. (2011). Adult pancreatic acinar cells dedifferentiate to an embryonic progenitor phenotype with concomitant activation of a senescence programme that is present in chronic pancreatitis. Gut, 60(7), 958–966.

Pogue-Geile, K. L., Chen, R., Bronner, M. P., Crnogorac-Jurcevic, T., Moyes, K. W., Dowen, S., … Brentnall, T. A. (2006). Palladin mutation causes familial pancreatic cancer and suggests a new cancer mechanism. PLoS Medicine, 3(12), e516.

Prévot, P.-P., Simion, A., Grimont, A., Colletti, M., Khalaileh, A., Van den Steen, G., … Jacquemin, P. (2012). Role of the ductal transcription factors HNF6 and Sox9 in pancreatic acinar-to-ductal metaplasia. Gut, 61(12), 1723–32.

Rakonczay, Z., Jármay, K., Kaszaki, J., Mándi, Y., Duda, E., Hegyi, P., … Takács, T. (2003). NF-kappaB activation is detrimental in arginine-induced acute pancreatitis. Free Radical Biology & Medicine, 34(6), 696–709.

Rambaldi, A., Young, D., & Griffin, J. (1987). Expression of the M-CSF (CSF-1) gene by human monocytes. Blood, 69(5).

Reichert, M., & Rustgi, A. K. (2011). Pancreatic ductal cells in development, regeneration, and neoplasia. The Journal of Clinical Investigation, 121(12), 4572–8.

Renner, I. G., Savage, W. T., Pantoja, J. L., & Renner, V. J. (1985). Death due to acute pancreatitis. A retrospective analysis of 405 autopsy cases. Digestive Diseases and Sciences, 30(10), 1005–18.

Reznik, R., Hendifar, A. E., & Tuli, R. (2014). Genetic determinants and potential therapeutic targets for pancreatic adenocarcinoma. Frontiers in Physiology, 5, 87.

Rodolosse, A., Chalaux, E., Adell, T., Hagège, H., Skoudy, A., & Real, F. X. (2004). PTF1alpha/p48 transcription factor couples proliferation and differentiation in the exocrine pancreas [corrected]. Gastroenterology, 127(3), 937–49.

Rohini, M., Menon, A. H., & Selvamurugan, N. (2018). Role of activating transcription factor 3 and its interacting proteins under physiological and pathological conditions. Int. J. Biol. Macromol. 120, 310-317.

Ron, D., & Walter, P. (2007). Signal integration in the endoplasmic reticulum unfolded protein response. Nature Reviews Molecular Cell Biology, 8(7), 519–529.

Rooman, I., & Real, F. X. (2012). Pancreatic ductal adenocarcinoma and acinar cells: a matter of differentiation and development? Gut, 61(3), 449–458.

Rosendahl, J., Witt, H., Szmola, R., Bhatia, E., Ózsvári, B., Landt, O., … Sahin-Tóth, M. (2008). Chymotrypsin C (CTRC) alterations that diminish activity or secretion are associated with chronic pancreatitis. Nature Genetics, 40(1), 78.

Roy, N., Takeuchi, K. K., Ruggeri, J. M., Bailey, P., Chang, D., Li, J., … Crawford, H. C. (2016). PDX1 dynamically regulates pancreatic ductal adenocarcinoma initiation and maintenance. Genes & Development, 30(24), 2669–2683.

Rukstalis, J. M., Kowalik, A., Zhu, L., Lidington, D., Pin, C. L., & Konieczny, S. F. (2003). Exocrine specific expression of Connexin32 is dependent on the basic helix-loop-helix transcription factor Mist1. Journal of Cell Science, 116(Pt 16), 3315–25.
Sah, R. P., Nagpal, S. J. S., Mukhopadhyay, D., & Chari, S. T. (2013). New insights into pancreatic cancer-induced paraneoplastic diabetes. Nature Reviews. Gastroenterology & Hepatology, 10(7), 423.

Saluja, A., Saito, I., Saluja, M., Houlihan, M. J., Powers, R. E., Meldolesi, J., & Steer, M. (1985). In vivo rat pancreatic acinar cell function during supramaximal stimulation with caerulein. American Journal of Physiology-Gastrointestinal and Liver Physiology, 249(6), G702–G710.

Sandgren, E. P., Luetteke, N. C., Palmiter, R. D., Brinster, R. L., & Lee, D. C. (1990). Overexpression of TGF alpha in transgenic mice: induction of epithelial hyperplasia, pancreatic metaplasia, and carcinoma of the breast. Cell, 61(6), 1121–35.

Schenk, M., Schwartz, A. G., O'Neal, E., Kinnard, M., Greenson, J. K., Fryzek, J. P., … Garabrant, D. H. (2001). Familial Risk of Pancreatic Cancer. JNCI Journal of the National Cancer Institute, 93(8), 640–644.

Schenker, S., & Montalvo, R. (1998). Alcohol and the pancreas. Recent Developments in Alcoholism: An Official Publication of the American Medical Society on Alcoholism, the Research Society on Alcoholism, and the National Council on Alcoholism, 14, 41–65.

Schneider, A., Barmada, M. M., Slivka, A., Martin, J. A., & Whitcomb, D. C. (2004). Clinical characterization of patients with idiopathic chronic pancreatitis and SPINK1 Mutations. Scandinavian Journal of Gastroenterology, 39(9), 903–904.

Schneider, G., & Schmid, R. M. (2003). Genetic alterations in pancreatic carcinoma. Molecular Cancer, 2(1), 15.

Schubbert, S., Shannon, K., & Bollag, G. (2007). Hyperactive Ras in developmental disorders and cancer. Nature Reviews. Cancer, 7(4), 295–308.

Selig, L., Sack, U., Gaiser, S., Klöppel, G., Savkovic, V., Mössner, J., … Bödeker, H. (2006). Characterisation of a transgenic mouse expressing R122H human cationic trypsinogen. BMC Gastroenterology, 6, 30.

Sendler, M., Beyer, G., Mahajan, U. M., Kauschke, V., Maertin, S., Schurmann, C., … Mayerle, J. (2015). Complement Component 5 Mediates Development of Fibrosis, via Activation of Stellate Cells, in 2 Mouse Models of Chronic Pancreatitis. Gastroenterology, 149(3), 765–776.e10.

Sendler, M., Dummer, A., Weiss, F. U., Krüger, B., Wartmann, T., Scharffetter-Kochanek, K., … Mayerle, J. (2013). Tumour necrosis factor α secretion induces protease activation and acinar cell necrosis in acute experimental pancreatitis in mice. Gut, 62(3), 430–439.

Sharan, S. K., Morimatsu, M., Albrecht, U., Lim, D.-S., Regel, E., Dinh, C., … Bradley, A. (1997). Embryonic lethality and radiation hypersensitivity mediated by Rad51 in mice lacking Brca2. Nature, 386(6627), 804–810.

Shi, C., Washington, M. K., Chaturvedi, R., Drosos, Y., Revetta, F. L., Weaver, C. J., … Means, A. L. (2014). Fibrogenesis in pancreatic cancer is a dynamic process regulated by macrophage-stellate cell interaction. Laboratory Investigation; a Journal of Technical Methods and Pathology, 94(4), 409–21.

Shi, G., DiRenzo, D., Qu, C., Barney, D., Miley, D., & Konieczny, S. F. (2013). Maintenance of Acinar Cell Organization is Critical to Preventing Kras-Induced Acinar-Ductal Metaplasia. Oncogene, 32(15), 1950.

Shroff, S., Rashid, A., Wang, H., Katz, M. H., Abbruzzese, J. L., Fleming, J. B., & Wang, H. (2014). SOX9: a useful marker for pancreatic ductal lineage of pancreatic neoplasms. Human Pathology, 45(3), 456–463.

Singh, A., Greninger, P., Rhodes, D., Koopman, L., Violette, S., Bardeesy, N., & Settleman, J. (2009). A gene expression signature associated with "K-Ras addiction" reveals regulators of EMT and tumor cell survival. Cancer Cell, 15(6), 489–500.

Siveke, J. T., Lubeseder–Martellato, C., Lee, M., Mazur, P. K., Nakhai, H., Radtke, F., & Schmid, R. M. (2008). Notch Signaling Is Required for Exocrine Regeneration After Acute Pancreatitis. Gastroenterology, 134(2), 544–555.e3.

Song, H. M., Park, G. H., Eo, H. J., & Jeong, J. B. (2016). Naringenin-Mediated ATF3 Expression Contributes to Apoptosis in Human Colon Cancer. Biomolecules & Therapeutics, 24(2), 140–146.

Stanger, B. Z., & Hebrok, M. (2013). Control of Cell Identity in Pancreas Development and Regeneration. Gastroenterology, 144(6), 1170–1179.

Steinberg, W., & Tenner, S. (1994). Acute Pancreatitis. New England Journal of Medicine, 330(17), 1198–1210. https://doi.org/10.1056/NEJM199404283301706
Stolzenberg-Solomon, R. Z., Graubard, B. I., Chari, S., Limburg, P., Taylor, P. R., Virtamo, J., & Albanes, D. (2005). Insulin, Glucose, Insulin Resistance, and Pancreatic Cancer in Male Smokers. JAMA, 294(22), 2872.

Su, K. H., Cuthbertson, C., & Christophi, C. (2006). Review of experimental animal models of acute pancreatitis. HPB: The Official Journal of the International Hepato Pancreato Biliary Association, 8(4), 264–86.

Suh, H., Pillai, K., & Morris, D. L. (2017). Mucins in pancreatic cancer: biological role, implications in carcinogenesis and applications in diagnosis and therapy. American Journal of Cancer Research, 7(6), 1372–1383.

Suyama, K., Ohmuraya, M., Hirota, M., Ozaki, N., Ida, S., Endo, M., … Yamamura, K.-I. (2008). C/EBP homologous protein is crucial for the acceleration of experimental pancreatitis. Biochemical and Biophysical Research Communications, 367(1), 176–82.

Takács, T., Czakó, L., Morschl, E., László, F., Tiszlavicz, L., Rakonczay, Z., & Lonovics, J. (2002). The role of nitric oxide in edema formation in L-arginine-induced acute pancreatitis. Pancreas, 25(3), 277–82.

Tani, S., Itoh, H., Okabayashi, Y., Nakamura, T., Fujii, M., Fujisawa, T., … Otsuki, M. (1990). New model of acute necrotizing pancreatitis induced by excessive doses of arginine in rats. Digestive Diseases and Sciences, 35(3), 367–74.

Thompson, M. R., Xu, D., & Williams, B. R. G. (2009). ATF3 transcription factor and its emerging roles in immunity and cancer. Journal of Molecular Medicine (Berlin, Germany), 87(11), 1053–60.

Tramacere, I., Scotti, L., Jenab, M., Bagnardi, V., Bellocco, R., Rota, M., … La Vecchia, C. (2010). Alcohol drinking and pancreatic cancer risk: a meta-analysis of the dose-risk relation. International Journal of Cancer, 126(6), 1474-86.

Trust, M. D., Sheffield, K. M., Boyd, C. A., Benarroch-Gampel, J., Zhang, D., Townsend, C. M., … Riall, T. S. (2011). Gallstone pancreatitis in older patients: Are we operating enough? Surgery, 150(3), 515–25.

Tsunoda, Y., Yoshida, H., & Owyang, C. (1996). Structural requirements of CCK analogues to differentiate second messengers and pancreatic secretion. The American Journal of Physiology, 271(1 Pt 1), G8-19.

Vacaru, A. M., Vitale, J., Nieves, J., & Baron, M. H. (2014). Generation of Transgenic Mouse Fluorescent Reporter Lines for Studying Hematopoietic Development. Methods in Molecular Biology (Clifton, N.J.), 1194, 289.

van Asperen, C. J., Brohet, R. M., Meijers-Heijboer, E. J., Hoogerbrugge, N., Verhoef, S., Vasen, H. F. A., … Netherlands Collaborative Group on Hereditary Breast Cancer (HEBON), b. (2005). Cancer risks in BRCA2 families: estimates for sites other than breast and ovary. Journal of Medical Genetics, 42(9), 711–9.

van der Heijden, M. S., Brody, J. R., Dezentje, D. A., Gallmeier, E., Cunningham, S. C., Swartz, M. J., … Kern, S. E. (2005). In vivo Therapeutic Responses Contingent on

Fanconi Anemia/BRCA2 Status of the Tumor. Clinical Cancer Research, 11(20), 7508–7515.

Vishal, M., Swetha, R., Thejaswini, G., Arumugam, B., & Selvamurugan, N. (2017). Role of Runx2 in breast cancer-mediated bone metastasis. International Journal of Biological Macromolecules, 99, 608–614.

Von Hoff, D. D., Ervin, T., Arena, F. P., Chiorean, E. G., Infante, J., Moore, M., … Renschler, M. F. (2013). Increased survival in pancreatic cancer with nab-paclitaxel plus gemcitabine. The New England Journal of Medicine, 369(18), 1691–703.

Vrieling, A., Bueno-de-Mesquita, H. B., Boshuizen, H. C., Michaud, D. S., Severinsen, M. T., Overvad, K., … Riboli, E. (2010). Cigarette smoking, environmental tobacco smoke exposure and pancreatic cancer risk in the European Prospective Investigation into Cancer and Nutrition. International Journal of Cancer, 126(10), 2394-403.

Waddell, N., Pajic, M., Patch, A.-M., Chang, D. K., Kassahn, K. S., Bailey, P., … Grimmond, S. M. (2015). Whole genomes redefine the mutational landscape of pancreatic cancer. Nature, 518(7540), 495–501.

Wagner, M., Lührs, H., Klöppel, G., Adler, G., & Schmid, R. M. (1998). Malignant transformation of duct-like cells originating from acini in transforming growth factor transgenic mice. Gastroenterology, 115(5), 1254–62.

Wang, Q., Mora-Jensen, H., Weniger, M. A., Perez-Galan, P., Wolford, C., Hai, T., … Ye, Y. (2009). ERAD inhibitors integrate ER stress with an epigenetic mechanism to activate BH3-only protein NOXA in cancer cells. Proceedings of the National Academy of Sciences of the United States of America, 106(7), 2200–5.

Wang, Z., Xu, D., Ding, H.-F., Kim, J., Zhang, J., Hai, T., & Yan, C. (2015). Loss of ATF3 promotes Akt activation and prostate cancer development in a Pten knockout mouse model. Oncogene, 34(38), 4975-84.

Wang, Z., & Yan, C. (2016). Emerging roles of ATF3 in the suppression of prostate cancer. Molecular & Cellular Oncology, 3(1), e1010948.

Weissmueller, S., Manchado, E., Saborowski, M., Morris, J. P., Wagenblast, E., Davis, C. A., … Lowe, S. W. (2014). Mutant p53 drives pancreatic cancer metastasis through cell-autonomous PDGF receptor β signaling. Cell, 157(2), 382–394.

Wescott, M. P., Rovira, M., Reichert, M., von Burstin, J., Means, A., Leach, S. D., & Rustgi, A. K. (2009). Pancreatic Ductal Morphogenesis and the Pdx1 Homeodomain Transcription Factor. Molecular Biology of the Cell, 20(22), 4838–4844.

Westphalen, C. B., & Olive, K. P. (2012). Genetically Engineered Mouse Models of Pancreatic Cancer. The Cancer Journal, 18(6), 502–510.

Whitcomb, D. C., Gorry, M. C., Preston, R. A., Furey, W., Sossenheimer, M. J., Ulrich, C. D., … Ehrlich, G. D. (1996). Hereditary pancreatitis is caused by a mutation in the cationic trypsinogen gene. Nature Genetics, 14(2), 141–145.

Wu, X., Nguyen, B.-C., Dziunycz, P., Chang, S., Brooks, Y., Lefort, K., … Dotto, G. P. (2010). Opposing roles for calcineurin and ATF3 in squamous skin cancer. Nature, 465(7296), 368–372.

Xia, B., Sheng, Q., Nakanishi, K., Ohashi, A., Wu, J., Christ, N., … Livingston, D. M. (2006). Control of BRCA2 Cellular and Clinical Functions by a Nuclear Partner, PALB2. Molecular Cell, 22(6), 719–729.

Xiao, X., Fischbach, S., Zhang, T., Chen, C., Sheng, Q., Zimmerman, R., … Gittes, G. K. (2017). SMAD3/Stat3 Signaling Mediates β-Cell Epithelial-Mesenchymal Transition in Chronic Pancreatitis–Related Diabetes. Diabetes, 66(10), 2646–2658.

Yadav, D., & Lowenfels, A. B. (2006). Trends in the epidemiology of the first attack of acute pancreatitis: a systematic review. Pancreas, 33(4), 323–30.

Yadav, D., & Lowenfels, A. B. (2013). The epidemiology of pancreatitis and pancreatic cancer. Gastroenterology, 144(6), 1252–61.

Yadav, D., & Whitcomb, D. C. (2010). The role of alcohol and smoking in pancreatitis. Nature Reviews Gastroenterology & Hepatology, 7(3), 131–145.

Yan, C., Wang, H., & Boyd, D. D. (2002). ATF3 represses 72-kDa type IV collagenase (MMP-2) expression by antagonizing p53-dependent trans-activation of the collagenase promoter. The Journal of Biological Chemistry, 277(13), 10804–12.

Yauch, R. L., Gould, S. E., Scales, S. J., Tang, T., Tian, H., Ahn, C. P., … de Sauvage, F. J. (2008). A paracrine requirement for hedgehog signalling in cancer. Nature, 455(7211), 406–410.

Yin, X., Wolford, C. C., Chang, Y.-S., McConoughey, S. J., Ramsey, S. A., Aderem, A., … Carpenter, W. (2010). ATF3, an adaptive-response gene, enhances TGF {beta} signaling and cancer-initiating cell features in breast cancer cells. Journal of Cell Science, 123(Pt 20), 3558–65.

Ying, H., Kimmelman, A. C., Lyssiotis, C. A., Hua, S., Chu, G. C., Fletcher-Sananikone, E., … DePinho, R. A. (2012). Oncogenic Kras maintains pancreatic tumors through regulation of anabolic glucose metabolism. Cell, 149(3), 656–70.

Zeng, M., Lu, J., Li, L., Feru, F., Quan, C., Gero, T. W., … Gray, N. S. (2017). Potent and Selective Covalent Quinazoline Inhibitors of KRAS G12C. Cell Chemical Biology, 24(8), 1005–1016.e3.

Zhan, X., Wang, F., Bi, Y., & Ji, B. (2016). Animal models of gastrointestinal and liver diseases. Animal models of acute and chronic pancreatitis. American Journal of Physiology. Gastrointestinal and Liver Physiology, 311(3), G343-55.

Zhang, Y., Crawford, H. C., & Pasca di Magliano, M. (2019). Epithelial-Stromal Interactions in Pancreatic Cancer. Annual Review of Physiology, 81(1), annurev-physiol-020518-114515.

CHAPTER 6

6 APPENDICES

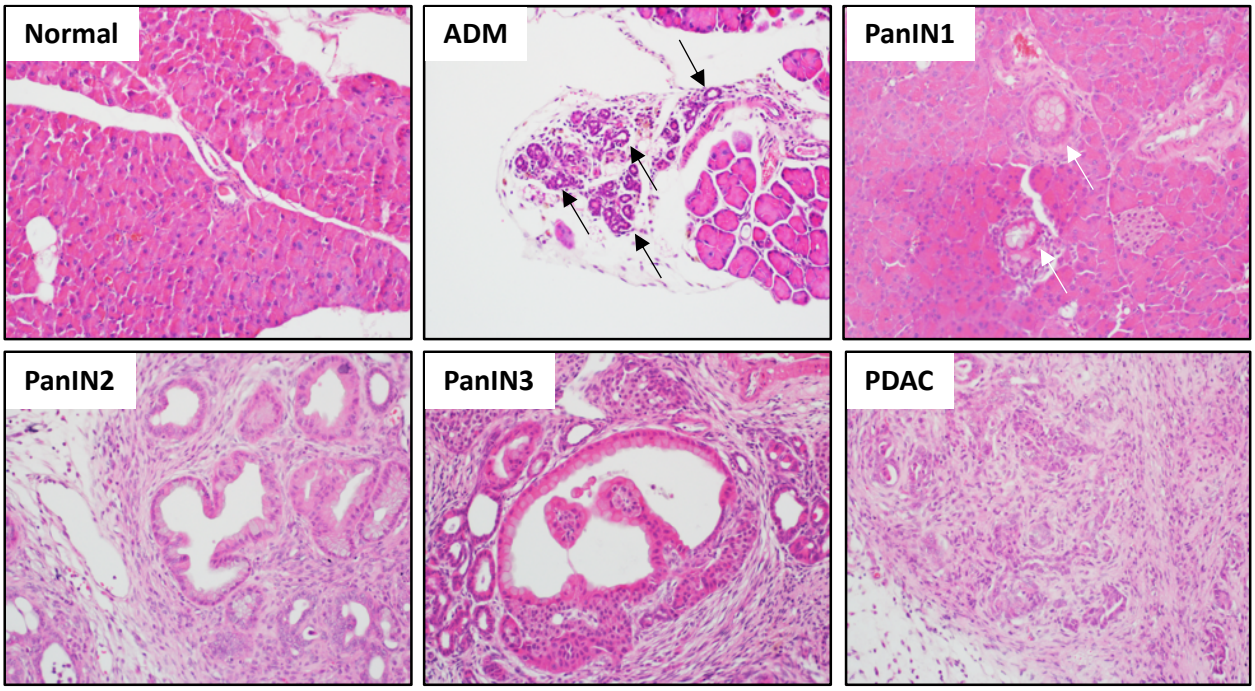

Appendix 1. ADM and PanIN lesion grade classification based on cellular morphology. Representative H&E images show ADM and varying stages of PanIN lesions. Putative ADM was classified based on cuboidal cellular morphology (black arrow points to ADM). PanIN1 lesions were classified based on columnar cellular morphology (white arrow points to PanIN1 lesions). PanIN2 and PanIN3 lesions were classified based on the loss of cellular polarity along with nuclear atypia. PDAC was classified according to a subset of cancerous cells encapsulated by fibrosis and inflammatory cells.

Curriculum Vitae

Name: Nawab Azizi

Post-Secondary Education:

The University of Western Ontario 2017 - 2019
Master of Science

The University of Guelph 2013 - 2017
Bachelor of Science, Honours

Honours and Awards:

Cancer Research and Technology Transfer (CaRTT) Scholarship 2017 - 2018
The University of Guelph Entrance Scholarship 2013 - 2014

Technical Laboratory Experience:

Victoria Research Labs, Children's Health Research Institute
Supervisor: Dr. Christopher Pin
Lab Research assistant May - August 2017

The University of Guelph, Department of Human Health and Nutritional Sciences
Supervisor: Dr. Marica Bakovic
Lab Research Assistant 2016 - 2017

Teaching Experience:

The University of Western Ontario, Department of Physiology and Pharmacology
Physiology and Pharmacology 3000E 2017 - 2019

Conferences:

American Pancreatic Association (APA) Annual Meeting, Miami, Florida, USA (2018)

Canadian Developmental Biology Conference, Mont-Tremblant, Quebec, Canada (2017)